IN THE UNITED STATES PATENT AND TRADEMARK OFFICE

In re application of	:	**Confirmation No. 1374**
Chise MUKAIDANI et al.	:	Attorney Docket No. 2004_1544A
Serial No. 10/509,032	:	Group Art Unit 1632
Filed February 9, 2005	:	Examiner Marcia S. Noble
A METHOD OF PROLIFERATING HUMAN HEPATOCYTES AND A METHOD FOR OBTAINING HUMAN HEPATOCYTES	:	**Mail Stop: AF**

DECLARATION UNDER 37 C.F.R. § 1.132

Commissioner for Patents
P.O. Box 1450
Alexandria, VA 22313-1450

Sir:

I, Chise Mukaidani, the undersigned, a citizen of Japan, residing at 6091-11, Misonou, Saijou-cho, Higashihiroshima-shi, Hiroshima, Japan, do hereby declare:

1. That I am an inventor of the above-identified application.

2. That I graduated from Department of Biologym, Faculty of Science, Nara Women's University, Japan.

3. That I currently work at PhoenixBio Co., Ltd (3-4-1 Kagamiyama, Higashihiroshima, Hiroshima 739-0024, Japan).

4. That I published papers and was received awards as listed below.

Publications

1. Utoh R, Tateno C, Yamasaki C, Hiraga N, Kataoka M, Shimada T, Chayama K, and Yoshizato K. Hepatitis B Virus-Infectibility of Chimeric Mice with Liver Repopulated by Serially Subcultured Human Hepatocytes. Hepatology (in press).
2. Masumoto N, Tateno C, Tachibana A, Utoh R, Morikawa Y, Shimada T, Momisako H, Itamoto T, Asahara T, Yoshizato K. GH enhances proliferation of human

ATTACHMENT A

hepatocytes grafted into immunodeficient mice with damaged liver.J Endocrinol. 194:529-37, 2007.

3. Hiraga N, Imamura M, Tsuge M, Noguchi C, Takahashi S, Iwao E, Fujimoto Y, Abe H, Maekawa T, Ochi H, Tateno C, Yoshizato K, Sakai A, Sakai Y, Honda M, Kaneko S, Wakita T, Chayama K. Infection of human hepatocyte chimeric mouse with genetically engineered hepatitis C virus and its susceptibility to interferon. FEBS Lett. 581:1983-7, 2007
4. Okumura H, Katoh M, Sawada T, Nakajima M, Soeno Y, Yabuuchi H, Ikeda T, Tateno C, Yoshizato K, Yokoi T. Humanization of excretory pathway in chimeric mice with humanized liver. Toxicol Sci. 97:533-8, 2007.
5. Katoh M, Sawada T, Soeno Y, Nakajima M, Tateno C, Yoshizato K, Yokoi T. In vivo drug metabolism model for human cytochrome P450 enzyme using chimeric mice with humanized liver. J Pharm Sci. 96:428-37, 2007.
6. Kakinuma S, Asahina K, Okamura K, Teramoto K. Tateno C, Yoshizato K. Tanaka Y, Yasumizu T, Sakamoto N, Watanabe M, Teraoka H. Human cord blood cells transplanted into chronic-damaged liver exhibit similar characteristics to functional hepatocytes. Transplantation Proceeding 39:240-233, 2007
7. Yoshitsugu H, Nishimura M, Tateno C, Kataoka M, Takahashi E, Soeno Y, Yoshizato K, Yokoi T, Naito S. Free Full TextEvaluation of human CYP1A2 and CYP3A4 mRNA expression in hepatocytes from chimeric mice with humanized liver. Drug Metab Pharmacokinet. 21:465-74, 2006.
8. Yatsuji H, Noguchi C, Hiraga N, Mori N, Tsuge M, Imamura M, Takahashi S, Iwao E, Fujimoto Y, Ochi H, Abe H, Maekawa T, Tateno C, Yoshizato K, Suzuki F, Kumada H, Chayama K. Emergenece of a novel lamivudine-resistant hepatitis B virus variant with a substitution outside the YMDD motif. Antimicrobiral Agent and Chenotherapy 50: 3867-3874, 2006
9. Aoki K, Kashiwagura Y., Horie T, Sato H, Tateno C, Ozawa N, and Yoshizato K. Characterization of Humanized liver from chimeric mice using coumarin as a human CYP2A6 and mouse CYP2A5 probe. Drug Metab. Pharmacokinet. 21:277-285, 2006
10. Okamura K, Asahina K, Fujimori H, Ozeki R, Shimizu-saito K, Tanaka Y, Teramoto K, Arii S, Takae K, Kataoka M, Soeno Y, Tateno C, Yoshizato K, and Teraoka H: Generation of hybrid hepatocytes by cell fusion from monky embryoid body cells in the injured mouse liver. Histochem Cell Biol 125:247-257, 2006
11. Emoto E, Tateno C, Hino H, Amano H, Imaoka Y, Asahina K, Asahara T, and Yoshizato K: Efficient In Vivo Xenogeneic Retroviral Vector-Mediated Gene Transduction into Human Hepatocytes. HUMAN GENE THERAPY 16:1168-1174, 2005
12. Katoh M., Matsui T., Okamura H., Nakajima M.,Nishimura M., Naito S., Tateno C., Yoshizato K., Yokoi T. Expression of human phase II enzymes in chimeric mice with humanized liver. Drug Metabolism and Disposition. 33:1333-1340, 2005
13. Tsuge M, Hiraga N, Takaishi H, Noguchi C, Oga H, Imamura M, Takahashi S, Iwao E, Fujimoto Y, Ochi H, Chayama K, Tateno C, Yoshizato K: Infection of human hepatocyte chimeric mouse with genetially engineered

hepatitis B virus. Hepatology 42:1046-1054, 2005
14. Katoh M, Matsui T, Nakajima M, Tateno C, Soneno Y, Horie T, Iwasaki K, Yoshizato K, and Yokoi T: In vivo induction of human cytochrome P450 enzymes expressed in chimeric mice with human hepatocytes. Drug Metab Dispos 33:754-763, 2005
15. Nishimura M, Yoshitsugu H, Yokoi T, Tateno C, Kataoka M, Horie T, Yoshizato K, Naito S. Evaluation of Mrna expression of human drug-metabolizing enzymes and transporters in chimeric mouse with humanized liver. Xenobiotica 35:877-890, 2005
16. Nishimura M, Yokoi T, Tateno C, Kataoka M, Takahashi E, Horie T, Yoshizato K, and Naito S: Induction of Human CYP1A2 and CYP3A4 in Primary Culture of Hepatocytes from Chimeric Mice with Humanized Liver. Drug Metabolism and Pharmacokinetics. 20:121-126, 2005
17. Katoh M, Matsui T, Nakajima M, Tateno C, Kataoka M, Soeno Y, Horie T, Iwasaki K, Yoshizato K, and Yokoi T: Expression of Human CYPs in Chimeric Mice with Humanaized Liver. Drug Metab Dispos 32:1402-1410, 2004
18. Tateno C, Yoshizane Y, Saito N, Kataoka M, Utoh R, Yamasaki C, Tachibana A, Soeno Y, Asahina K, Hino H, Asahara T, Yokoi T, Furukawa T, Yoshizato K: Near-completely humanized liver in mice shows human-type metabolic responses to drugs. Am J Pathol 165:901-912, 2004

Awards

1. Award for the Japan Society for Organ Preservation and Medical Biolody in 2004

2. DMPK editor's award for the most excellent article in 2005, The Japanese Society for the Study of Xenobiotics

5. That I have read the specification and claims of the above-identified application as well as the Reply filed May 17, 2007. I have also read the Office Actions, including the most recent dated August 10, 2007, which includes a rejection of claims 1, 7-10 and 16-18 under 35 USC 112, first paragraph, as not enabled.

6. That in order to show that the claimed invention is enabled for proliferating human hepatocytes in immunodeficient hepatopathy mice, I have under my control and direction conducted the following experiment, the particulars and results of which are attached herewith.

Experiment

A. Animals

A chimeric mouse carrying proliferated human hepatocytes in the liver was prepared by transplanting human hepatocytes into the liver of an immunodeficient hepatopathy mouse, uPA(+/+)/Rag2 knockout/γc knockout mouse (uPA/Rag2-KO/γc-KO mouse).

Rag2-KO/γc-KO mouse (obtain from Taconic Inc. U.S.A.) is an immunodeficiency mouse not having B cells and T cells due to knockout of Rag2 gene. Further, the mouse has no NK activity because IL-2 receptor γ chain is knocked out.

The uPA/Rag2-KO/γc-KO mice were obtained by mating a uPA(+/+)/SCID male mouse (Example 1 of this application) and a Rag2-KO/γc-KO female mouse.

B. Transplantation of human hepatocytes into the uPA/Rag2-KO/γc-KO mouse

The uPA/Rag2-KO/γc-KO mouse, from 21 to 48 days old, was anesthetized by ether and incised about 5 mm at the flank, and then, 20 μl of cell suspension with concentration from 5 x 10^7 cells/ml (10 x 10^5 cells in total) was inoculated from a spleen head, and then stanched. As a hemostatic agent, 40 μl of an e-aminocaproic acid (SIGMA) solution (0.02 g/ml) was administered into the abdominal cavity, and then, after the spleen was returned to the abdominal cavity, the flank was sewed up.

After the surgery for transplanting human hepatocytes, the chimeric mouse was administered with Futhan in accordance with the schedule shown in Example 1 of this application.

C. Monitoring of human albumin in mouse blood

From 3 weeks after transplantation of human hepatocytes, 2 μl blood samples were taken from the tail of the chimeric mouse once per a week, and concentration of human albumin was measured.

Increased concentration of human albumin in blood was observed in all 11 mice (Fig. A). The highest value was over 14 mg/ml.

D. Induction of P450 isozymes in a liver of the chimeric mouse

Inducers for P450 isozymes were administered to the chimeric mouse and expression levels of each isozymes (mRNA and protein) were measured.

The chimeric mice, at 74 days after transplantation of human hepatocytes (concentration of human albumin was 4-15 mg/ml), were administered with Rifampicin (an inducer for CYP3A4) or 3-methylcholanthrene (3-MC; an inducer for CYP1A1 and CYP1A2). Rifampicin (50 mg/kg body weight) and 3-MC (20 mg/kg body weight) were administered intraperitoneally once per day for 4 days, respectively. As a control, uPA/SCID mouse (Example 1 of this application) was administered with Rifampicin.

After administration of the inducer, total RNA was isolated from a part of the liver of the chimeric mouse, and then expression level of mRNA for human P450 isozymes (CYP1A1, CYP1A2, CYP2C9, CYP2C19, CYP2D6 and CYP3A4) was assayed by real-time RT-PCR method. In addition, microsome was isolated from the other part of the liver and protein amount of CYP1A2 and CYP3A4 was measured by western blotting using a specific antibody for each protein.

The results are shown in Fig. B. The expression level of human CYP1A1 and CYP1A2 in the 3-MC-administered chimeric mice was about 4.9 and 3.5 times higher respectively, compared with non-administered mice. The expression level of human CYP3A4 in the Rifampicin-administered mice was 3.7 times higher compared with the non-administered mice. Furthermore, it should be noted that the Rifampisin-induction for CYP3A4 in uPA/Rag2-KO/γc-KO mouse was equivalent to that in uPA/SCID mouse.

Regarding to expression amount of each CYP protein, same results were obtained as mRNA expression level (data not shown).

E. Replacement of human hepatocytes in the chimeric mouse

Frozen sections of each lobe of the liver were prepared, followed by reacting with human specific cytokeratin 8/18 antibody and staining by peroxidase as Example 1 (2.6). With respect to each lobe of the liver, ratio of cytokeratin 8/18 positive areas in the total section area was

calculated.

Results are shown in Fig. C. In the chimeric mouse derived from uPA/Rag2-KO/γc-KO mouse, the human albumin value was correlated with replacement ratio of human hepatocytes.

Figures A, B and C, which are discussed above, are attached to this Declaration.

Conclusion

Based on the above noted experiment, as well as page 5, lines 3-12, and page 17, line 19 to page 20, line 18, it is my expert opinion and belief that the claimed invention is enabled for proliferating human hepatocytes in immunodeficient hepatopathy mice. In particular, the above experiment and noted specification disclosure, as well as the knowledge in the art, indicate that immunodeficient hepatopathy mice may be utilized in the claimed invention without undue experimentation.

I further declare that all statements made herein of my own knowledge are true and all statements made on information and belief are believed to be true; and further that these statements were made with the knowledge that willful false statements and the like so made are punishable by fine or imprisonment, or both, under Section 1001 of Title 18 of the United States Code and that such willful false statements may jeopardize the validity of this application or any patent issuing thereon.

Date: Feb 1, 2008

Chise Mukaidani

Chise MUKAIDANI

WMC/WRS/lq
Washington, D.C. 20006-1021
Telephone (202) 721-8200
Facsimile (202) 721-8250

Fig. A

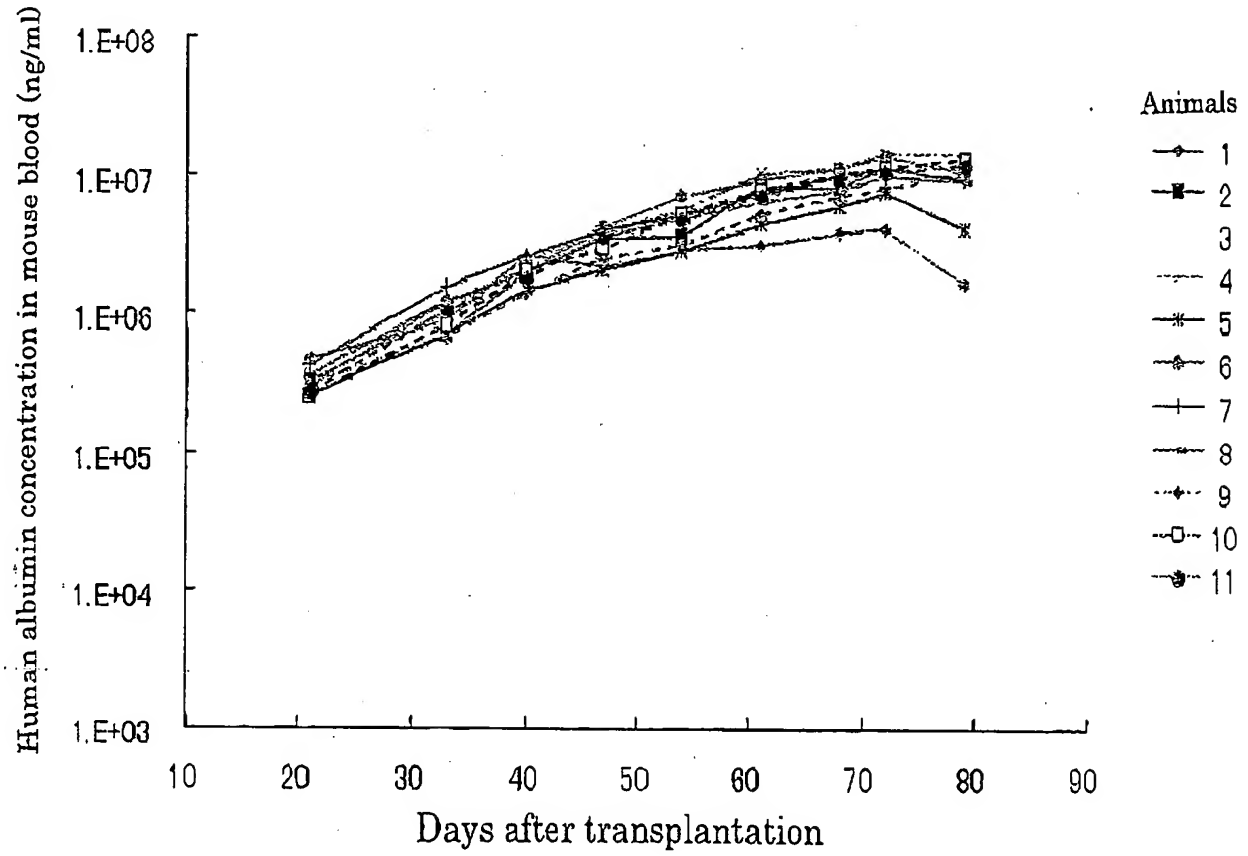

Fig. B

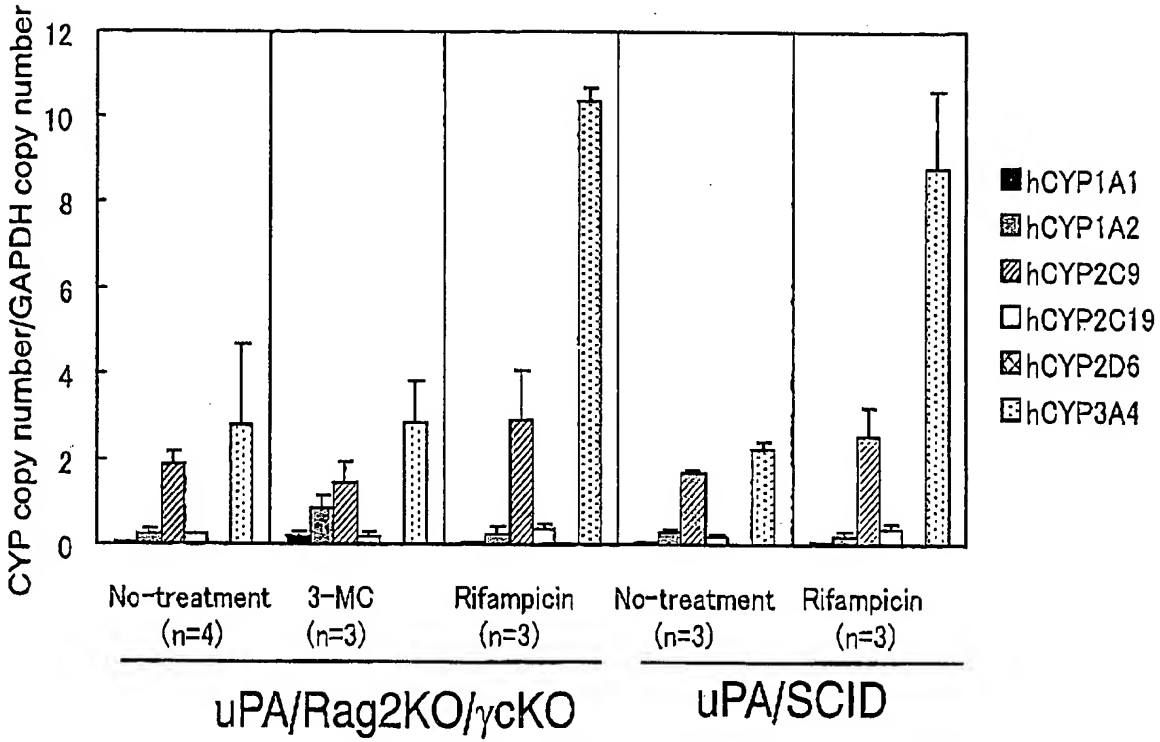

		hCYP1A1	hCYP1A2	hCYP2C9	hCYP2C19	hCYP2D6	hCYP3A4
uPA/Rag2KO/γcKO	No-treatment	1.00	1.00	1.00	1.00	1.00	1.00
	3-MC	4.88	3.51	0.76	0.84	0.95	1.02
	Rifampicin	1.05	0.98	1.52	1.54	0.95	3.74
uPA/SCID	No-treatment	1.00	1.00	1.00	1.00	1.00	1.00
	Rifampicin	1.14	0.69	1.52	1.99	0.90	3.99

Fig. C

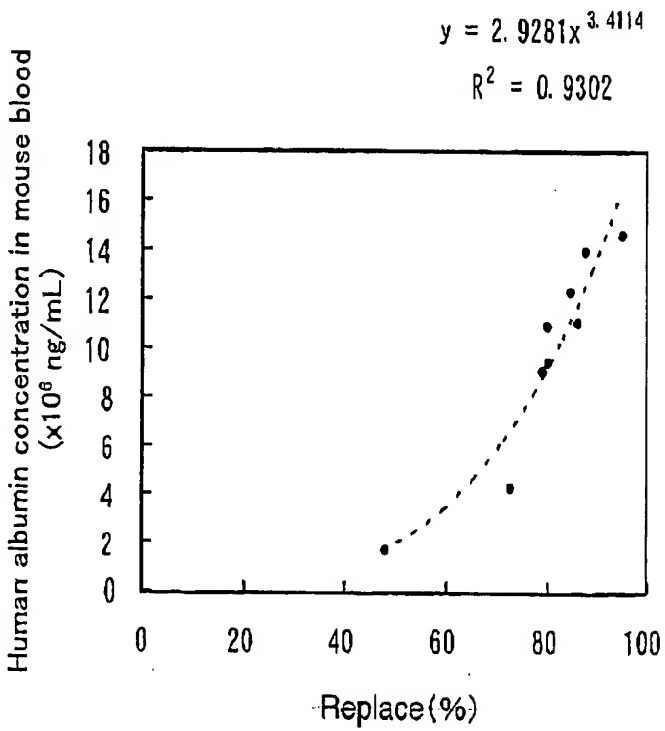
y = 2.9281x^3.4114
R^2 = 0.9302
Human albumin concentration in mouse blood (x10^6 ng/mL)
18
16
14
12
10
8
6
4
2
0
0
20
40
60
80
100
Replace(%)

'TY DOCKET #: 2004_1544A
nfirmation No. 1374
JR REF: 2004_1544A/WMC/00653
plicant: Chise MUKAIDANI et al.
ial No.: 10/509,032 **Filing Date:** February 9, 2005
le: A METHOD OF PROLIFERATING HUMAN HEPATOCYTES AND A METHOD FOR OBTAINING HUMAN HEPATOCYTES

eipt of the following papers is acknowledged:

PPLEMENTAL IDS, PTO-1449 FORM WITH 8 REFERENCES.

e: April 22, 2005 **Attorney:** WMC/dlk **[Check No._____]**

ATTACHMENT B

Sheet 1 of 1

INFORMATION DISCLOSURE STATEMENT

FORM PTO 1449 *(modified)*

U.S. DEPARTMENT OF COMMERCE
PATENT AND TRADEMARK OFFICE

LIST OF REFERENCES CITED BY APPLICANT(S)
(Use several sheets if necessary)

Date Submitted to PTO: April 22, 2005

ATTY DOCKET NO.	SERIAL NO.
2004_1544A	10/509,032
APPLICANT	
Chise MUKAIDANI et al.	
FILING DATE	**GROUP**
February 9, 2005	

U.S. PATENT DOCUMENTS

*EXAMINER INITIAL		DOCUMENT NUMBER	DATE	NAME	CLASS	SUBCLASS	FILING DATE IF APPROPRIATE
	AA						
	AB						
	AC						

FOREIGN PATENT DOCUMENTS

		DOCUMENT NUMBER	DATE	COUNTRY	CLASS	SUBCLASS	TRANSLATION YES	TRANSLATION NO
	AD							
	AE							

OTHER DOCUMENT(S) *(Including Author, Title, Date, Pertinent Pages, Etc.)*

	AF	J. L. Heckej et al., "Neonatal Bleeding in Transgenic Mice Expressing Urokinase-Type Plasminogen Activator", Cell, Vol. 62, pp. 447-456, August 10, 1990.
	AG	J. A. Rhim et al., "Replacement of Diseased Mouse Liver by Hepatic Cell Transplantation", Science, Vol. 263, pp. 1149-1152, February 25, 1994.
	AH	E. P. Sandgren et al., "Complete Hepatic Regeneration after Somatic Deletion of an Albumin-Plasminogen Activator Transgene", Cell, Vol. 66, pp. 245-256, July 26, 1991.
	AI	J. A. Rhim et al., "Complete Reconstitution of Mouse Liver with Xenogeneic Hepatocytes", Proc. Natl. Acad., USA, Vol. 92, pp. 4942-4946, May 1995.
	AJ	M. Dandri et al., "Woodchuck Hepatocytes Remain Permissive for Hepadnavirus Infection and Mouse Liver Repopulation after Cryopreservation", Hepatology, Vol. 34, No. 4, pp. 824-833, 2001.
	AK	M. Dandri et al., "Repopulation of Mouse Liver with Human Hepatocytes and *In Vivo* Infection with Hepatitis B Virus", Hepatology, Vol. 33, No. 4, pp. 981-987, 2001.
	AL	J. Petersen et al., "Liver Repopulation with Xenogenic Hepatocytes in B and T Cell-Deficient Mice Leads to Chronic Hepadnavirus Infection and Clonal Growth of Hepatocellular Carcinoma", Proc. Natl. Acad. Sci., USA, Vol. 95, pp. 310-315, January 1998.
	AM	D. F. Mercer et al., "Hepatitis C Virus Replication in Mice with Chimeric Human Livers", Nature Medicine, Vol. 7, No. 8, pp. 927-932, August 2001.

MINER | DATE CONSIDERED

NER: *Initial if reference considered, whether or not citation is in conformance with MPEP 609; Draw line through citation if not in conformance and not considered. Include copy i with next communication to applicant.*

ATTACHMENT C

•Cell, Vol. 62, 447–456, August 10, 1990.

Neonatal Bleeding in Transgenic Mice Expressing Urokinase-Type Plasminogen Activator

Janice L. Heckel,* Eric P. Sandgren,† Jay L. Degen,* Richard D. Palmiter,‡ and Ralph L. Brinster†
*Children's Hospital Research Foundation and Department of Pediatrics
University of Cincinnati College of Medicine
Cincinnati, Ohio 45229
†Laboratory of Reproductive Physiology
School of Veterinary Medicine
University of Pennsylvania
Philadelphia, Pennsylvania 19104
‡Howard Hughes Medical Institute and Department of Biochemistry
University of Washington
Seattle, Washington 98195

Summary

Spontaneous intestinal and intra-abdominal bleeding was observed in a high percentage of newborn transgenic mice carrying the murine urokinase-type plasminogen activator (uPA) gene linked to the albumin enhancer/promoter. These hemorrhagic events were directly related to transgene expression in the liver and the development of high plasma uPA levels. Two lines were established from surviving founder mice that displayed multigenerational transmission of the bleeding phenotype. Fatal hemorrhaging developed between 3 and 84 hr after birth in about half of the transgenic offspring of these lines; transgenic pups that did not bleed nevertheless passed the phenotype to their young. The phenotypic variability could not be explained by differences in transgene expression. All transgenic neonates were severely hypofibrinogenemic and displayed loss of clotting function that extended beyond the risk period for bleeding. These mice provide a means of studying the pathophysiology of plasminogen hyperactivation and evaluating therapeutic protocols designed to prevent bleeding.

Introduction

Hemostasis is maintained by an integrated system that promotes the formation and dissolution of fibrin. Loss of vascular integrity normally initiates a two-phase response involving platelet plug formation followed by coagulation factor–mediated deposition of a stable fibrin clot. Once vascular repair is completed, the fibrinolytic system removes the fibrin clot. Fibrinolysis is controlled in part by the conversion of plasminogen to the active serine protease, plasmin, by plasminogen activator (Collen and Lijnen, 1987). This process is also regulated by specific and fast-acting serine protease inhibitors, which include α2-antiplasmin (α2-AP) and plasminogen activator inhibitors (Collen and Lijnen, 1987; Saksela and Rifkin, 1988). Two plasminogen activators, tissue-type plasminogen activator (tPA) and urokinase-type plasminogen activator (uPA), have been identified in the plasma of mammals. These enzymes have distinct domain architecture and biochemical properties and are encoded by different genes located on separate chromosomes (Collen and Lijnen, 1987; Saksela and Rifkin, 1988; Danø et al., 1985). While plasma concentrations of both are similar, tPA is widely considered the more important in physiologic fibrinolysis. This view is supported by the unique fibrin binding property of tPA, which both enhances the efficiency of plasminogen activation and permits formation of plasmin directly on the fibrin substrate (Collen and Lijnen, 1987). The role of uPA in physiologic fibrinolysis is unknown.

Defects in the fibrinolytic system are known to produce hemorrhagic and thrombotic disorders. Congenital conditions include deficiency of α2-AP (Aoki et al., 1979, 1980; Miles et al., 1982), dysfunctional α2-AP (Kluft et al., 1987), dysplasminogenemias (Aoki et al., 1978; Kazama et al., 1981), plasminogen deficiency (Girolami et al., 1986; Lottenberg et al., 1985), and increased plasminogen activator activity (Booth et al., 1983; Aznar et al., 1984). Acquired disorders are more common and have been described in association with hepatic cirrhosis (Das and Cash, 1969), amyloidosis (Sane et al., 1989), acute leukemias (Imaoka et al., 1986; Gralnick and Abrell, 1973; Van Slyck et al., 1989), solid tumors (Tagnon, 1952; Pellman et al., 1986), and the use of thrombolytic therapy (Marder and Sherry, 1988; Rao, 1988). Despite potential bleeding complications, the administration of plasminogen activators has become an attractive strategy in the treatment of thrombotic disorders including myocardial infarction. While some of the bleeding problems observed with this therapy appear related to catheterization procedures, spontaneous bleeding from remote sites (e.g., the gastrointestinal tract) has been noted (Rao, 1988).

Because of the intricacies of the coagulation and fibrinolytic pathways, a complete understanding of these systems may be difficult to achieve using in vitro or short-term in vivo studies. Genetic manipulation of the coagulation and fibrinolytic systems in transgenic mice provides a promising new experimental approach to study hemostasis. In this study, we have applied this approach to explore the effects of elevated plasma plasminogen activator levels. In particular, we investigated whether enhanced plasminogen activation would result in spontaneous hemorrhage, and, if so, what biochemical consequences contribute to the bleeding diathesis.

Results

Transgenic mice with elevated plasma uPA levels were generated using a construct that targets uPA production to the hepatocyte. This chimeric gene (Alb–uPA) consists of the albumin enhancer/promoter, the murine uPA gene body, and the 3′ untranslated and flanking sequences of the human growth hormone (hGH) gene, which were incorporated to provide a means to distinguish transgene-derived from endogenous mRNA (see Figure 1). Injection

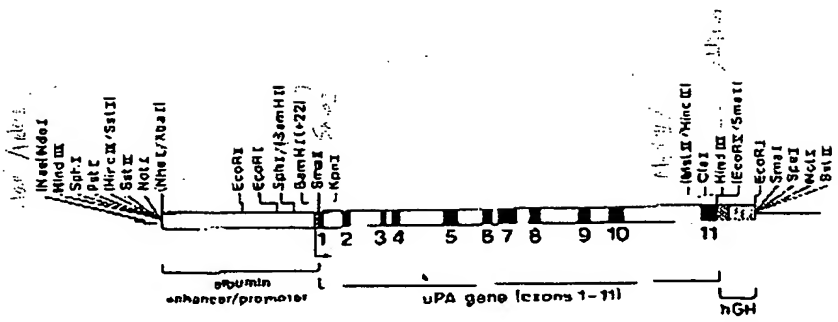

Figure 1. Map of the Alb–uPA Transgene

The Alb–uPA construct contained the following major elements: a 2.9 kb NheI–BamHI fragment of the plasmid EB3alb-hGH (Pinkert et al., 1987) containing the murine albumin enhancer/promoter and 22 nucleotides of exon 1; a portion of the murine uPA gene (Friezner-Degen et al., 1987) extending from 5′ noncoding sequences in exon 1 (position +43) to 3′ noncoding sequences in exon 11 (position +5753); and a 0.8 kb SmaI–EcoRI fragment of the hGH gene containing 100 nucleotides of hGH 3′ noncoding sequences and the hGH polyadenylation site. The components were joined using oligonucleotide linkers as described in Experimental Procedures. The exon sequences derived from the albumin, uPA, and hGH gene are indicated by the horizontal cross-hatched, filled-in, and diagonally cross-hatched regions, respectively. The 3′-flanking sequences of the hGH gene are stippled. The exons of the composite gene are numbered 1 to 11 with the transcription initiation site indicated with an arrow. Bluescript (Stratagene) vector sequences are indicated by thin lines. For simplicity, restriction endonuclease cleavage sites within the fully sequenced uPA (Friezner-Degen et al., 1987) and hGH (Seeburg, 1982) gene elements have not been indicated; selected sites found at the linker junctions are shown. Restriction endonuclease cleavage sites lost during subcloning are shown in parentheses.

of the Alb–uPA construct into fertilized mouse eggs resulted in a total of 183 mice, of which 56 carried one or more copies of the transgene.

Hepatic Expression of uPA Causes Neonatal Bleeding

During the 2 days following birth, 17 Alb–uPA founder mice developed internal bleeding (see Figure 2); each was subsequently confirmed to carry the uPA transgene. Bleeding into intestine (13 mice) or abdominal cavity (4 mice) was first detectable between 3 and 52 hr after birth. Mice subsequently became icteric and then died within 10 hr (plasma bilirubin in two affected animals was 5.7 and 12.9 mg/dl, compared with 0.2–1.2 mg/dl in nontransgenic mice). From these observations, two findings stand out: no mice displayed any sign of bleeding during or shortly after birth, and by 3 days postpartum all susceptible mice had died.

To explore the relationship between bleeding and uPA transgene expression, tissue and plasma samples were collected from affected and age-matched control mice and examined for transgene products. As shown in Table 1, transgene mRNA levels in the livers of affected neonates were as high as 6500 molecules per cell (compared with <10 for endogenous uPA). In addition, liver plasminogen mRNA was equally abundant in transgenic and nontransgenic mice, indicating the absence of any general impairment of liver-specific mRNA production in the transgenic animals (Table 1). Samples of lung, kidney, and intestine from seven affected mice were also analyzed for transgene mRNA. All intestinal samples were negative, and few transgene-derived transcripts were detected in any of the remaining samples with the exception of one mouse exhibiting 240 molecules per cell in the lung (data not shown).

The relative uPA levels in plasma were measured with a simple zymography assay. In this system, plasma proteins are electrophoretically fractionated on nonreducing SDS–polyacrylamide gels containing both plasminogen and casein. When renatured, the separated plasminogen activators catalyze localized plasminogen-dependent caseinolysis detected as "lytic zones" in amido black–stained gels. The method provides both a comparative analysis of plasminogen activator levels and information regarding the size of the plasminogen activators present. Plasma uPA concentration was extremely high in transgenic mice and nearly undetectable in control neonates (Figure 3A): assay of serially diluted plasma from animal 1942-1 showed uPA activity to be approximately 200 times that of control plasma (Figure 3B). To compare the levels of plasma plasminogen activator activity in individual mice, the amount of caseinolytic activity in a standard amount of plasma was arbitrarily assigned a value of + (control) to ++++ (transgenic mouse 1942-1). As summarized in Table 1, plasma uPA activity appeared to be related to the level of hepatic transgene mRNA. In all transgenic mice examined, the majority of the plasma plasminogen activator

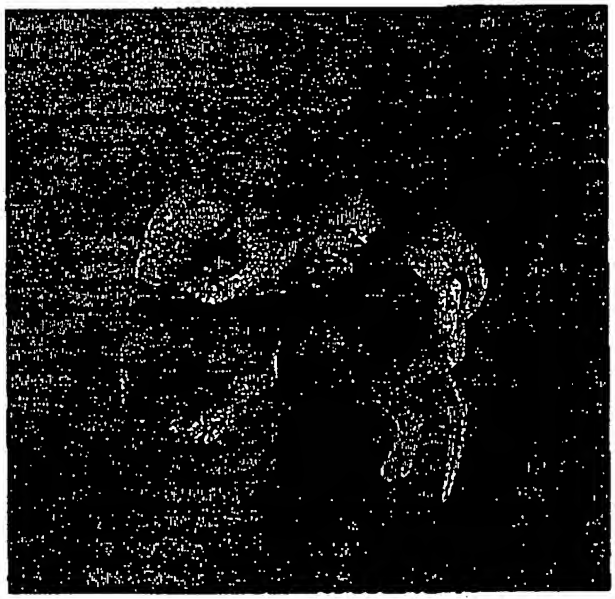

Figure 2. Gross Appearance of Live Alb–uPA Transgenic Founder Displaying the Bleeding Phenotype

The transgenic mouse (top) is icteric and contains blood in its intestine (dark patch in the caudal abdomen indicated by arrows). Milk is present in the stomach of both mice. The transgenic mouse is an albino, and thus lacks retinal pigment.

Table 1. Expression of uPA Transgene in Founder Mice Displaying the Bleeding Phenotype

Mouse	Liver mRNA (Molecules/Cell) uPA[a]	Plasminogen[a]	Plasma uPA[b]
1356-1	870	ND[c]	ND
1356-5	650	190	ND
1356-7	280	ND	ND
1940-2	3200	280	+ + +
1942-1	6500	380	+ + + +
1942-2	4800	660	+ + +
1947-5	5800	380	+ + + +
1949-1	1500	740	+ + +
1951-1	2700	770	+ + +
Control 1	<10	290	+
Control 2	<10	450	+
Control 3	<10	480	+

[a] uPA mRNA and plasminogen mRNA levels were established by solution hybridization assay using specific cDNA probes; see Experimental Procedures for details.
[b] uPA levels in plasma were established by zymography assay (see text and Experimental Procedures for details). The relative uPA activity observed in each sample was assigned a value ranging from + + + + (activity observed in plasma collected from transgenic founder 1942-1; see Figure 3) to + (activity observed in plasma collected from nontransgenic control animals; see Figure 3). The values assigned were not linearly related to activity.
[c] ND, not determined.

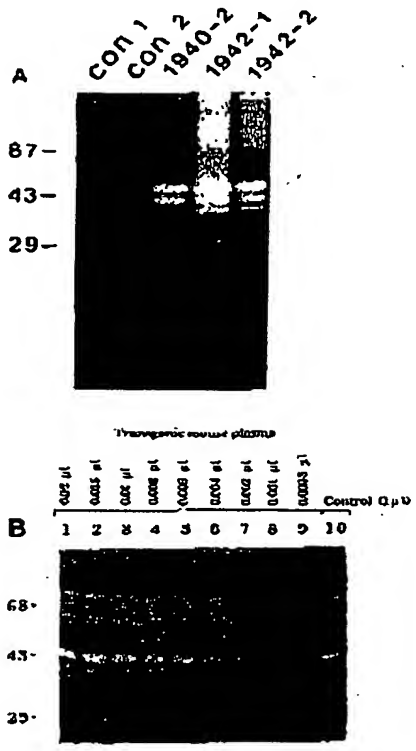

Figure 3. Zymographic Analysis of Plasma Plasminogen Activator Levels in Alb–uPA Mice

(A) Plasminogen activator activity in electrophoretically fractionated plasma samples (1 μl) collected from Alb–uPA transgenic neonates displaying bleeding phenotype (1940-2, 1942-1, 1942-2) and control mice (con 1 and con 2). For a detailed description of the zymographic detection of plasminogen activators, see text and Experimental Procedures. For the purpose of comparison, the plasminogen activator levels in control, 1940-2, and 1942-1 plasma samples were assigned an arbitrary value of +, + + +, and + + + +, respectively (for summary see Table 1). The relative migration of bovine serum albumin (68,000), ovalbumin (43,000), and carbonic anhydrase (29,000) molecular weight standards is indicated at left.

(B) Plasminogen activator activity in serially diluted plasma collected from transgenic mouse 1942-1 (lanes 1–9; plasma volume indicated above each lane).

had a molecular weight of approximately 45,000, which is similar to the size of mature murine uPA. A set of three bands was consistently observed in the range of 40,000 to 45,000 daltons, and samples containing the highest total activity displayed an additional band with apparent molecular weight of 30,000. Urine samples (a rich source of uPA) from control mice contained similar bands of activity, suggesting that these species arise from uPA and its proteolytic derivatives and that the 30,000 molecular weight species is the plasmin degradation product termed low molecular weight urokinase. Covalent complexes of uPA with inhibitor(s) may account for at least part of the heterogeneous high molecular weight activity noted on gels.

Two Established Transgenic Lines Display Multigenerational Transmission of the Bleeding Phenotype

Thirty-nine of 56 Alb–uPA transgenic founder animals did not bleed, and three of these died of unknown causes as neonates. A sample of liver was obtained by partial hepatectomy from each of the remaining 36 mice at 4 weeks of age and examined for transgene expression. Only 2 of the 36 samples contained transgene-derived mRNA, but at near-background levels for the assay (10–20 molecules per cell). Nevertheless, these mice, designated 1353-8 and 1944-6, were bred, and their offspring were analyzed for the transgene. Three of 33 1353-8 offspring and 12 of 48 1944-6 offspring analyzed at weaning inherited the transgene, consistent with germline mosaicism in both founder mice. However, occasional newborn offspring of each parent developed abdominal or intestinal bleeding and subsequently died. When surviving offspring of these founder mice were bred and the litters weaned, only 29 of 122 (1353-8) and 10 of 61 (1944-6) second to fourth generation offspring carried the transgene. The deviation from the expected 50% transgene transmission ratio was a consequence of the bleeding and death of approximately one-half (1353-8) or two-thirds (1944-6) of all transgene-positive mice. Like the founder Alb–uPA mice that bled as neonates, affected line 1353-8 and 1944-6 offspring appeared normal at birth but then developed fatal hemorrhaging into the abdominal cavity or intestinal tract between 3 and 84 hr postpartum. Transgenic mice that survived beyond 4 days did not bleed, but nevertheless passed the neonatal bleeding phenotype to offspring.

To characterize the biochemistry of bleeding in these lines, transgene expression and plasma uPA levels were measured. Liver and plasma samples were collected from mice ranging in age from fetal day 18 (2 days before birth) to postnatal day 10. Liver samples were subsequently

Table 2. Analysis of Perinatal Alb–uPA Mice from Established Lines

Age (Line)[a]	No. Mice	Appearance	Liver mRNA (Molecules/Cell)[b] uPA	Liver mRNA (Molecules/Cell)[b] Plasminogen	Plasma uPa (Relative Level)[c]
fd.18 (1353-8)	4	normal	1400 ± 140	250 ± 60	+ + +
fd.18 (control)	1	normal	<10	200	+
d.1–2 (1353-8)	10	abdominal bleed	600 ± 280	470 ± 130	+ + +
d.1–2 (1353-8)	11	normal	600 ± 210	270 ± 50	+ + +
d.1–2 (1944-6)	2	GI/abdominal bleed	870 ± 340	240 ± 80	ND
d.1–2 (1944-6)	2	normal	2000 ± 300	ND[d]	+ + + +
d.1–2 (control)	2	normal	<10	410 ± 40	+
d.4–5 (1353-8)	3	normal	480 ± 300	680 ± 50	+ +
d.4 (1944-6)	1	normal	450	ND	+ +
d.4 (control)	2	normal	<10	330 ± 180	+
d.7–10 (1353-8)	10	normal	440 ± 170	ND	+ +
d.8–10 (control)	2	normal	<10	ND	+

[a] fd.18 = fetal day 18 (ca. 24–48 hr before expected birth); d = day after birth.
[b] uPA and plasminogen mRNA levels established by solution hybridization assay using specific cDNA probes (see Experimental Procedures). Data expressed as mean value ± standard deviation.
[c] uPA activity in plasma established by zymography (see Experimental Procedures). Highest relative uPA activity is expressed as + + + + and trace uPA activity is expressed as +.
[d] ND, not determined.

analyzed for transgene-derived uPA mRNA and plasminogen mRNA levels, and plasma samples were analyzed for plasminogen activator activity (Table 2). Abundant transgene mRNA was present in the livers of all transgenic offspring, generally in excess of the endogenous plasminogen mRNA levels. The transgene mRNA levels were generally greater in fetal than postnatal mice, yet fetal animals never displayed a bleeding phenotype and there was no indication of fetal loss of transgenic animals. Surprisingly, the transgene mRNA levels in hemorrhaging and nonhemorrhaging day 1 and day 2 neonates were not significantly different, and these levels were occasionally less than those in mice greater than 4 days old, which never bleed. These results argue that the phenotypic difference in transgenic neonates is not simply due to variation in transgene expression.

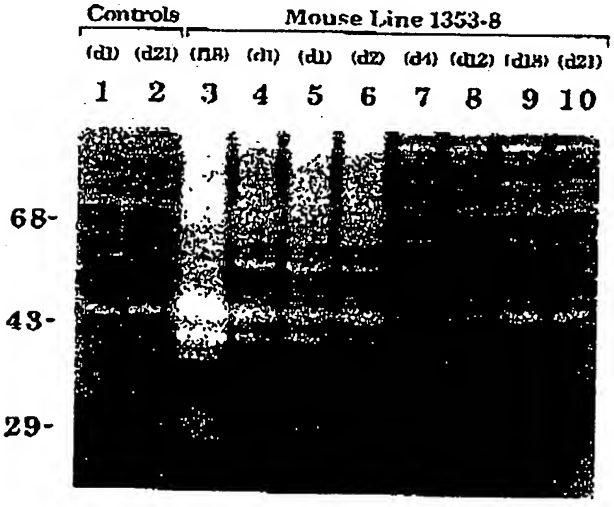

Figure 4. Plasma Plasminogen Activator Levels Decrease As a Function of Age in Alb–uPA Mice

Zymographic analysis of plasma (0.5 μl) plasminogen activator levels in control (lanes 1 and 2) and line 1353-8 transgenic mice (lanes 3–10) ranging in age from fetal day 18 to postnatal day 21. Plasma sample analyzed in lane 5 was collected from a transgenic mouse displaying the bleeding phenotype; all other mice appeared grossly normal. Lane 1, day 1 control; lane 2, day 21 control; lane 3, fetal day 18; lane 4, day 1; lane 5, day 1; lane 6, day 2; lane 7, day 4; lane 8, day 12; lane 9, day 18; lane 10, day 21.

Fetal and neonatal transgenic mice also had uniformly high plasma plasminogen activator activity as detected by zymography (Table 2). Analysis of serially diluted plasma collected from a 1-day-old line 1353-8 neonate showed that the uPA level was about 100 times that of an age-matched control (data not shown). Like hepatic uPA mRNA, plasma uPA levels were highest in fetal animals and decreased with age (see representative results in Figure 4 and summary in Table 2). However, variations in plasma uPA levels in day 1 and day 2 neonates did not distinguish between the bleeding and nonbleeding animals.

Alb–uPA Mice Are Hypofibrinogenemic

The physiological basis of the bleeding phenotype in Alb–uPA transgenic mice was also investigated. Platelets are one of the first responsive elements to bleeding, and variability in platelet number could explain why only some transgenic animals bleed. To examine this possibility, platelets were counted in whole-blood samples collected from both affected and unaffected line 1353-8 mice at 2 days of age. Among nontransgenic, age-matched mice the mean platelet count was 610 ± 90 × 10^3/μl (n = 8, range 500 × 10^3 to 740 × 10^3). Bleeding transgenic mice had a mean platelet count of 800 ± 260 × 10^3/μl (n = 4, range 460 × 10^3 to 1100 × 10^3). Two transgenic mice that were not bleeding had counts of 1000 × 10^3 and 2400 × 10^3/μl. Platelet numbers in both groups of trans-

Table 3. Thrombin-Mediated Clotting Times of Whole Blood Collected from 1-Day-Old Control and Line 1353-8 Transgenic Mice

Mouse	DNA Status[a]	Appearance	Clotting Time[b]
18-21	–	normal	17 s
18-22	+	GI/abdominal bleed	>30 min
18-23	+	intestinal bleed	>30 min
18-24	+	intestinal bleed	>30 min
18-25	+	intestinal bleed	>30 min
18-26	+	normal	>30 min
18-27	–	normal	15 s
18-28	–	normal	14 s
18-29	–	normal	15 s
18-30	+	normal	>30 min
18-31	–	normal	11 s
18-32	+	normal	>30 min

[a] Presence of uPA transgene was established by dot blot analysis of tail DNA.
[b] Whole-blood thrombin time; clotting times were measured with a stopwatch following addition of excess thrombin as described in Experimental Procedures.

genic animals were slightly increased relative to the controls, so platelet deficiency does not cause the bleeding phenotype.

To characterize clotting function in transgenic mice, we initially measured spontaneous clotting time. Whole blood from newborn nontransgenic mice placed on a glass slide at room temperature spontaneously clotted in 2 min. However, blood collected from line 1353-8 and 1944-6 neonates uniformly failed to clot even after 30 min (data not shown). We next determined thrombin-mediated clotting times. Because thrombin directly converts fibrinogen to fibrin, thrombin times provide a functional assay of blood fibrinogen. A prolonged thrombin time indicates either decreased fibrinogen or the presence of anticoagulants such as fibrin(ogen) degradation products. Whole-blood samples obtained from 1-day-old line 1353-8 littermates were mixed with excess thrombin on glass slides, and the clotting time was measured. A plasmin inhibitor, ε-amino-n-caproic acid, was included in assay mixtures to limit plasmin degradation of newly formed clots. The results (Table 3) indicate that blood collected from both bleeding and nonbleeding transgenic mice uniformly failed to clot even after extended incubation (>30 min), whereas nontransgenic littermates had clotting times of less than 20 s. To examine the possibility that absence of thrombin-mediated clot formation was a consequence of anticoagulant activity (e.g., fibrin(ogen) degradation products) rather than low fibrinogen, thrombin times were measured in 1:1 mixtures of blood from transgenic and control animals. Failure of mixed blood thrombin times to normalize indicates the presence of anticoagulants, since thrombin times are normal in blood with half-normal fibrinogen concentration. The thrombin times obtained in mixtures of transgenic and nontransgenic blood resembled control mouse values, indicating that clotting dysfunction was due, at least in part, to hypofibrinogenemia.

Because mice over 4 days of age do not hemorrhage, we determined thrombin clotting time in older animals to ascertain if they displayed restored clotting function. Thrombin times were measured for mice ranging in age from fetal day 18 to postnatal day 21 (Table 4). Remarkably, the absence of clotting function extended many days beyond the neonatal period in which animals display the bleeding phenotype. These results indicate that the decline in plasma plasminogen activator levels observed during the first days after birth is insufficient to restore clotting function. Some recovery of clotting function may develop after 1–3 weeks, as is suggested by the appearance of very loose clots in blood from single 8- and 16-day-old transgenic mice. However, it was not until mice reached 21 days of age that thrombin reproducibly induced clot formation. Thus, while the loss of clotting function likely predisposes animals to hemorrhage, this is apparently insufficient to cause the bleeding phenotype.

Because the functional assay indicated a deficit of plasma fibrinogen, fibrinogen mRNA and protein levels were examined in line 1353-8 mice. Total RNA extracts from the livers of transgenic and control neonates were analyzed by Northern blot hybridization using rat fibrinogen cDNA probes specific for the Aα Bβ, and γ chain mRNA species. Transgenic and age-matched control mice possessed similar mRNA levels for all three chains (Figure 5), indicating that hypofibrinogenemia in transgenic mice does not result from a decline in fibrinogen mRNA. Plasma fibrinogen was measured by Western blot analysis (Figure 6). Whole blood was analyzed to reduce sample handling time and decrease artifactual losses in vitro. Rabbit antiserum raised against rat fibrinogen was used to detect fibrinogen and fibrinogen-related antigen. The pattern of staining observed with control adult mouse

Table 4. Age-Dependent Thrombin-Mediated Clotting Times in Line 1353-8 Transgenic Mice

Age (Days)	No.[a]	Appearance	Clotting Time[b]
Fetal 18	3	normal	>30 min
Fetal 19	4	normal	>30 min
1	5	bleeding	>30 min
	8	normal	>30 min
4	1	bleeding	>30 min
	6	normal	>30 min
7–8	8	normal	>30 min
	1	normal	5–10 min[c]
10	4	normal	>30 min
12	1	normal	>30 min
14	4	normal	>30 min
16	2	normal	>30 min
	1	normal	10–15 min[c]
18	4	normal	>30 min
21	2	normal	20, 23 s[c]

[a] Total number of mice analyzed.
[b] Whole-blood thrombin time; clotting times were measured with a stopwatch following addition of excess thrombin as described under Experimental Procedures. Clotting times in nontransgenic littermate control mice were measured at each age and ranged from 30 s in fetuses (n = 8) to 5–20 s in 1- to 21-day-old mice (n = 69).
[c] Loose clots with fibrin tags.

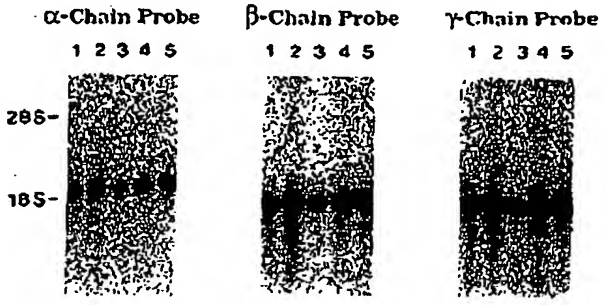

Figure 5. Northern Blot Analysis of Fibrinogen mRNA

Total RNA extracts from the livers of control and line 1353-8 transgenic mice were subjected to denaturing agarose gel electrophoresis (12 μg per lane), transferred to nitrocellulose, and hybridized to ^{32}P-labeled cDNA probes complementary to rat Aα (left), Bβ (middle), and γ (right) fibrinogen mRNA. Lanes 1, nontransgenic day 2 neonate; lanes 2, transgenic day 2 neonate not displaying bleeding phenotype; lanes 3, transgenic day 2 neonate displaying bleeding phenotype; lanes 4, nontransgenic day 6 neonate; lanes 5, transgenic day 6 neonate. The relative positions of the 28S and 18S ribosomal RNAs are indicated.

plasma was similar to that seen with purified rat fibrinogen. Three major bands were resolved that correspond to the known sizes of the Aα, Bβ, and γ chains of fibrinogen. The Bβ chain stained most heavily, suggesting that the most avid or abundant antibodies in the antiserum are specific for the Bβ chain. The fibrinogen chains were easily detected in blood from nontransgenic 2-day-old neonates, whereas little staining was observed in equal volumes of blood collected from transgenic neonates. We estimate that fibrinogen levels in these animals were 10%–20% of control values. Fibrinogen levels in bleeding animals were not appreciably different from those in nonbleeding, 2-day-old transgenic neonates. By day 6, the level of fibrinogen in transgenic mouse blood was about 30% of the level observed in a control day 6 mouse. This is consistent with earlier observations that as transgenic mice age, the plasma level of plasminogen activator declines and clotting function is slowly restored.

Discussion

Severe neonatal bleeding occurs with a high frequency in transgenic mice in which uPA gene expression is targeted to liver. Hepatocyte-specific uPA production results in elevated circulating uPA, fibrinogen depletion, and neonatal death in most mice that express the transgene. The commonly identified sites of bleeding in these mice are the abdominal cavity and the intestinal tract. Abdominal cavity bleeding may be secondary to perforation of an intestinal intramural hematoma or splenic rupture. While the reason for gastrointestinal tract involvement is uncertain, it is not due to local tissue transgene expression. Interestingly, similar episodes of gastrointestinal or intra-abdominal bleeding are frequently observed in human newborns with vitamin K deficiency (Oski, 1982) as well as in patients with hemophilia (Baehner and Strauss, 1966), von Willebrand's disease (Eichelberger and Randolph, 1986), thrombocytopenia (Eichelberger and Randolph, 1986), α2-AP deficiency (Kordich et al., 1985), and undergoing thrombolytic therapy (Rao, 1988). Thus, the gastrointestinal system appears profoundly vulnerable to disorders in the fibrinolytic and coagulation systems, and this sensitivity is reproduced in transgenic mice.

Two lines of Alb–uPA mice have been established in which about half of the transgenic offspring develop fatal bleeding. Bleeding always occurs during a 4 day window after birth; no animals experience a hemorrhagic event after this period even though their clotting times exceed 30 min. The incomplete penetrance of the bleeding phenotype in the two transgenic lines raises the question of what factors might contribute to the onset of bleeding. The variable occurrence of bleeding cannot be explained by quantitative differences in transgene expression or plasma plasminogen activator activity, since these parameters appeared relatively uniform in animals of any given age irrespective of phenotype. However, an age-dependent drop in transgene expression and plasma uPA levels and subsequent restoration of clotting function may partly explain

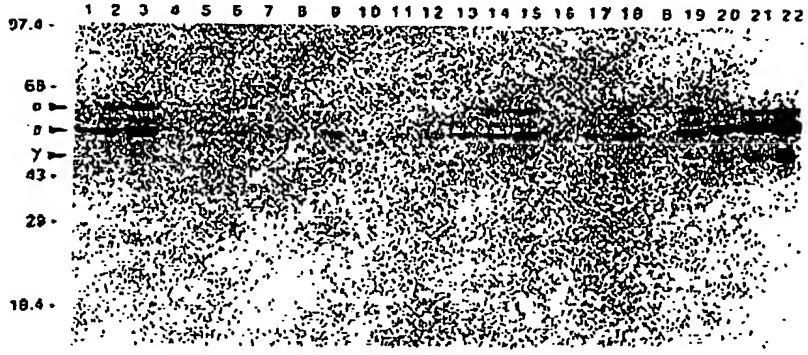

Figure 6. Western Blot Analysis of Whole-Blood Fibrinogen in Transgenic Neonates

Whole-blood samples collected from 1353-8 lineage transgenic mice and control mice were subjected to SDS–polyacrylamide gel electrophoresis. Fibrinogen was detected using a rabbit antiserum raised against rat fibrinogen using a Western blot procedure described in Experimental Procedures. Samples containing 0.02 μl, 0.04 μl, and 0.08 μl of whole blood were analyzed simultaneously for each mouse examined. Lanes 1–3, nontransgenic day 2 neonate; lanes 4–6, transgenic day 2 neonate with no apparent hemorrhaging; lanes 7–9, transgenic day 2 neonate with hemorrhaging into the gastrointestinal tract; lanes 10–12 transgenic day 2 neonate with hemorrhaging into the abdominal cavity; lanes 13–15, nontransgenic day 6 neonate; lanes 16–18, transgenic day 6 neonate; lane B, no sample applied; lane 19, 0.04 μl of plasma collected from nontransgenic adult; lane 20–22, 20, 40, and 60 ng of purified rat fibrinogen. The relative positions of the molecular weight standards phosphorylase B (97,400), bovine serum albumin (68,000), ovalbumin (43,000), carbonic anhydrase (29,000), and β-lactoglobulin (18,400) are indicated at left. α, fibrinogen Aα chain; β, fibrinogen Bβ chain; γ, fibrinogen γ chain.

the absence of hemorrhagic events in older animals and may contribute to the survival of individuals and maintenance of the lines. This loss of transgene expression occurred in both Alb–uPA lines generated, and thus is unlikely to be dependent on the site of transgene integration. The mechanism underlying this loss of expression is currently being investigated; this phenomenon has not been observed with other transgenes containing the albumin enhancer/promoter (E. P. S., unpublished data). The observation that blood from unaffected transgenic mice failed to clot spontaneously or in the presence of excess thrombin excludes differences in functional levels of plasminogen activator or inhibitors as the cause of phenotypic variability. Further evidence for the uniform activity of plasminogen activator was the severe depression of blood fibrinogen levels in all transgenic mice relative to age-matched controls, as measured by Western blot. Since plasminogen, fibrinogen, and transgene-encoded uPA would probably move down the same intracellular secretory pathway, plasminogen activation and plasmin-mediated fibrinogenolysis could potentially occur both within the hepatocyte prior to secretion and in the circulation. The loss of clotting function in fetal mice also argues that maternal inhibitors are not responsible for the absence of intrauterine hemorrhaging.

Because the initial response to loss of vascular integrity is vessel spasm and platelet plug formation, platelet deficiency could contribute to a bleeding event. Although platelet function was not assessed, platelet counts were, in fact, slightly increased in transgenic mice. The apparent increase in platelet number may represent reactive thrombocytosis, which is associated with metabolic stress, inflammation, or acute blood loss (Addiego et al., 1974). We also considered the syndrome of disseminated intravascular coagulation as a possible cause of bleeding in the mice. However, the absence of thrombocytopenia and the absence of thrombi within kidney microvasculature (data not shown) argue against this possibility. A third potential cause of bleeding was decreased coagulation factor synthesis secondary to transgene-mediated liver failure. However, total plasma protein levels were similar in control and transgenic mice (data not shown), and both groups displayed comparable levels of the liver-specific mRNA species encoding plasminogen and fibrinogen. Finally, a major dominant effect of genetic background on phenotype can be excluded because when transgenic line 1353-8 mice were backcrossed to either parental strain (C57BL/6 or SJL), both affected and unaffected transgenic offspring were obtained (data not shown). Additional backcrosses will be required to determine whether a more subtle genetic influence is present.

The nature of the critical characteristic that distinguishes those mice that bleed from those that do not thus remains uncertain. It is possible that microvascular trauma may result in hemorrhage in affected animals. The source of this trauma may be parturition, with associated pelvic transit and umbilical tearing, or the passage of material through the gastrointestinal tract. This concept is consistent with the absence of bleeding diatheses among fetuses. The observation that bleeding does not occur immediately at birth suggests that all transgenic neonates are protected for a brief period. This can be incorporated into the general framework of the trauma hypothesis. The formation of a platelet plug would act as the initial response to vascular injury, thus immediate bleeding could not occur. However, failure to stabilize the platelet plug with a fibrin clot would ultimately result in renewed and sustained bleeding. Failure to generate a clot could be caused by the decline of coagulation function that accompanies hypofibrinogenemia. This model proposes that the difference between bleeding and nonbleeding mice is happenstance trauma.

Regardless of cause, the variability of symptoms within litters of Alb–uPA transgenic mice is consistent with the phenotypic variation observed among humans with several disorders, specifically congenital deficiency of α2-AP (Aoki, 1989; Booth et al., 1983), congenital excess of plasminogen activator (Aoki, 1989; Booth et al., 1983), or the administration of plasminogen activator therapy (Rao, 1988). In these conditions, fibrin(ogen)olysis secondary to an increase in fibrinolytic system components leads to bleeding manifestations that include umbilical stump hemorrhage (Aoki, 1989), mucous membrane bleeding (Aoki, 1989; Miles et al., 1982), subcutaneous ecchymoses (Booth et al., 1983; Francis, 1989; Miles et al., 1982), hemarthroses (Aoki et al., 1979; Booth et al., 1983; Miles et al., 1982; Francis, 1989), GI bleeding (Rao, 1988), and/or central nervous system hemorrhage (Booth et al., 1983; Francis, 1989).

The transgenic lines described above provide an easily manipulated experimental system to examine events leading to hemorrhage due to hypofibrinogenemia from any cause. In particular, these animals may serve as in vivo models for the study of congenital and acquired disorders of fibrinolysis. This system can also be used to test clinical protocols for limiting the hemorrhagic complications now associated with use of plasminogen activators in the treatment of thrombotic disorders, including acute myocardial infarction. Finally, this study illustrates the utility of applying transgenic methodology to the investigation of the complex system of hemostasis in vivo.

Experimental Procedures

Construction of the Alb–uPA Fusion Gene and Production of Transgenic Mice

A 14.5 kb SalI fragment of cosMuPA-1 (Friezner-Degen et al., 1987), containing the entire murine uPA gene (~6.7 kb) as well as 7.5 kb of 5′-flanking sequence and 0.3 kb of 3′-flanking sequence was subcloned into the SalI site of pUC19. The plasmid was linearized at a unique EcoRV site located approximately 2.5 kb upstream of the site of transcription initiation and digested with exonuclease Bal31 under reaction conditions designed to limit cleavage to less than 3 kb. Synthetic KpnI linkers were added and the products circularized. One product plasmid (pPD-uPA5.2) had a KpnI linker introduced within exon 1 (position +43) and included the entire protein coding region. A derivative of pPD-uPA5.2 was subsequently prepared that eliminated all but 10 nucleotides downstream of the translation termination codon. To do this, a 5.75 kb KpnI–MaeIII fragment of pPD-uPA5.2 was isolated, the ends generated by MstII cleavage made blunt using the Klenow fragment of E. coli DNA polymerase, and then ligated into Bluescript (SK) (Stratagene) KpnI–HincII vector. The deleted 3′ noncoding and flanking sequences were replaced with 3′ noncoding and flanking sequences of the hGH gene using the following two-step procedure. First, a 627 bp SmaI–EcoRI fragment of the hGH gene (Seeburg, 1982)

containing 100 nucleotides of 3′ noncoding sequences and the polyadenylation site was subcloned into Bluescript EcoRV–EcoRI vector. Second, the hGH element was excised using flanking ClaI and SpeI polylinker sites and ligated into uPA gene body plasmid. The product plasmid (puPA-hGH) contained properly oriented uPA and hGH gene elements separated by 21 nucleotides of polylinker DNA.

The murine albumin enhancer/promoter was then joined to exon 1 of uPA using a three-step protocol. First, a unique NaeI site located in the Bluescript vector sequences of puPA-hGH (~320 upstream of the exon 1 KpnI linker) was converted to a unique NdeI site by introduction of a synthetic NdeI linker (product plasmid = puPA-hGH/Nde). Second, a derivative of the albumin gene was prepared that placed unique NdeI and KpnI sites upstream and downstream, respectively, of the critical enhancer/promoter elements. This was done by subcloning the 2.3 kb NheI–BamHI fragment of EB.Salb-hGH (Pinkert et al., 1987) into Bluescript XbaI–BamHI vector and then transferring the insert using the flanking SalI and BamHI sites to pUC18 HincII–BamHI vector (SalI ends were made blunt using T4 DNA polymerase). The product (pUC18-Alb[e/p]) contained a NdeI site located in pUC18 vector sequences ~225 nucleotides upstream of the enhancer/promoter element and contained a KpnI site located in polylinker sequences immediately downstream of the albumin transcription initiation site. Finally, the ~2.5 kb NdeI–KpnI fragment of pUC18-Alb(e/p) was isolated and subcloned into puPA-hGH/Nde NdeI–KpnI vector to produce the product (pAlb-uPA) illustrated in Figure 1. An 8.7 kb SalII fragment of pAlb-uPA was isolated and microinjected into fertilized mouse eggs for the generation of transgenic mice (Brinster et al., 1985). Transgenic pups were identified as previously described (Pinkert et al., 1987) using hGH-specific hybridization probes.

Tissue Collection

Mice of various ages were killed by decapitation, and whole blood was immediately collected into heparinized hematocrit tubes, then centrifuged for 5 min to separate plasma from cells. Plasma was retained and frozen in liquid nitrogen. The livers and occasionally additional tissues were exposed by dissection, and all or a portion of each was placed into foil and frozen in liquid nitrogen for subsequent analyses.

Isolation of Total Cellular RNA

Total RNA was isolated from mouse tissues by a modification of the guanidine isothiocyanate/CsCl centrifugation method of Chirgwin et al. (1979). Briefly, tissue fragments (100–500 mg) were ground with mortar and pestle under liquid nitrogen. The powder was homogenized in extraction buffer (2.5 ml) consisting of 25 mM sodium citrate (pH 7.0), 4 M guanidine isothiocyanate, 0.2 M β-mercaptoethanol, and 0.2% sarkosyl. Homogenates were transferred to SW60 ultracentrifuge tubes (Beckman) and underlaid with a 1 ml CsCl cushion (10 mM Tris–HCl [pH 7.5] containing 5.7 M CsCl and 0.1 M EDTA). RNA was pelleted by centrifugation at 35,000 rpm for 15 hr at 25°C. The RNA was resuspended in 10 mM Tris–HCl (pH 7.5), heated to 68°C for 3 min, ethanol precipitated, and finally dissolved in 100–200 μl of water. RNA concentrations were determined spectrophotometrically using an extinction coefficient of 20 at 260 nm for a 1 mg/ml solution.

Quantitative Solution Hybridization Assay of uPA mRNA

Transgene-derived uPA mRNA levels in total RNA extracts were established using a solution hybridization assay (Durnam and Palmiter, 1983) and a synthetic oligonucleotide probe (5′-TTATAGGACAAGGCTGGTGGGCACTGGAG-3′) complementary to the hGH portion of the Alb–uPA transgene. Oligonucleotide (8.5 pmol) was end labeled with [γ-^{32}P]ATP and T4 polynucleotide kinase to a specific activity of ~3000 Ci/mmol (Omitz et al., 1985) and isolated on a 12% acrylamide–urea gel (Omitz et al., 1985). The ^{32}P-labeled probe was eluted overnight at 37°C in 1.0 ml of 0.5 M ammonium acetate containing 1 mM EDTA, purified by chromatography on a NENSORB 20 cartridge (New England Nuclear), and redissolved in 1 mM Tris–HCl (pH 7.5) containing 0.5 mM EDTA and 0.1% SDS.

Hybridization mixtures (30 μl) contained test nucleic acids, 10,000 cpm ^{32}P-labeled probe, 20 mM Tris–HCl (pH 7.5), 0.6 M NaCl, 4 mM EDTA, 0.1% SDS, 20% formamide, and 10 ng of M13mp9 carrier DNA. The mixtures were covered with paraffin oil and incubated approximately 15 hr at 50°C. Hybridization was detected by digestion of unhybridized probe with S1 nuclease as described previously (Durnam and Palmiter, 1983), except that the reaction mixtures were incubated at 45°C. To convert hybridized radioactivity to molecules of transgene-derived uPA mRNA, a standard curve was established using recombinant M13mp19 single-stranded DNA containing the 627 bp SmaI–EcoRI element of the hGH gene incorporated into the chimeric Alb–uPA transgene. The average cellular uPA mRNA level was calculated using the known size of the M13 standard (7880 nucleotides) and the following values for the RNA content of neonatal mouse tissues: lung, 2.8 μg/10^8 cells; liver, 10.9 μg/10^8 cells; kidney, 6.1 μg/10^8 cells; intestine, 9.8 μg/10^8 cells. These RNA values were established as previously described (Baetge et al., 1988).

Zymographic Analysis of Plasminogen Activator in Plasma

Plasma samples were placed in sample buffer containing 2% SDS, 60 mM Tris–HCl (pH 6.8), 10% glycerol, and 0.002% bromophenol blue. Proteins were electrophoretically fractionated on nonreducing SDS–acrylamide (12.5%) gels (Laemmli, 1970) cast with 0.4% nonfat dry milk and 20 μg/ml human plasminogen. The gels were washed twice for 30 min in 2.5% Triton X-100 and then incubated for 16 hr at 37°C in 0.1 M glycine (pH 8.0). The caseinolytic activity was detected by staining the gel for 2 hr in 10% acetic acid, 15% isopropanol, 0.1% amido black and destaining in 10% acetic acid, 20% methanol.

Western Blot Immunodetection of Fibrinogen

Samples of whole blood (5 μl) were collected from decapitated mice and dispensed into 195 μl of 60 mM Tris–HCl (pH 6.8) containing 2% SDS, 0.7 M β-mercaptoethanol, 0.004% bromophenol blue, and 10% glycerol (elapsed time <10 s). The samples were heated to 100°C for 5 min to denature and reduce proteins and then serially diluted in sample buffer to final concentrations of 0.08, 0.04, and 0.02 μl whole blood per 20 μl. The proteins present in 20 μl aliquots were fractionated by SDS–polyacrylamide gel (10% acrylamide) electrophoresis (Laemmli, 1970) and then electrophoretically transferred (250 mA for 15 hr at 4°C) to Immobilon (Millipore) using a Transphor (Hoefer) blotting cell and a Tris–glycine buffer system (25 mM Tris, 192 mM glycine, 0.1% SDS, 20% methanol). Fibrinogen was detected using a rabbit antiserum raised against rat fibrinogen (kindly provided by R. F. Doolittle, University of California, San Diego) and the Vectastain ABC (Vector) avidin–biotin peroxidase staining system. Briefly, blots were incubated 2 hr at room temperature in buffer A (20 mM Tris–HCl [pH 7.5] containing 0.15 M NaCl, 0.2% Tween-20 (Sigma), and 10% nonfat dry milk) and then incubated an additional 2 hr at room temperature in fibrinogen antiserum diluted 1:500 in buffer A. The membranes were extensively washed in buffer A and transferred to buffer A containing 7.5 μg/ml affinity-purified biotinylated goat anti-rabbit immunoglobulin antibody (Vector). After a 1 hr incubation, the membranes were washed extensively in buffer A and then rinsed briefly in buffer A lacking nonfat dry milk. The membranes were incubated for 1 hr at room temperature with the avidin–biotin peroxidase complex formed by combining 100 μl each of Vectastain reagents A and B in 10 ml of buffer A lacking nonfat dry milk. Finally, the blots were washed extensively in buffer A, rinsed in 20 mM Tris–HCl (pH 7.5), 0.15 M NaCl, and stained in 100 mM Tris–HCl (pH 7.5) containing 0.8 mg/ml diaminobenzidine, 0.4 mg/ml $NiCl_2$, and 0.01% H_2O_2.

Northern Blot Analysis

Total RNA samples were electrophoretically fractionated on denaturing agarose gels and blotted onto BA85 nitrocellulose filters (Schleicher and Schuell) as described previously (Bell et al., 1990). Filters were prehybridized for 2 hr at 60°C in 5× SSC containing 0.04% Ficoll 400, 0.04% bovine serum albumin, 0.04% polyvinylpyrrolidine (1× SSC = 15 mM sodium citrate [pH 7.5], 0.15 M NaCl). Hybridization reactions were carried out for 15 hr at 60°C in prehybridization solution (10 ml) containing 1 mM EDTA, 0.5% SDS, and 10 × 10^6 cpm heat-denatured ^{32}P-labeled (Feinberg and Vogelstein, 1983) rat fibrinogen cDNA probes (specific activity 2–4 × 10^8 cpm/μg). The fibrinogen Aα, Bβ, and γ chain probes (kindly provided by G. Crabtree, Stanford University) were the 1.4 kb PstI fragment of pαFib, the 1.2 kb PstI fragment of pβFib$_2$, and the 1.7 kb PstI fragment of pγFib1, respectively (Crabtree and Kant, 1981). Blots were removed from hybridization mixtures, washed extensively at 60°C in 5× SSC, 0.5% SDS, and exposed to Kodak X-Omat XAR-5 film at −70°C with intensifying screens.

Clotting Time Measurement

Blood (20 µl) was collected from a decapitated mouse in a disposable plastic pipette tip and was mixed with 5.2 µl of a solution of thrombin (Sigma) and ε-amino-n-caproic acid (Sigma) on a glass slide, such that the final concentration of thrombin was 80 U/ml and that of the acid was 0.24 M. Clotting time was measured with a stopwatch, the endpoint being loss of free fluid motion and formation of a visible clot. Samples were monitored for 30 min. For blood mixing studies, 8 µl of transgenic and 8 µl of nontransgenic mouse blood were mixed together with 2 µl of thrombin solution on a glass slide, such that the final thrombin concentration was 120 U/ml, and clotting time was measured. This value was compared with clotting times of individual blood samples collected from the same mice and assayed as described above.

Platelet Counts

Whole blood (10 µl) was collected from a decapitated mouse and added to 1 or 4 ml of a 1% ammonium oxalate solution to lyse red blood cells. Platelets were counted in a hemacytometer.

Acknowledgments

We are grateful to Dr. Russell F. Doolittle (University of California, San Diego) for his constructive suggestions and providing fibrinogen antiserum and purified rat fibrinogen. We thank Dr. Gerald R. Crabtree (Stanford University) for providing cDNA clones encoding all three chains of rat fibrinogen. We gratefully acknowledge Janice Hagedorn for her assistance in preparing the manuscript. This work was supported by National Institutes of Health grants to J. L. D. (CA44611), R. D. P. (HD09172), and R. L. B. (CA38635). J. L. H. is a fellow of the William Cooper Procter Research Scholar Program at the Children's Hospital of Cincinnati and a recipient of an American Cancer Society Career Development Award (CDA89-134). E. P. S. is a fellow of the Veterinary Medical Scientist Training Program at the University of Pennsylvania.

The costs of publication of this article were defrayed in part by the payment of page charges. This article must therefore be hereby marked "*advertisement*" in accordance with 18 U.S.C. Section 1734 solely to indicate this fact.

Received April 16, 1990; revised May 24, 1990.

References

Addiego, J. E., Mentzer, W. C., and Dallman, P. R. (1974). Thrombocytosis in infants and children. *J. Pediatr. 85*, 805–807.

Aoki, N. (1989). Hemostasis associated with abnormalities of fibrinolysis. *Blood Rev. 3*, 11–17.

Aoki, N., Morai, M., Sakata, Y., Yoshida, N., and Matsuda, M. (1978). Abnormal plasminogen. A hereditary molecular abnormality found in a patient with recurrent thrombosis. *J. Clin. Invest. 63*, 877–884.

Aoki, N., Saito, H., Kamiya, T., Kaie, K., Sakata, Y., and Kabakura, M. (1979). Congenital deficiency of α2-plasmin inhibitor associated with severe hemorrhagic tendency. *J. Clin. Invest. 63*, 877–884.

Aoki, N., Sakata, Y., Matsuda, M., and Tateno, K. (1980). Fibrinolytic status in a patient with congenital deficiency of α-2-plasmin inhibitor. *Blood 55*, 483–488.

Aznar, J., Estellés, A., Vila, V., Regañón, E., España, F., and Villa, P. (1984). Inherited fibrinolytic disorder due to an enhanced plasminogen activator level. *Thromb. Haemost. 52*, 198–200.

Baehner, R. L., and Strauss, H. S. (1966). Hemophilia in the first year of life. *N. Engl. J. Med. 275*, 524–528.

Baetge, E. E., Behringer, R. R., Messing, A., Brinster, R. L., and Palmiter, R. D. (1988). Transgenic mice express the human phenylethanolamine N-methyltransferase gene in adrenal medulla and retina. *Proc. Natl. Acad. Sci. USA 85*, 3648–3652.

Bell, S. M., Brackenbury, R. W., Leslie, N. D., and Degen, J. L. (1990). Plasminogen activator gene expression is induced by the *src* oncogene product and tumor promoters. *J. Biol. Chem. 265*, 1333–1338.

Booth, N. A., Bennett, B., Wijngaards, G., and Grieve, J. H. K. (1983). A new life-long hemorrhagic disorder due to excess plasminogen activator. *Blood 61*, 267–275.

Brinster, R. L., Chen, H. Y., Trumbauer, M. E., Yagle, M. K., and Palmiter, R. D. (1985). Factors affecting the efficiency of introducing foreign DNA into mice by microinjecting eggs. *Proc. Natl. Acad. Sci. USA 82*, 4438–4442.

Chirgwin, J. M., Przybyla, A. E., MacDonald, R. J., and Rutter, W. J. (1979). Isolation of biologically active ribonucleic acid from sources enriched in ribonuclease. *Biochemistry 18*, 5294–5299.

Collen, D., and Lijnen, H. R. (1987). Fibrinolysis and the control of hemostasis. In The Molecular Basis of Blood Diseases, G. Stamatoyannopoulos, A. W. Nienhuis, P. Leder, and P. W. Majerus, eds. (Philadelphia: W. B. Saunders Co.), pp. 662–688.

Crabtree, G. R., and Kant, J. A. (1981). Molecular cloning of cDNA for the α, β, and γ chains of rat fibrinogen. *J. Biol. Chem. 256*, 9718–9723.

Danø, K., Andreasen, P. A., Grøndahl-Hansen, J., Kristensen, D., Nielsen, L. S., and Skriver, L. (1985). Plasminogen activators, tissue degradation, and cancer. *Adv. Cancer Res. 44*, 139–265.

Das, P. C., and Cash, J. D. (1969). Fibrinolysis at rest and after exercise in hepatic cirrhosis. *Br. J. Haematol. 17*, 431–443.

Durnam, D. M., and Palmiter, R. D. (1983). A practical approach for quantitating specific mRNAs by solution hybridization. *Anal. Biochem. 131*, 385–393.

Eichelberger, M. R., and Randolph, J. G. (1986). Abdominal trauma. In Pediatric Surgery, K. J. Welch, J. G. Randolph, M. M. Ravitch, J. A. O'Neill, and M. I. Rowe, eds. (Chicago: Yearbook Medical Publishers, Inc.), pp. 145–174.

Feinberg, A. P., and Vogelstein, B. (1983). A technique for radiolabelling DNA restriction endonuclease fragments to high specific activity. *Anal. Biochem. 132*, 6–13.

Francis, R. B. (1989). Clinical disorders of fibrinolysis: a critical review. *Blut 59*, 1–14.

Friezner-Degen, S., Heckel, J., Reich, E., and Degen, J. L. (1987). The murine urokinase-type plasminogen activator gene. *Biochemistry 26*, 8270–8279.

Girolami, A., Marafioti, F., Rubertelli, M., and Cappellato, M. G. (1986). Congenital heterozygous plasminogen deficiency associated with a severe thrombotic tendency. *Acta Haematol. 75*, 54–57.

Grainick, H. R., and Abrell, E. (1973). Studies of the procoagulant and fibronolytic activity of promyelocytes in acute promyelocytic leukemia. *Br. J. Haematol. 24*, 89–99.

Imaoka, S., Veda, T., Shibata, H., Masaoka, T., Ogawa, M., Sasaki, Y., Iwanaga, T., and Terasawa, T. (1985). Fibrinolysis in patients with acute promyelocytic leukemia and disseminated intravascular coagulation during heparin therapy. *Cancer 56*, 1738–1738.

Kazama, M., Tahara, C., Suzuki, Z., Gohchi, K., and Abe, T. (1981). Abnormal plasminogen, a case of recurrent thrombosis. *Thromb. Res. 21*, 517–522.

Kluft, C., Nieuwenhuis, H. K., Rijken, D. C., Groeneveld, F., Wijngaards, G., van Berkel, W., Dooijewaard, G., and Sixma, J. J. (1987). Alpha-2-antiplasmin Enschede: a dysfunctional alpha-2-antiplasmin molecule, associated with an autosomal recessive hemorrhagic disorder. *J. Clin. Invest. 80*, 1391–1400.

Kordich, L., Feldman, L., Porterie, P., and Lago, O. (1985). Severe hemorrhagic tendency in heterozygous α2-antiplasmin deficiency. *Thromb. Res. 40*, 845–851.

Laemmli, U. K. (1970). Cleavage of structural proteins during the assembly of the head of bacteriophage T4. *Nature 227*, 680–685.

Lottenberg, R., Dolly, F. R., and Kitchens, C. S. (1985). Recurring thromboembolic disease and pulmonary hypertension associated with severe hypoplasminogenemia. *Am. J. Hematol. 19*, 181–193.

Marder, V. J., and Sherry, S. (1988). Thrombolytic therapy: current status. *N. Engl. J. Med. 318*, 1512–1520.

Miles, L. A., Plow, E. F., Donnelly, K. J., Hougie, C., and Griffin, J. H. (1982). A bleeding disorder due to deficiency of α-2-antiplasmin. *Blood 59*, 1246–1257.

Ornitz, D. M., Palmiter, R. D., Hammer, R. E., Brinster, R. L., Swift, G. H., and MacDonald, R. J. (1985). Specific expression of an elastase-human growth hormone fusion gene in pancreatic acinar cells of transgenic mice. *Nature 313*, 600–602.

Oski, F. A. (1982). Blood coagulation and its disorders in the newborn. In Hematologic Problems in the Newborn, F. A. Oski, and J. L. Naiman, eds. (Philadelphia: W. B. Saunders Co.), pp. 137–174.

Pellman, C., Aldion, H. C., and Phillips, L. L. (1966). Manifestation and management of hypofibrinogenemia and fibrinolysis in patients with carcinoma of the prostate. J. Urol. 96, 375–379.

Pinkert, C. A., Ornitz, D. M., Brinster, R. L., and Palmiter, R. D. (1987). An albumin enhancer located 10 kb upstream functions along with its promoter to direct efficient, liver-specific expression in transgenic mice. Genes Dev. 1, 268–276.

Rao, A. K. (1988). Thrombolysis in myocardial infarction (TIMI) trial-phase I: hemorrhagic manifestations and changes in plasma fibrinogen and the fibrinolytic system in patients treated with recombinant tissue plasminogen activator and streptokinase. J. Am. Coll. Cardiol. 11, 1–11.

Saksela, O., and Rifkin, D. B. (1988). Cell-associated plasminogen activation: regulation and physiological functions. Annu. Rev. Cell Biol. 4, 93–126.

Sane, D. C., Pizzo, S. V., and Greenberg, C. S. (1989). Elevated urokinase-type plasminogen activator level and bleeding in amyloidosis: case report and literature review. Am. J. Hematol. 31, 53–57.

Seeburg, P. H. (1982). The human growth hormone gene family: nucleotide sequences show recent divergence and predict a new polypeptide hormone. DNA 1, 239–249.

Tagnon, H. J. (1952). Fibrinolysis in metastatic cancer of the prostate. Cancer 5, 9–12.

Van Slyck, E. J., Raman, S. B. K., and Janakiraman, N. (1989). Primary fibrinolysis in acute monocytic leukemia. Henry Ford Hosp. Med. J. 37, 33–38.

Note Added in Proof

The two Alb-uPA transgenic mice described in this paper have been assigned the following genetic designations: 1353-8,Tg(Alb-1,Plau)Bri-44; 1944-6,Tg(Alb-1,Plau)Bri45.

Dixon, in (37)] with the following modifications: Fusion proteins were bound to glutathione agarose, and the recombinant portion was eluted for 30 min in 10 ml of 50 mM tris (pH 8.0), 150 mM NaCl, 2.5 mM $CaCl_2$, and 0.1% β-mercaptoethanol with thrombin (4 μg ml^{-1}). Phenylmethylsulfonyl fluoride (0.6 mM) was added to the protein elution, and the sample concentrated to 0.5 ml. The protein was further purified by gel filtration on a Superose 12 sizing column (Pharmacia, Piscataway, NJ) in HBS-T20 buffer. Control preparations were prepared identically from lysates expressing only the GST protein.

39. SPR detection experiments were performed with the BIAcore apparatus (Pharmacia Biosensor). All protein immobilizations were performed in 25 mM acetate buffer (pH 4.0), 15 mM NaCl, 0.05% Tween-20. The carboxylated dextran matrix of the flow cell was first activated with 1-ethyl-3-(3-dimethylaminopropyl)carbodiimide and *N*-hydroxysuccinimide, which allowed the subsequent cross-linking of injected protein through primary amine groups [B. Johnsson *et al.*, *Anal. Biochem.* 198, 268 (1991)]. After the protein was cross-linked to the flow cell, the reactive groups were blocked by the injection of an excess of primary amines, 1 M ethanolamine (pH 8.5). Data for BIAcore SPR detection experiments were collected at 5 Hz. All binding was done in HBS-T20 buffer at room temperature.
40. We thank R. Granzow and J. Pevsner for critical support and discussions and S. Bajjaleh for editorial reading of the manuscript. Supported by the National Institute of Mental Health (R.H.S.). N.C. is a Medical Scientist Training Program trainee funded by the National Institute of General Medical Sciences.

17 November 1993; accepted 10 January 1994

Replacement of Diseased Mouse Liver by Hepatic Cell Transplantation

Jonathan A. Rhim, Eric P. Sandgren,* Jay L. Degen, Richard D. Palmiter, Ralph L. Brinster†

Adult liver has the unusual ability to fully regenerate after injury. Although regeneration is accomplished by the division of mature hepatocytes, the replicative potential of these cells is unknown. Here, the replicative capacity of adult liver cells and their medical usefulness as donor cells for transplantation were investigated by transfer of adult mouse liver cells into transgenic mice that display an endogenous defect in hepatic growth potential and function. The transplanted liver cell populations replaced up to 80 percent of the diseased recipient liver. These findings demonstrate the enormous growth potential of adult hepatocytes, indicating the feasibility of liver cell transplantation as a method to replace lost or diseased hepatic parenchyma.

Despite its highly specialized function, the liver is unique in its capacity to regenerate, even within the adult organism. The primary model of this process, two-thirds partial hepatectomy in the rat, has allowed investigation of molecular events that underlie the regenerative process (*1*). While much has been learned about liver regeneration, many questions regarding the proliferative capacity of adult liver cells remain. After partial hepatectomy, much of the lost liver mass is restored by the division of fully differentiated hepatocytes (*1*, *2*). However, because only one to two rounds of hepatocellular division are required to restore the liver mass after partial hepatectomy, the extent of the regenerative capacity of hepatocytes is unknown. Certain pathological processes may reflect a finite capacity for hepatocyte replication. In gene therapy protocols, in which therapeutic genes are delivered to the liver via genetically modified hepatocytes, expression of the introduced gene declines over time (*3*, *4*). This diminution of gene expression may be due to gradual loss of the modified cells because of a limited capacity to divide, either as a result of an inherent restriction in their replicative potential or as a result of changes acquired during their manipulation in culture, and is an especially serious problem given the very low colonization of host liver (less than 1%) that has been achieved in experimental models using hepatocellular transplantation (*3*–*5*). Finally, in conditions of severe liver injury, restoration of liver mass may be primarily accomplished not by hepatocytes but by the expansion of hepatocyte precursors (stem cells) that subsequently differentiate into hepatocytes. The existence of liver stem cells, their replicative potential, and their role in liver regeneration remain controversial (*6*, *7*).

We recently described a model of liver regeneration in albumin-urokinase (Alb-uPA) transgenic mice [TgN(Alb1Plau)-144Bri, TgN(Alb1Plau)145Bri], in which hepatocyte-targeted expression of a hepatotoxic transgene creates a functional liver deficit (*8*) resulting in a chronic stimulus for liver growth. Because of the stimulus for liver growth present in these mice, a small number of hepatic cells in young mice that stochastically delete the deleterious transgene are selectively expanded. Each cell gives rise to a clone of hepatocytes that forms a nodule (*8*). By 8 to 12 weeks of age, transgenic mouse livers have been completely replaced by the nodular, clonal growth of these transgene-deficient cells (referred to as "red nodules"). The observation that the regenerating nodules in these livers were composed of normal appearing hepatocytes suggested that mature hepatocytes may indeed possess considerable replicative capacity. However, we could not rule out the possibility that the progenitor cells of these nodules, instead of being hepatocytes, were actually undifferentiated cells with a much greater replicative capacity than the hepatocytes to which they gave rise. Furthermore, even if nodule progenitor cells were hepatocytes, they were of fetal or early postnatal origin; cells at this stage display a much higher mitotic index than the adult hepatocytes, which are of greatest interest biologically and medically.

To determine the replicative capacity of adult liver cells, we transplanted cells isolated from adult mouse livers into Alb-uPA transgenic mice, then studied their growth. Marking of donor cells at the genetic level can be accomplished with retroviral transduction of hepatocytes (*9*), but for our studies we wished to avoid methods that might alter the replicative potential of the cells or mark only subpopulations of liver cells. We therefore transplanted cells freshly isolated from two groups of transgenic mice. The first, EL-*myc* [TgN(Ela1Myc)159Bri], carried the rat elastase enhancer-promoter fused to the mouse *c-myc* structural gene (*10*). This transgene is not expressed in liver; however, there are approximately nine copies per cell, facilitating detection of donor hepatocyte DNA within recipient livers. This lineage is congenic in C57BL/6 (B6). Second, we generated B6 donor transgenic mouse lines that carried the mouse metallothionein-I gene promoter plus flanking sequences fused to a modified β-galactosidase (β-gal) structural gene (MT-*lacZ*) (*11*). The protein product of this transgene is targeted to the cell nucleus as a result of the presence of the SV40 large T-antigen nuclear localization signal peptide. The MT promoter is active in liver of transgenic mice, and its expression can be induced up to 10-fold by administration of heavy metal

J. A. Rhim, Department of Animal Biology, School of Veterinary Medicine, University of Pennsylvania, Philadelphia, PA 19104, USA, and Department of Pathology and Laboratory Medicine, University of Pennsylvania School of Medicine, Philadelphia, PA 19104, USA.
E. P. Sandgren and R. L. Brinster, Department of Animal Biology, School of Veterinary Medicine, University of Pennsylvania, Philadelphia, PA 19104, USA.
J. L. Degen, Children's Hospital Research Foundation and Department of Pediatrics, University of Cincinnati College of Medicine, Cincinnati, OH 45229, USA.
R. D. Palmiter, Howard Hughes Medical Institute and Department of Biochemistry, University of Washington SL-15, Seattle, WA 98195, USA.

*Present address: Department of Pathobiological Sciences, School of Veterinary Medicine, University of Wisconsin–Madison, Madison, WI 53706, USA.
†To whom correspondence should be addressed.

tions (12). β-Galactosidase activity can be visibly detected with the synthetic substrate 5-bromo-4-chloro-3-indolyl-β-D-galactoside (X-gal).

Two MT-*lacZ* lineages (containing the transgene at different genomic locations) were established and designated 4560-2 [TgN(MTnlacZ)203Bri] and 4580-2 [TgN-(MTnlacZ)204Bri]. After induction with cadmium and incubation with X-gal (13), transgenic livers were stained homogeneously blue. Microscopic examination revealed β-gal activity localized to hepatocyte nuclei (Fig. 1A).

For all transplantation experiments, liver cell suspensions were freshly prepared by two-step EDTA-collagenase perfusion (14), then centrifuged twice at 50*g* to enrich for hepatocytes. Cellular viability ranged from 50 to 85% as measured by trypan blue exclusion. Each suspension was kept on ice and transferred within 2 hours. Approximately 80 to 85% of the cells in the preparations were hepatocytes morphologically; however, small nonhepatocytic cells were also present (Fig. 1B).

In the hemizygous Alb-uPA transgenic mice used in our experiments, the regenerative stimulus is present as long as transgene-expressing liver remains, for ~6 to 8 weeks after birth. Thus, to optimize assessment of cellular replicative ability, cells must be transferred into transgenic recipients as soon after birth as possible. Donor cells were introduced into the spleen of mice within the first 2 weeks of life (15). Recipient mice were generally maintained for an additional 4 to 6 weeks and killed; livers were then analyzed for the presence of donor cells and their progeny.

In two initial experiments, ~10^4 liver cells isolated from adult El-*myc* transgenic mice were injected into spleens of 5- to 11-day-old Alb-uPA recipients. Four to 6 weeks later, the recipients were killed and their livers removed and analyzed by polymerase chain reaction and Southern (DNA) blot hybridization. All six recipient mice transplanted with adult El-*myc* cells displayed evidence of donor cells in one or more portions of liver. Phosphoimage analysis of Southern blots indicated that, in some liver samples, more than 50% of the cells were donor-derived (16). In contrast, no signal was observed in livers of similarly treated control mice lacking the Alb-uPA transgene. Given that individual samples examined were often greater than 2.0 mm^3 in size and contained many more cells than the total number transplanted, these results strongly suggested that extensive donor cell expansion occurred within recipient liver.

To determine both the extent and pattern of colonization of donor cells and their progeny in the recipient livers, we injected donor cells harvested from liver of adult

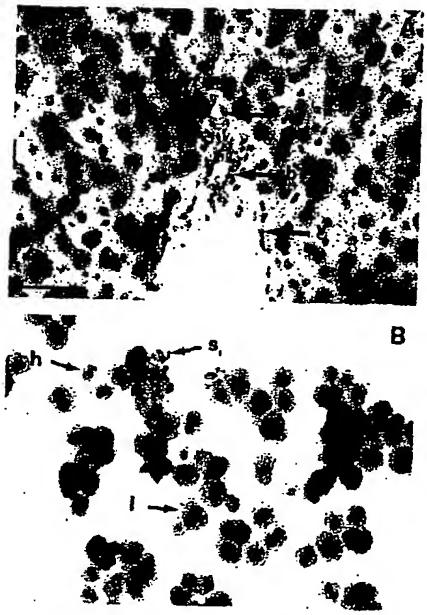

Fig. 1. X-gal staining of MT-*lacZ* donor liver after cadmium induction. A frozen section (A) or a liver cell suspension (B) from MT-*lacZ* transgenic liver was stained with X-gal (13) and counterstained with nuclear fast red. In the frozen section (A), a portal triad is shown containing an arteriole (a), a bile duct (b), and a vein (v). Hepatocyte nuclei show strong X-gal staining. Neither biliary cell nor endothelial cell nuclei had any detectable β-gal activity; they are stained red. Scale bar, 40 μm. In the cell preparation (B), over 80% of the cells are hepatocytes (l); they are large, round to polygonally shaped cells with abundant cytoplasm and one or two centrally placed nuclei. In most hepatocytes the β-gal activity is confined to the nucleus; in others, the activity is also present within the cytoplasm. A few hepatocytic cells showed no evidence of β-gal activity (h); their nuclei stained red. In addition to hepatocytes, other cells with smaller nuclei, less cytoplasm, and no evidence of β-gal activity were also present (s). We found that the location and intensity of X-gal staining in hepatocytes varied with different fixation protocols for cell suspensions. Staining was much more uniform and predictable in frozen sections where variation in intensity appeared related primarily to the plane of section relative to the hepatocyte nucleus.

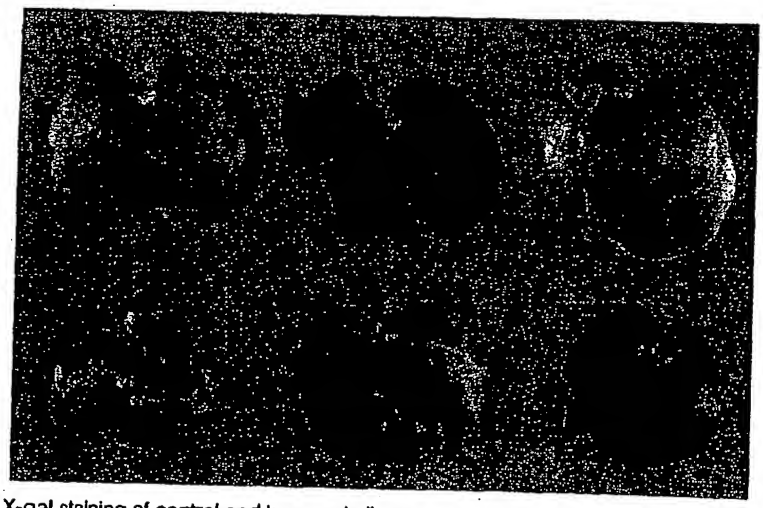

Fig. 2. X-gal staining of control and transgenic livers transplanted with MT-*lacZ* cells. Livers from a nontransgenic control (top, left), an MT-*lacZ* positive control (top, center), a control mouse lacking the Alb-uPA transgene transplanted with MT-*lacZ* cells (top, right), and three livers from Alb-uPA transgenic mice receiving MT-*lacZ* cells (bottom) were stained with X-gal after cadmium induction. Unstained liver represents red areas of endogenous cells (r) that had lost transgene expression as well as residual transgene-expressing white parenchyma (w). No gross blue staining was detected in the nontransgenic liver transplanted with MT-*lacZ* cells (top, right).

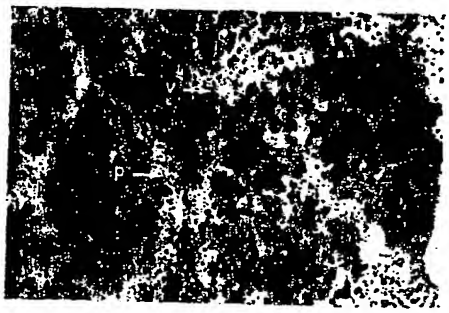

Fig. 3. Histology of Alb-uPA transgenic liver receiving MT-*lacZ* cells. A frozen section of Alb-uPA transgenic liver transplanted with MT-*lacZ* cells 4.5 weeks previously was incubated with X-gal and counterstained with nuclear fast red. The liver parenchyma was almost completely replaced by MT-*lacZ* hepatocytes, nearly all of which displayed intense nuclear blue staining with little variation among cells. The MT-*lacZ* cells have become associated with portal triads, central veins, and sinusoidal cells. Biliary nuclei from a portal area (p), endothelial nuclei from a central vein (v), and sinusoidal cell nuclei were stained red. A small residual area of transgene-expressing liver is seen in the lower right corner of the figure.

MT-*lacZ* mice into spleens of 10-day-old Alb-uPA mice. Transgenic recipients were administered cadmium 4 to 5 weeks after transplant, then killed, and their livers stained with X-gal. No gross blue staining was present in livers of control recipients lacking the Alb-uPA transgene (Fig. 2, top right). Microscopic examination of these livers did show single isolated blue cells (*16*). In contrast, large areas of blue staining, comprising up to 80% of the liver, were readily apparent on gross examination of transgenic recipient livers (Fig. 2, bottom), indicating that the donated MT-*lacZ* cells had expanded substantially. Microscopically, the blue stained areas were composed of hepatocytes with blue nuclear staining (Fig. 3). Examination of the spleens of recipient animals showed no evidence of donated liver cells (*16*).

Close inspection of chimeric livers revealed that the growth of the transplanted cells was nodular (Fig. 2). The apparently solid blue areas were themselves composed of several thousand confluent blue nodules. The nodules were of markedly uniform size (Table 1). This uniformity of donor nodule size contrasts with the much greater size variation of endogenous (transgene-deficient) red nodules identified in two of the mice (Table 1), caused by either the variable onset of growth of red nodules in these mice or by a difference in the growth potential of red nodule progenitor cells.

The nodular appearance of the donor-derived cells suggested that they, like their transgene-deficient endogenous counterparts, grew by clonal expansion at the expense of the surrounding diseased, transgene-expressing liver. By comparing the volume of a blue nodule to the volume of a blue cell, the number of cells comprising the nodule can be calculated. Using this result, one can determine the number of cell doublings required to form the nodule (*17*), assuming that blue nodules are derived from the expansion of one progenitor cell. On the basis of these calculations, the progenitor cells appear mitotically equivalent (Table 1, last column); that is, each gave rise to approximately the same number of descendants during the 4.5-week in vivo incubation period. Thus, donated liver cells underwent extensive growth within the transgenic liver, dividing at least 12 times. Reconstitution of an entire liver from one hepatocyte would require 28 cell doublings.

The growth of transgenic livers transplanted with MT-*lacZ* cells was appropriately regulated. By 6 weeks after transplant, the liver weight to body weight ratio of transgenic recipients was no different than that of nontransgenic controls (*16*). In addition, the livers of older animals were not grossly enlarged. No tumors have been observed in animals up to 6 months after transplantation.

To assess the functional competency of Alb-uPA/MT-*lacZ* chimeric livers, we performed two experiments. First, the blood concentrations of albumin, total protein, and bilirubin, molecules whose concentration is dependent on hepatic sufficiency, were compared in recipient and control mice; the values were similar (*16*). Second, a sensitive test of liver cell function and adequacy is the mitotic index of hepatocytes after injury or loss of liver mass (*1*). Therefore, Alb-uPA/MT-*lacZ* chimeric livers of 49-day-old mice were subjected to two-thirds partial hepatectomy, and the mitotic index was determined 44 hours later (the time of peak mitotic activity in mouse hepatocytes). We also determined the responses of donor and endogenous liver present in the same mouse, thus providing an internal control to eliminate variation between animals. The overall mitotic response of the Alb-uPA/MT-*lacZ* chimeric livers (including both donor and endogenous areas) was elevated compared to non-

Table 1. Donor and endogenous nodule size. Nodule diameter was measured from X-gal–stained livers of three Alb-uPA mice transplanted with MT-*lacZ* cells in each of two separate experiments by means of a dissecting microscope equipped with a calibrated measuring reticle. Fifty donor cell–derived (blue) nodules were measured from each liver. Twenty spontaneously arising, endogenous nodules (unstained) were measured in two livers. Note the large standard deviation in endogenous nodule size compared to that of donor nodules. The number of donor cell doublings needed to generate a nodule of average size was calculated for each animal by determining the number of MT-*lacZ* cells within the nodule and assuming that each nodule was clonally derived (*17*).

Experiment number	Percentage of liver replaced	Type of nodules measured	Average nodule diameter ± SD (mm)	Average doublings per donor cell
1	5	Donor	0.70 ± 0.24	14
	40	Donor	0.50 ± 0.15	12
	80	Donor	0.64 ± 0.16	13
		Endogenous	1.25 ± 1.08	16
3	30	Donor	0.56 ± 0.15	13
		Endogenous	1.26 ± 1.02	16
	60	Donor	0.57 ± 0.18	13
	70	Donor	0.52 ± 0.11	12

Table 2. Fraction of transplanted liver cells giving rise to recipient liver nodules. MT-*lacZ* liver cells were injected intrasplenically into day 10 Alb-uPA transgenic pups. After 32 days the livers were stained with X-gal and the number of blue nodules calculated by dividing the volume of the replaced portion of liver by the volume of the average blue nodule (*19*). Each nodule was assumed to be clonally derived (*8*). In experiments 2 and 3 and in a separate experiment, nontransgenic pups were injected with MT-*lacZ* cells. Their livers were removed after 3 days, stained with X-gal, and the number of MT-*lacZ* cells determined and used to calculate the seeding efficiency (number of cells detected in nontransgenic recipient livers divided by the number of viable cells injected into the spleen) of the liver. The efficiencies were as follows: experiment 2, 0.1 to 1.2% ($n = 2$); experiment 3, 3.5 to 17.0% ($n = 3$); and additional experiment, 2.0 to 6.4% ($n = 2$). Because only a small fraction of the injected cells reach the liver, the calculated percentage of injected cells giving rise to nodules (shown in the last column) is likely to significantly underestimate the fraction of injected cells capable of giving rise to nodules.

Experiment number	Viable cells injected	Recipient animal	Percentage of liver replaced	Number of nodules per recipient liver	Percentage of injected cells giving rise to nodules
1	120,000	1	5	400	0.3
		2	40	3300	2.8
		3	80	6500	5.4
2	88,000	1	5	400	0.5
		2	70	5700	6.5
		3	70	5700	6.5
3	75,000	1	30	2400	3.2
		2	60	4900	6.5
		3	70	5700	7.6
4	170,000	1	50	4100	2.4
		2	60	4900	2.9
		3	70	5700	3.4

transgenic control livers (1.5 ± 0.4%, n = 3, and 0.7 ± 0.1%, n = 2, respectively), possibly reflecting the regenerative state of the transgenic livers. Hepatocytes of donor (1.6 ± 0.3%, n = 3) and endogenous (1.4 ± 0.6%, n = 3) origin within transgenic host liver responded nearly identically to this test of regenerative function.

By comparing the number of blue nodules in the recipient liver to the number of injected cells, it is possible to estimate the fraction of cells with extensive growth potential within the donor cell population. Of 12 animals from four separate experiments, the percentage of injected cells giving rise to blue nodules ranged from 0.3 to 7.6% (Table 2). These percentages strongly support the conclusion that hepatocytes were the progenitors of at least some of the blue nodules, since 0.3%, and certainly 7.6%, is an unreasonably high frequency for a distinct class of cells with unique replicative potential (that is, stem cells). Although there were nonparenchymal contaminant cells within our donor cell preparations (Fig. 1B), it is very unlikely that this population of cells would be selectively taken up by the recipient liver and account for all of the blue nodules. Indeed, the percentage of adult hepatocytes that can function as nodule progenitor cells is most likely appreciably higher than 7.6% considering that the percentage of injected cells reaching the livers of seven control mice evaluated over three experiments never exceeded 17.0% (Table 2, legend).

We have shown that progeny of nonautologous transplanted adult liver cells can replace almost the entire mouse hepatic parenchyma because of the substantial replicative capacity of the mature hepatocyte. On the basis of our results, we propose that transplanted adult hepatocytes can undergo at least 12 cell doublings and still retain the ability to respond to partial hepatectomy with one or two additional divisions. Although we cannot rule out the possibility that the progenitor cells of the nodules represent a subpopulation of hepatocytes, we note that, should such subpopulations exist, our model is ideal for determining their replicative potential.

Our findings suggest that preparation of a donor cell population will not be the principal difficulty facing medical use of hepatic cell transplantation; rather, success is likely to depend on provision of a suitable internal environment in which transplanted cells can survive and grow. Transgene-expressing Alb-uPA hepatocytes are at a growth disadvantage compared to regenerating transgene-deficient liver (8) and are apparently also functionally compromised, since a strong hepatic growth environment is present in Alb-uPA liver despite a normal hepatic mass (8). However, hepatic architecture and the complement of liver cells (including endothelium, biliary epithelium, Kupffer cells, and Ito cells) remain relatively normal. Thus, in young Alb-uPA recipients, the physical microenvironment is permissive for survival and function of transplanted cells, while the functional deficit of endogenous hepatocytes stimulates the subsequent expansion of this donor cell population. These characteristics of the model suggest it will be extremely valuable to test the replicative potential of various cell donor populations, including hepatocytes manipulated for gene therapy.

Our findings have several medical implications. First, immediate transplantation of currently available human liver cell populations may save patients with fulminant hepatic failure where liver architecture is preserved (18). Second, the approach of transplanting genetically engineered hepatocytes to correct a metabolic defect appears likely to succeed as long as a suitable microenvironment for growth of these cells can be provided. Finally, Alb-uPA mice backcrossed onto an immunodeficient genetic background should accept xenogeneic cell transplants and could in principle be reconstituted with human liver cells. Thus, this approach of cell transplantation into Alb-uPA mice can also be used to characterize the regenerative potential of human liver cell populations and to study the biology of human hepatocytes within an intact liver in a controlled experimental setting.

REFERENCES AND NOTES

1. N. Fausto, In *Hepatology, A Textbook of Liver Disease*, D. Zakim and T. D. Boyer, Eds. (Saunders, Philadelphia, ed. 3, 1990), pp. 49–65; G. K. Michalopoulos, *FASEB J.* 4, 176 (1990).
2. Although some investigators believe that hepatocytes are not all at the same maturational stage and that multiple subpopulations of hepatocytes exist that may differ in their growth properties, we will follow the convention accepted by the majority of investigators who believe hepatocytes are best thought of as one mature population. Therefore, we use "hepatocyte" to refer to "liver parenchymal cells."
3. J. W. Wilson *et al.*, *Proc. Natl. Acad. Sci. U.S.A.* 87, 8437 (1990).
4. M. A. Kay *et al.*, *Ibid.* 89, 89 (1992).
5. K. P. Ponder *et al.*, *Ibid.* 88, 1217 (1991).
6. N. Fausto, N. L. Thompson, L. Braun, In *Cell Separation: Methods and Selected Applications*, T. G. Pretlow and T. P. Pretlow, Eds. (Academic Press, New York, 1987), vol. 4, pp. 45–77.
7. S. Sell, *Cancer Res.* 50, 3811 (1990); S. H. Sigal, S. Brill, A. S. Florino, L. M. Reid, *Am. J. Physiol.* 263, G139 (1992).
8. E. P. Sandgren *et al.*, *Cell* 66, 245 (1991).
9. D. Armentano, A. R. Thompson, G. Darlington, S. L. C. Woo, *Proc. Natl. Acad. Sci. U.S.A.* 87, 6141 (1990); J. M. Wilson, D. E. Johnston, D. M. Jefferson, R. C. Mulligan, *ibid.* 85, 4421 (1988).
10. E. P. Sandgren, C. J. Quaife, A. G. Paulovich, R. D. Palmiter, R. L. Brinster, *Ibid.* 88, 93 (1991).
11. The MT-*lacZ* transgene is composed of the mouse metallothionein-I gene promoter and flanking DNA fused to the bacterial *lacZ* gene encoding β-gal with a nuclear localization sequence. The mouse metallothionein-I gene promoter (−588 to +68) was fused to the nuclear *lacZ* construct with protamine I intron and 3′-untranslated region described previously [E. H. Mercer, G. W. Hoyle, R. P. Kapur, R. L. Brinster, R. D. Palmiter, *Neuron* 7, 703 (1991)]. This gene was then inserted into the Eco RI site of the MT 5′/3′ vector that carries 10 kb of sequence flanking the MT-II gene and 7 kb flanking the MT-I gene that have been shown to enhance expression of several genes [R. D. Palmiter, E. P. Sandgren, D. M. Koeller, R. L. Brinster, *Mol. Cell. Biol.* 13, 5266 (1993)]. These flanking sequences contain deoxyribonuclease-hypersensitive sites that appear to be important for enhanced expression.
12. R. D. Palmiter, H. Y. Chen, R. L. Brinster, *Cell* 29, 701 (1982).
13. To induce expression of the MT-*lacZ* transgene, we injected mice intraperitoneally with 1 mg of Cd^{2+} per kilogram of body weight at 20 hours and 6 hours before the mice were killed. β-Galactosidase activity was detected with X-gal as described [E. H. Mercer, G. W. Hoyle, R. P. Kapur, R. L. Brinster, R. D. Palmiter, *Neuron* 7, 703 (1991)], except that frozen sections were fixed in 0.5% glutaraldehyde in phosphate-buffered saline for 30 min at 4°C before incubation with X-gal.
14. J. E. Klaunig *et al.*, *In Vitro* 17, 913 (1981).
15. Liver cell suspensions were introduced into 10-day-old mice by intrasplenic injection. Mice were anesthetized by inhalation of methoxyflurane (Metofane). The spleen was exteriorized through a small left flank incision. A 30-gauge needle stabilized by a micromanipulator was introduced into the spleen, and the chilled cell suspension was slowly injected in a volume of 5 to 10 μl. The spleen was then gently returned to the abdominal cavity and the abdominal musculature and skin sutured. The mice were allowed to recover overnight before being returned to their mother. Mice were housed and maintained in accordance with the institutional animal care and use committee guidelines of the University of Pennsylvania.
16. J. A. Rhim, E. P. Sandgren, J. L. Degen, R. D. Palmiter, R. L. Brinster, unpublished data.
17. Providing that each nodule is clonally derived, the number of cell doublings can be calculated on the basis of the number of MT-*lacZ* cells within a nodule. For the average blue nodule with a diameter of 0.58 mm (representing the average of all the nodule diameters shown in Table 1), the volume is 0.102 mm^3. For an average blue hepatocyte with a diameter of 0.03 mm, the volume is 0.000014 mm^3. Therefore, the number of blue cells in the average nodule equals the volume of a whole nodule divided by the volume of a blue hepatocyte = 7300 cells per average nodule. The number of cell doublings needed to give 7300 cells is 2^n = 7300, or n = 13.
18. E. A. Jones and D. F. Schafer, In *Hepatology, A Textbook of Liver Disease*, D. Zakim and T. D. Boyer, Eds. (Saunders, Philadelphia, ed. 3, 1990), pp. 460–492.
19. The average mass of a 6-week-old Alb-uPA/MT-*lacZ* chimeric liver is approximately 0.83 g, with a volume of approximately 830 mm^3. The volume of the average blue nodule is 0.102 mm^3 (*17*). The number of blue nodules in a completely replaced liver equals the volume of the whole liver divided by the volume of the average nodule = 8100 nodules. In a 70% replaced liver, the number of blue nodules is 8100 × 0.70 = 5700.

20. We are grateful to G. Michalopoulos, N. Fausto, J. Klaunig, M. DeFrances, T. Baker, and J. Wu for helpful suggestions on adult mouse liver cell preparations. We thank M. Avarbock, K. Clegg, and N. Jensen for technical assistance and C. Pope for secretarial help. Supported in part by National Institutes of Health grants HD-23857 to R.L.B. and HD-09172 to R.D.P. and by a National Grant-in-Aid (92-1103) from the American Heart Association with funds contributed in part by the AHA, Ohio affiliate (J.L.D.). This study was done during the tenure of an Established Investigatorship (93002570) from the American Heart Association (J.L.D.). J.A.R. is a resident in pathology at the University of Pennsylvania School of Medicine.

17 September 1993; accepted 4 January 1994

Cell, Vol. 66, 245–256, July 26, 1991, Copyright © 1991 by Cell Press

Complete Hepatic Regeneration after Somatic Deletion of an Albumin–Plasminogen Activator Transgene

Eric P. Sandgren,* Richard D. Palmiter,† Janice L. Heckel,‡ Cynthia C. Daugherty,‡ Ralph L. Brinster,* and Jay L. Degen‡
*Laboratory of Reproductive Physiology
School of Veterinary Medicine
University of Pennsylvania
Philadelphia, Pennsylvania 19104
†Howard Hughes Medical Institute
and Department of Biochemistry
University of Washington
Seattle, Washington 98195
‡Children's Hospital Research Foundation
and Department of Pediatrics
University of Cincinnati College of Medicine
Cincinnati, Ohio 45229

Summary

We previously demonstrated that expression of an albumin–urokinase-type plasminogen activator (Alb–uPA) fusion construct in transgenic mice resulted in elevated plasma uPA concentration, hypofibrinogenemia, and neonatal hemorrhaging. Two lines of Alb–uPA mice were established in which only one half of the transgenic pups died at birth; surprisingly, plasma uPA concentrations in survivors gradually returned to normal by 2 months of age. The basis for this phenomenon is DNA rearrangement within hepatocytes that affects the transgene tandem array and abolishes transgene expression. Transgene-deficient cells selectively proliferate relative to surrounding liver, and this process culminates in replacement of the entire liver by clonal hepatic nodules derived from transgene-deficient progenitor cells. In some cases as few as two nodules can reconstitute over 90% of liver mass, highlighting the remarkable regenerative capacity of individual liver cells.

Introduction

Transgenic mouse technology has provided the means to create and analyze models of genetic diseases affecting virtually any organ to which transgene expression can be directed (reviewed in Jaenisch, 1988; Hanahan, 1989). Because of its involvement in many diseases of medical importance, the liver has been a frequent target for this type of analysis. Among transgenes reported to be associated with liver lesions are those encoding growth hormone, which alters hepatocyte size and nuclear characteristics (Quaife et al., 1989); oncogenes, which induce hepatic tumors (Messing et al., 1985; Held et al., 1989; Sandgren et al., 1989; Sepulveda et al., 1989); the hepatitis B virus large envelope polypeptide, which induces hepatocellular necrosis and carcinoma formation in adults (Chisari et al., 1985, 1987, 1989); transforming growth factor α, which causes both tumors and excessive liver growth (Sandgren et al., 1990; Jhappan et al., 1990); and a variant form of α_1-antitrypsin (AAT), which reproduces some characteristics of AAT deficiency disease in humans, including neonatal and adult hepatitis (Dycaico et al., 1988; Carlson et al., 1989).

Because of the liver's large synthetic and secretory capability, targeting transgene expression to this organ also serves as a way to determine the systemic influence of overproduction of biologically potent molecules. We previously used this approach to study the consequences of inappropriate plasminogen activator expression in vivo by introducing into mice a transgene bearing the urokinase-type plasminogen activator (uPA) coding sequence fused to the albumin enhancer/promoter (Heckel et al., 1990). Plasminogen activators catalyze the proteolytic cleavage and activation of plasminogen to plasmin, which in turn degrades fibrin clots (Collen and Lijnen, 1987). uPA also has been implicated in biological processes involving tissue remodeling or destruction, including ovulation, mammary gland involution, and metastasis (Danø et al., 1985; Collen and Lijnen, 1987; Saksela and Rifkin, 1988). We predicted that expression of the albumin–uPA fusion construct (Alb–uPA) might disrupt hemostasis through the plasmin intermediate either by inducing rapid breakdown of fibrin clots or direct fibrinogenolysis. As expected, in many transgenic founder mice this construct directed high-level uPA expression to hepatocytes, resulting in elevated plasma uPA and fatal hemorrhaging in newborns. Two lines of Alb–uPA transgenic mice were established from surviving founder mice that expressed lower levels of uPA. In these lines, about half of the transgenic neonates bled into either intestine or abdomen and died within 4 days of birth, whereas the remaining transgenic offspring appeared normal and survived. Transgenic fetuses and both bleeding and nonbleeding transgenic neonates displayed marked hypofibrinogenemia and unclottable blood, and we concluded that any injury sufficient to initiate bleeding was rapidly fatal in affected mice (Heckel et al., 1990).

A general expectation in experiments of this type is that transgene expression will be stable over time in targeted cells. Unexpectedly, surviving mice in both of the Alb–uPA lines showed a gradual decrease in the level of plasma uPA activity accompanied by a restoration of clotting function that was complete between 1 and 2 months of age (Heckel et al., 1990; E. P. S., unpublished data). Production of uPA, when directed by the albumin enhancer/promoter, should persist for as long as hepatocytes remain functional, so we were curious to understand the basis of this unusual phenotype. We now report that uPA is cytotoxic for hepatocytes and that inactivation of transgene expression by DNA rearrangement in isolated hepatocytes is followed by repopulation of the entire liver by cells that no longer produce uPA.

Figure 1. Gross Appearance of Alb–uPA Transgenic Mouse Liver

Livers were removed from 5-week-old male mice. The liver to the left is from a nontransgenic control mouse, that in the center from a hemizygous line 1353-8 transgenic mouse, and that to the right from a homozygous line 1353-8 transgenic mouse. Note the large red nodules in the hemizygote's liver and their absence from the homozygote's liver.

Results

Transgene Expression Is Hepatotoxic

It was immediately apparent upon inspection of the liver of 3- to 5-week-old Alb–uPA transgenic mice that this organ was profoundly abnormal. The liver consisted of smooth, pale to nearly white tissue (hereafter referred to as "white liver") surrounding multiple reddish nodules ranging from less than 1 mm to over 1 cm in diameter (Figure 1). The same gross features were present in each of two independently generated lines of Alb–uPA transgenic mice, indicating that this phenomenon is unrelated to the site of transgene integration. Livers of younger transgenic mice tended to be uniformly pale, and red foci were not grossly visible in mice under 1 week of age. By 6–8 weeks, the entire liver was composed of confluent red nodules, and in some mice as few as two or three large nodules comprised the majority of the liver mass. These findings suggested that the white areas represented original transgenic liver tissue and that postnatal changes in some aspect of liver function or development had given rise to red nodular growths that eventually replaced white parenchyma.

Microscopic examination of fixed liver revealed two cellular populations. The first, occupying red areas, contained variably sized but otherwise normal hepatocytes that displayed occasional mitotic figures and that were mildly disorganized in relation to vascular sinusoids (compare Figures 2A and 2B). The second, occupying white areas, contained small hepatocytes with prominent cytoplasmic vacuolization (Figure 2B). A few individual hepatocytes in white areas showed evidence of degeneration, although large foci of necrosis were not observed. There was no histological indication of hepatic fibrosis or compromised circulation in white portions of the liver, but osmicated tissue sections demonstrated the presence only in white tissue of an increased amount of fat (data not shown), a possible contributor to the pallor. At the red–white interface, red areas often seemed to be compressing surrounding white areas, suggesting that red foci were expanding. Once the process of expansion was complete, livers composed of confluent red nodules did not appear to retain any white parenchyma.

White and red liver tissue from transgenic mice of several ages were examined further by electron microscopy. In 1-month-old mice, hepatocytes from red nodules resembled normal hepatocytes in nontransgenic liver (compare Figures 3A and 3B with 3C and 3D). Hepatocytes from the white areas showed progressive degenerative changes with fragmentation and disintegration of the most severely affected cells. Cytoplasm of intact hepatocytes contained varying numbers of membrane-limited, electron-lucent, single or multivesicular bodies in a finely granular matrix, and they were often lined at the cytoplasmic face by ribosomes, suggesting an origin from rough endoplasmic reticulum (RER) (Figures 3E and 3F). Although their exact chemical composition is unknown, the multivesicular bodies may represent compartmentalization of substances whose progression through the ER has been disrupted. Other organelles appeared normal until the onset of cellular degeneration.

Matings were established between transgenic mice to generate homozygotes that carried two copies of the transgene array, and these mice provided the first clinical evidence for a deleterious effect of hepatic uPA expression in adult mice. Between 3 and 6 weeks of age, most homozygotes developed severe edema and subsequently died. At necropsy, their livers were pale and displayed few or no grossly visible red nodules (Figure 1, right). Examination of blood chemistry from these mice was consistent with a diagnosis of liver insufficiency (Table 1). Most significantly, serum total protein and albumin concentrations were re-

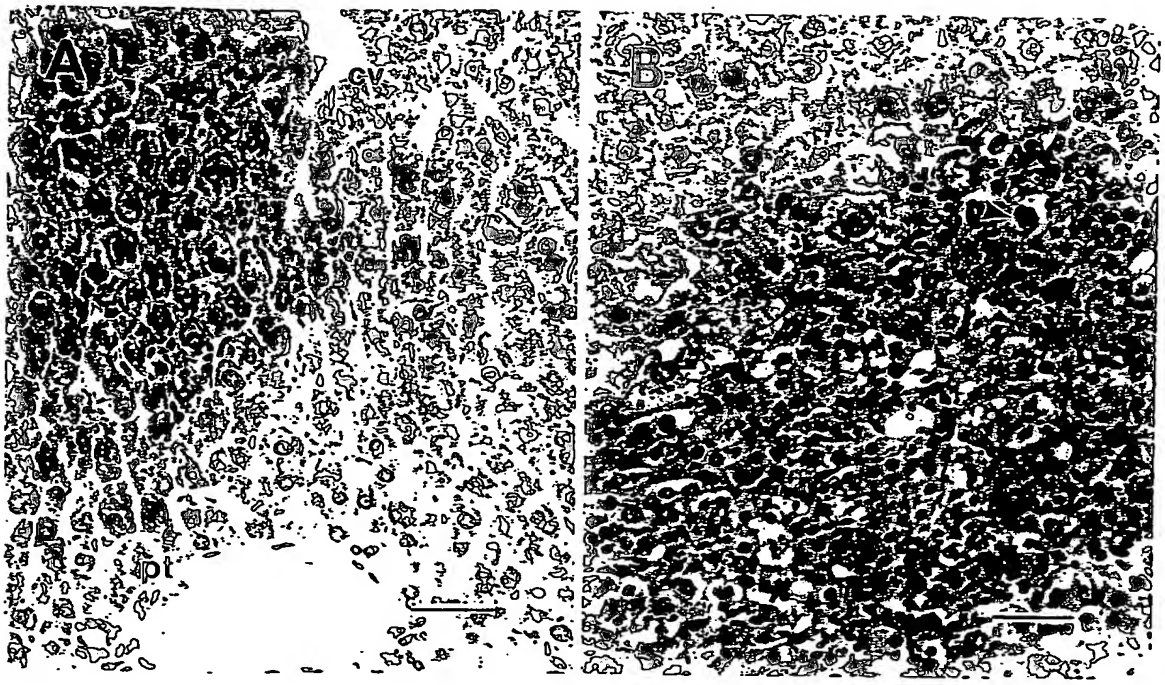

Figure 2. Histopathology of Alb–uPA Transgenic Mouse Liver

(A) Liver from a 4.5-week-old nontransgenic control mouse. The photograph spans a lobule. Note the uniform size and arrangement of the hepatocytes.

(B) Liver from a 4.5-week-old hemizygous line 1353-8 transgenic mouse spanning a red–white interface. Note the disarrayed hepatocytes of variable size in the red area (above). Hepatocytes in the white area (below) are generally small and often show fine cytoplasmic vacuolization. Eosinophilic, necrotic hepatocytes are present (arrowhead).

cv, central vein; pt, portal tract; arrowhead, necrotic hepatocyte; bar, 33 μm.

duced at least 4-fold, and the resulting loss of vascular oncotic pressure would be sufficient to produce edema. The level of circulating uPA was also reduced at least 4-fold relative to neonates, although it remained greater than in hemizygotes of the same age (Figure 4). Given that plasma uPA levels are elevated for several weeks before the development of edema, the reduction of plasma proteins (other than plasminogen and fibrinogen) is not likely due to proteolysis. Furthermore, we did not detect an increase in urine protein in these mice (data not shown), suggesting that the cause of low serum protein is decreased hepatic production. The serum concentration of the enzyme alanine aminotransferase, a marker of hepatocellular damage (Stolz and Kaplowitz, 1990), was mildly elevated, probably reflecting continued focal hepatocyte death. Interestingly, plasma bilirubin was not increased (Table 1). In the liver, bilirubin is conjugated with glucuronates and then excreted into bile. Homozygous mouse livers maintain this important metabolic function, indicating different sensitivities of the bile and protein secretory pathways to transgene toxicity. All values remained normal in hemizygotes (Table 1). Approximately 20% of homozygotes survived for more than 2 months. Microscopic examination of fixed liver sections indicated a greater density of red foci than typically observed in the livers of homozygous mice exhibiting liver failure (data not shown). We believe that these mice must possess a sufficient number of healthy hepatocytes within red foci to avoid excessively low plasma protein concentration.

Transgene expression was measured in both red nodules and white liver parenchyma to determine the relationship between uPA production and the two types of liver tissue. Surprisingly, while white tissue continued to express high levels of uPA mRNA, all samples from red nodules lacked detectable transgene expression (Table 2). The levels of albumin and plasminogen mRNAs in red liver were the same as controls (Table 2), indicating that the unexpected lack of transgene expression was not due to a general effect on liver-specific gene expression. In contrast, the levels of albumin and plasminogen mRNAs were reduced slightly in white liver compared with red nodules or control liver samples from nontransgenic mice (Table 2). One interesting exception was α-fetoprotein production, which was actually increased in white liver relative to red nodules by 5- to 20-fold (Table 2). Production of α-fetoprotein has similarly been reported to increase in response to certain liver toxins, such as CCl_4 (4-fold increase) or ethionine administered in a choline-deficient diet (40-fold increase) (see Fausto, 1990). It therefore appears that loss of uPA expression is correlated with enhanced hepatic growth and a return to normal cellular morphology and function in red liver.

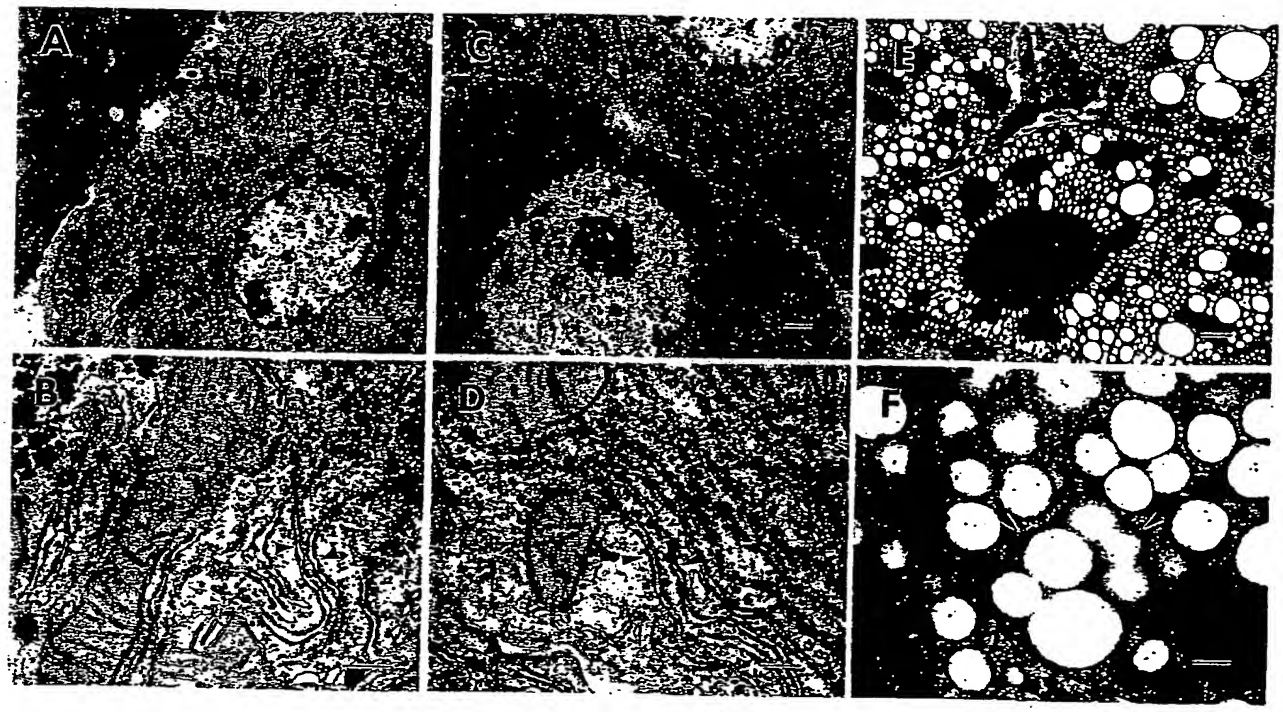

Figure 3. Ultrastructure of Alb–uPA Transgenic Mouse Liver

(A) Low magnification of a hepatocyte from a 4.5-week-old nontransgenic control mouse.

(B) High magnification detail of control hepatocyte cytoplasm. Note the lamellar nature of the RER (arrowheads) and the generally narrow RER lumens.

(C) Low magnification of a red focus hepatocyte from a 4.5-week-old line 1353-8 transgenic mouse.

(D) High magnification detail of red focus hepatocyte cytoplasm. Ultrastructural features closely resemble those of the control mouse. Arrowheads indicate RER.

(E) Low magnification of a white area hepatocyte from the mouse pictured in (C) and (D). Note the vacuolated appearance of the hepatocyte cytoplasm.

(F) High magnification detail of white area hepatocyte cytoplasm. The ER, often decorated by ribosomes (arrowheads), is distended by single or multiple electron-lucent vacuoles or vesicles surrounded by a finely granular, faintly fibrillar material.

Low magnification bar, 1 μm; high magnification bar, 0.25 μm.

Development of Clonal Hepatic Nodules Accompanies Stochastic Transgene Loss

Two general mechanisms could account for loss of transgene expression in red nodules. The first consists of modifications of transgene expression in trans, such as changes in concentration of trans-acting factors that influence transgene expression. The second consists of modifications in cis, including covalent modifications such as methylation, which inactivate transgene transcription, and mutations, ranging from point mutations to gross rearrangements. Loss of a positive trans-acting factor would be expected to reduce or eliminate endogenous albumin transcription, which was not observed. Furthermore, the number of transgene copies in homozygous mouse livers is only doubled, yet the reduction of red nodule development in these livers is extreme, arguing against specific trans-mediated inhibition of transgene expression as an explanation of the

Table 1. Blood Chemistry in Line 1353-8 Mice

Mice	Total Protein (g/dl)	Albumin (g/dl)	Bilirubin (mg/dl)	Alanine Aminotransferase (U/L)
Adult controls	5.0 ± 0.2 (7)	2.2 ± 0.1 (7)	0.2 ± 0.0 (5)	40 ± 11 (4)
Hemizygotes	5.0 ± 0.6 (6)	2.3 ± 0.2 (6)	0.5 ± 0.3 (4)	64 ± 23 (3)
Homozygotes (with edema)	<1.2 ± 0.3 (5)	<0.5 ± 0.2 (5)	0.2 ± 0.1 (7)	142 ± 33 (5)*

Data are presented as mean ± SD; the number of mice analyzed is given in parentheses. Mice were 4–6 weeks old when samples were collected. The lower limit of sensitivity of the automated clinical analyzer for total protein was 1.0 g/dl, and for albumin it was 0.4 g/dl. Individual values reported as <1.0 or <0.4 were assumed to equal 1.0 or 0.4 for purposes of these calculations.

* Excludes a high result (693 U/L) from one analyzed mouse.

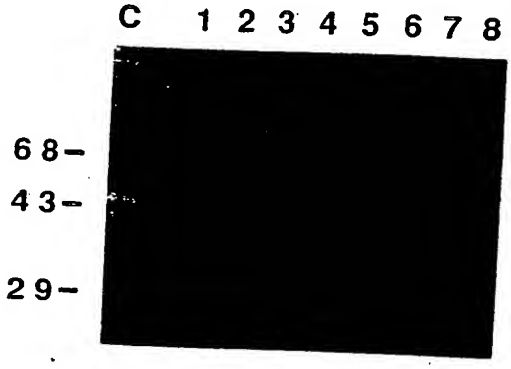

Figure 4. Plasma Plasminogen Activator Concentration in Alb–uPA Transgenic Mice

Zymographic analysis of plasminogen activator activity levels in plasma (0.5 μl) of 1-month-old nontransgenic (lanes 1 and 2), line 1353-8 hemizygous transgenic (lanes 3–5), and line 1353-8 homozygous transgenic mice (lanes 6–8). Plasma sample (0.5 μl) shown in lane C was collected from a 2-day-old line 1353-8 transgenic mouse displaying the bleeding phenotype. Note that the plasma concentration of uPA in homozygotes is greater than in hemizygotes, yet is still reduced at least 4-fold relative to newborn transgenic mice (lane C). For a description of the zymographic assay, see Experimental Procedures. The relative migration of the molecular weight standards, BSA (68,000), ovalbumin (43,000), and carbonic anhydrase (29,000), is indicated at the left margin.

phenotype. To identify possible cis-acting changes in the transgene array, we isolated white and red tissue samples from hemizygotes and measured their transgene DNA content by Southern blot analysis (Figure 5A). The blot was simultaneously hybridized with two probes, one that detects the transgene and one that detects the endogenous *Hox-1.4* gene, which serves as a control for DNA loading. In Figure 5A, DNA was digested with KpnI, which cuts once within the transgene. In each sample this generated a band of about 9 kb, the size of the injected DNA, plus additional faint bands that probably correspond to junction fragments. The presence of the band of unit transgene length suggests that the transgene integrated as a tandem head-to-tail repeat, as is usually the case in transgenic mice. The band at 11 kb corresponds to the *Hox-1.4* locus. Note that all red liver samples from both line 1353-8 and line 1944-6 mice show reduced hybridization of the transgene probe relative to the respective white liver sample or an unaffected tissue such as kidney; this indicates that loss of transgene DNA accompanies loss of transgene expression and red nodule development.

The residual transgene signal in red tissue could reflect either a remnant of the transgene array that remained in hepatocytes after an internal deletion, or it could represent the intact transgene array present in unaffected cells within the tissue, such as endothelial and Kupffer cells. To distinguish between these possibilities, DNA from red nodules and white parenchyma of hemizygous mice in each line was digested with enzymes that do not cut within the transgene. Transgene deletion by intrachromosomal recombination within the tandem array should generate a lower molecular weight band that might be detected if the trangene array happened to be flanked closely by restriction sites. Alternatively, complete deletion of the transgene array in hepatocytes but not nonhepatocytes should change only the hybridization intensity but not its pattern. Preliminary experiments with four enzymes (EcoRV, BglI, ApaI, and NdeI) did not reveal lower molecular weight bands in DNA from line 1944-6 red nodules after electrophoresis through a 0.7% agarose gel. However, both EcoRV and BglI revealed a lower molecular weight band in DNA from red nodules of a line 1353-8 mouse.

These experiments suggested that DNA rearrangement could be involved in transgene inactivation, at least in line 1353-8 liver. To examine this hypothesis in a liver cell population largely free of nonhepatocytes and to determine the frequency of transgene rearrangements, we isolated hepatocytes from five individual red nodules following collagenase perfusion of livers from four mice (see Experimental Procedures). DNA from these cells was digested with KpnI or EcoRV and analyzed by Southern blotting as before. When digested with KpnI, hepatocyte DNA from each nodule displayed the band of unit transgene length that was reduced in intensity relative to kidney (Figure 5C). When digested with EcoRV, hepatocyte DNA from four of the red nodules displayed a low molecular

Table 2. Gene Expression in Alb–uPA Mice

Mice (n)	Liver Sample	mRNA uPA (m/c)[a]	mRNA Plasminogen (m/c)[a]	Albumin (% Adult Control)	α-Fetoprotein (% Neonate Control)
Adult control (2)	Nontransgenic	<10	620 ± 220[b]	100 ± 6	<0.1
Neonate control (2)	Nontransgenic	—	—	—	100 ± 16
Line 1944-6 (4) (hemizygous)	White	660 ± 160	220 ± 50	44 ± 17	1.9 ± 0.8
	Red	<10	300 ± 50	93 ± 26	0.1 ± 0.2
Line 1353-8 (3) (hemizygous)	White	470 ± 90	240 ± 110	43 ± 22	2.1 ± 0.3
	Red	<10	690 ± 180	81 ± 11	0.3 ± 0.3
Line 1353-8 (5) (homozygous)	White	518 ± 141	278 ± 82	37 ± 14	4.6 ± 2.5

[a] m/c = molecules per cell, calculated as described in Experimental Procedures.
[b] Data are presented as mean ± SD. The number of samples analyzed is given in parentheses in the first column. Mice were 4–6 weeks old when tissues were collected.

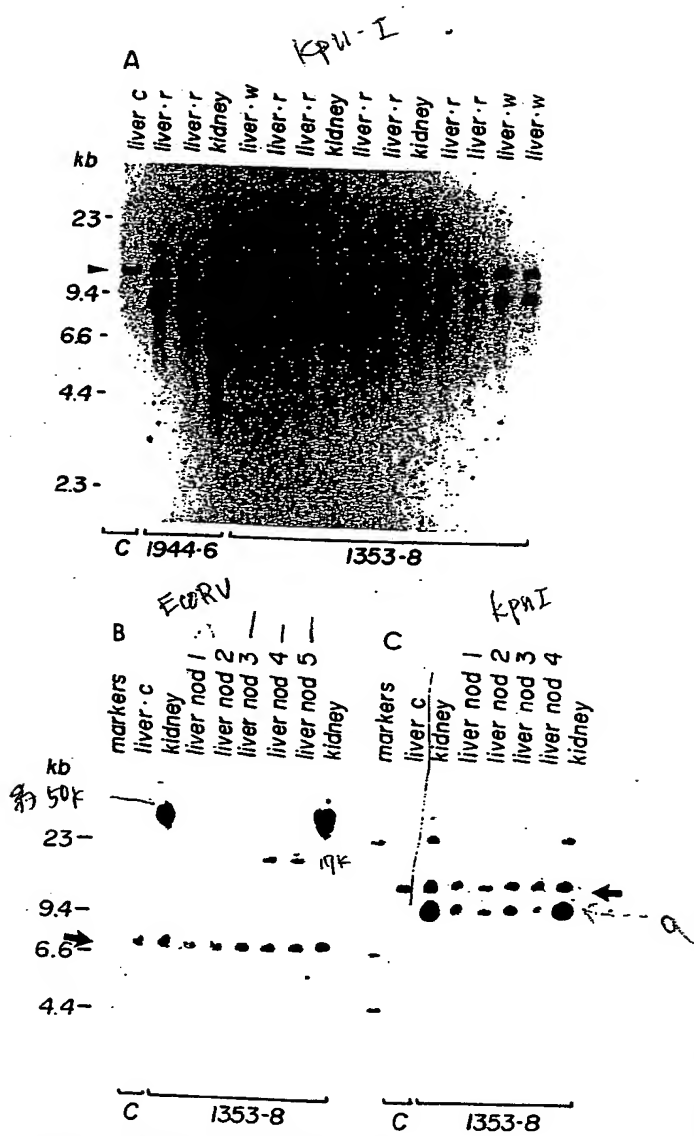

Figure 5. Southern Blot Analysis of the Alb–uPA Transgene

(A) DNA was isolated from liver or kidney, and 5 μg was digested with KpnI (an enzyme that cuts once within the transgene). The blot was hybridized with nick-translated fragments from the hGH gene, which detects the transgene, and the mouse *Hox-1.4* locus, which serves as an internal control for DNA loading. Samples were isolated from white liver areas (liver-w), from red liver nodules (liver-r), or from kidney. Marginal arrowhead indicates the Hox-1.4 band. Note the decreased intensity of the red liver transgene bands relative to those in white liver or kidney. Measurement of transgene copy number by quantitative dot hybridization (data not shown) indicated that line 1944-6 has about ten copies of the transgene in germline DNA, which is reduced about 4-fold in red liver nodule cells. Line 1353-8 has about four copies, and this is reduced to the equivalent of about one copy in red liver nodule cells. (B) DNA was isolated from a purified population of red nodule hepatocytes and digested with EcoRV. The blot was hybridized with both growth hormone and Hox-1.4 (arrow) probes. Nodules 1 and 2 were from the same mouse; 3–5 were from different mice. The kidney samples represent the unrearranged locus. Liver C is from a nontransgenic mouse. Note the transgene bands at 8 or 17 kb from all red nodules but number 3. The simplest explanation of the faint high molecular weight transgene band in the liver nodule lanes is that it represents unrearranged transgene in contaminating cells, although it may reflect a complex pattern of transgene integration or rearrangement in this line of mice (see text).

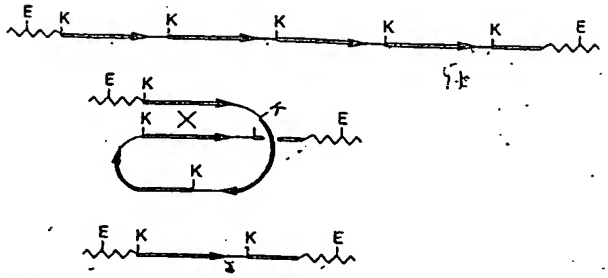

Figure 6. Representative Intrachromosomal Transgene Deletion Event

The transgene is depicted as an arrow, with the thin line representing the albumin enhancer/promoter, the bold line representing the mouse uPA gene, the arrowhead representing the hGH sequence (complementary to the hybridization probe), and the wavy line representing mouse chromosomal DNA. Quantitation of transgene copy number in line 1353-8 mice suggests that there are about four copies. Restriction sites are indicated as follows: K for KpnI and E for EcoRV. The rearrangement depicted would produce a 9 kb band following KpnI digestion and a 17 kb band following EcoRV digestion.

weight transgene band of about 8 or 17 kb (Figure 5B); note the unit transgene length difference in size. DNA from the remaining nodule (number 3) displayed no low molecular weight band despite the reduced intensity of the 9 kb KpnI band (Figure 5C). These data and those from four additional red nodule DNA samples revealed a 17 kb EcoRV band in five of nine nodules, the 8 kb band in two nodules, and no lower molecular weight band in two nodules. Thus, at least three different rearrangements have been detected, and each nodule contains only one, suggesting that all of the hepatocytes within a nodule are clonally derived. Given the unit transgene length band in the KpnI digests of all nodules, the presence of a band of less than 9 kb in some EcoRV digests is puzzling, since EcoRV should cut only outside the transgene array. Perhaps transgene deletion can involve flanking DNA, or a rearrangement or mutational event accompanied transgene integration in the line 1353-8 founder mouse, as reported for other transgenic mouse lineages (see Wilkie and Palmiter, 1987). A complete characterization will likely require cloning and sequencing of the transgene locus before and after rearrangement. Despite this complication, we believe that a somatic intrachromosomal recombination event similar to that diagrammed in Figure 6 is the principal mechanism for loss of transgene expression in line 1353-8 mouse liver. Although one or more unit length KpnI fragments remain after the deletion, mRNA analysis suggests that they are nonfunctional.

If partial transgene deletion in individual hepatocytes accounts for loss of uPA expression and subsequent clonal expansion of affected cells, then homozygous transgenic mice (carrying two genomic copies of the transgene array) should show a greatly reduced incidence of red nodule development. In these mice, the appearance of a red

(C) The same DNA samples used in (B) were digested with KpnI. The blot was hybridized with both growth hormone and Hox-1.4 (arrow) probes. There was insufficient DNA from nodule 5 for this blot, but an earlier blot showed it to contain the typical 9 kb band.

nodule progenitor cell would presumably require two independent deletion events. As noted earlier, red nodule number was reduced in homozygotes (Figure 1). Five livers from 4.5- to 5-week-old homozygous line 1353-8 mice were serially sectioned and examined microscopically. The numbers of macro- and microscopic red foci observed in these mice were 11, 20, 30, 42, and approximately 250, for an average of 71. The total number of hepatocyte nuclei in three 4- to 6-week-old homozygous mouse livers was also determined (see Experimental Procedures). Assuming 2.1×10^9 hepatocyte nuclei per liver and independent transgene rearrangement events in homozygous liver cells, there were approximately 1.4×10^{-4} productive rearrangements per cell division (see Experimental Procedures for a detailed calculation). Homozygotes from line 1944-6 almost never survive to be weaned, possibly due to a greater susceptibility to neonatal bleeding. In the one homozygous mouse liver examined, no red foci could be positively identified. Using the assumptions noted above, we calculate fewer than 1.6×10^{-5} productive rearrangements per cell division in this liver.

Clonal Hepatic Nodules Resemble Regenerating Liver

The apparent expansion of red liver nodules in Alb–uPA transgenic mice suggested that these nodules represented regenerating liver. The liver is a remarkable organ in that, following a toxic insult that causes hepatocellular death, such as CCl_4 administration, or following partial (two thirds) hepatectomy, remaining hepatocytes are induced to proliferate; after approximately 2 weeks the liver will regain (but not exceed) its entire pretreatment mass (reviewed in Fausto, 1990; Michalopoulos, 1990). Hepatocytes relieved from the deleterious effects of Alb–uPA transgene expression might also be expected to proliferate. We therefore conducted several experiments to determine the regenerative character of red liver.

One-month-old mice from each transgenic line plus two nontransgenic control mice were administered [^{3}H]thymidine and sacrificed 1 hr later. Sections of fixed liver were coated with a radiosensitive emulsion, developed, and examined to determine the location and number of cells undergoing DNA synthesis (Table 3). The fraction of labeled nuclei was twice as high in red nodules as in white liver, consistent with a selective growth advantage by red nodule hepatocytes. Hepatic nuclei were also analyzed for ploidy by flow cytometry. The percentage of liver nuclei with tetraploid or octaploid DNA content was greatly increased in red nodules and slightly decreased in white liver parenchyma compared with controls (Table 3). This suggests that red nodule cells were in a stage of rapid proliferation such as occurs after repeated partial hepatectomy, during which development of polyploid hepatocyte nuclei is a more frequent event (Brodsky and Uryvaeva, 1977).

To determine whether white liver parenchyma grows at a normal rate during early postnatal mouse development, we compared liver weight as a percent of body weight between line 1353-8 and line 1944-6 transgenic mice and nontransgenic littermate controls (data not shown). At 15 days of age in hemizygotes when transgenic livers appeared almost entirely white and at 1 month of age when line 1353-8 livers averaged 20% white, and line 1944-6 livers averaged 80% white, relative liver weights were not significantly different between mice of similar age. Even in line 1353-8 homozygotes, relative liver weights resembled controls at 1 month. Thus, despite the toxic influence of uPA expression, hepatocytes within white areas still proliferate. Furthermore, at 2 and 3 months when hemizygous transgenic livers appeared entirely red, relative liver weights remained normal.

Finally, several 4- to 5-week-old transgenic mice from line 1353-8 were subjected to partial (two thirds) hepatectomy. Remaining liver was collected between 24 and 98 hr later and examined microscopically. At 24 hr, no mitotic figures were observed in either red or white liver. At 2–4 days posthepatectomy, mitotic figures were visible in both liver populations, though at a much lower frequency in white parenchyma (Table 3). Remarkably, nonhepatocytes throughout white portions of the liver did proliferate. By 4 days posthepatectomy, biliary-like cells were observed in large numbers in white liver, often extending between and isolating largely nonproliferating hepatocytes (data not shown). Thus, in addition to having a greater fraction of cycling cells than white liver, red liver possesses the ability to respond further to the strong mi-

Table 3. Cell Cycle Characteristics of Alb–uPA Liver Cells

Mice	Liver Sample	% [^{3}H]Thymidine-Labeled Hepatocyte Nuclei	Ploidy (%)			% Nuclei in Mitosis after Hepatectomy		
			2N	4N	8N	24 hr	52 hr	98 hr
Control	Nontransgenic	1.7 (4 week) 0.4 (5 week)	83	17	0	—	—	—
Line 1353-8	White	1.7	93	6.2	0.4	<0.01	0.2	0.1
	Red	3.7	72	24	3.4	<0.01	1.0	0.4
Line 1944-6	White	1.9	95	5.4	0	—	—	—
	Red	3.6	71	25	4.1	—	—	—

Mice were 3–5 weeks old at the time of analysis. To determine % nuclei labeled or in mitosis, the number of labeled hepatocyte nuclei or mitotic cells was counted in a large number of high power fields (400×) representing red or white liver; total hepatocyte number was estimated by counting all hepatocytes in one high power field for each tissue type. Each reported value reflects examination of between 8,000 and 17,000 hepatocytes from one mouse. Ploidy was determined by flow cytometry on two control liver samples and two white and four red liver samples from each line. Data are reported as mean percent of hepatic nuclei displaying each ploidy value.

totic stimulus of hepatectomy. Hepatocytes in white areas, although mitotically competent, do not proliferate much above a basal level, either because they lack the ability to be stimulated fully or lack the ability to respond.

Discussion

In two lines of Alb–uPA transgenic mice, loss of transgene expression in individual hepatocytes leads to polyclonal replacement of the entire liver by descendents of those cells. The loss of transgene expression appears to involve deletion of functional transgenes mediated by intrachromosomal recombination between transgene copies that are present in a linear array, although other mechanisms, including mitotic recombination, gene conversion, or nondisjunction may less frequently generate transgene loss. The clonal proliferation of transgene-deficient cells and the eventual loss of transgene-expressing hepatocytes imply that hepatocellular uPA production is cytotoxic and that a very few cells, in some cases three or fewer, can effectively reconstitute functional liver mass once relieved from that toxicity.

The principal ultrastructural defect that we have detected in white, transgene-expressing liver is transformation of a large portion of RER into RER-bounded multivesicular bodies, a lesion unlike any described in human liver disease. Similar ultrastructural changes have not been reported in transgenic mice expressing tissue plasminogen activator (Pittius et al., 1988) or uPA (E. P. S., unpublished data) in mammary epithelium, suggesting that certain characteristics specific to hepatocytes are necessary for the development of this lesion. An obvious candidate is the hepatocyte's ability to produce the uPA substrate plasminogen. By virtue of their signal peptides, uPA, plasminogen, and the plasmin substrate fibrinogen would all be synthesized at the surface of the RER, and all three would enter the same intracellular compartment. Activation of a few molecules of uPA could initiate a cascade of proteolysis within the RER, leading to intracellular degradation of fibrinogen and possibly other proteins that are either passengers within or intrinsic to the RER. The resulting diversion of RER from its roles in protein sorting and secretion and the cytoplasmic accumulation of RER-derived multivesicular bodies may compromise the hepatocyte's ability to carry out important biochemical functions or to replicate.

Two additional transgenic models of hepatic disease have been described in which the principal lesion appears to involve the hepatocyte secretory pathway. In humans, the most severe form of AAT deficiency disease is the result of a single amino acid substitution in AAT that interferes with intracellular transport of the protein and results in accumulation of unsecreted AAT in hepatocyte RER; similarly, transgenic mice expressing this mutant AAT gene display intracellular globules within the hepatocyte RER that contain mutant protein (Dycaico et al., 1988; Carlson et al., 1989). The most severely affected mice show retarded growth and multifocal hepatic inflammation and necrosis. Transgenic mice expressing the hepatitis B virus large envelope polypeptide under control of the albumin enhancer/promoter also develop liver lesions (Chisari et al., 1985, 1987, 1989). Long filaments composed of hepatitis B surface antigen accumulate in smooth ER, leading to hepatocellular degeneration, focal hepatic necrosis, and hepatocellular carcinomas in adults. In Alb–uPA transgenic mice, hepatic vesicles do not contain visible deposits of unsecreted protein of the types described in AAT or hepatitis B virus transgenics. Despite this difference, expression of each transgene results in hepatocellular injury and eventual death.

Perhaps the most intriguing feature of liver disease in Alb–uPA mice is that some liver cells escape cytotoxicity by inactivating transgene expression. This fact explains much of the phenotype that characterizes young adult mice, including the development of red liver nodules, the lack of transgene expression in those nodules, and the subsequent recovery of clotting function. The mechanism responsible for the loss of cytotoxic transgene expression appears to be homologous recombination by which active transgene copies present in a linear array are deleted. We estimate that this occurs in line 1353-8 mouse liver with a frequency of 1.4×10^{-4} per cell division, somewhat higher than the estimate of 2×10^{-5} recombinants per cell division between two linked viral thymidine kinase genes present in the genome of mouse L cells (Liskay et al., 1984). In line 1944-6, the upper limit of recombination frequency is 2×10^{-5}.

There is no reason to expect that similar events do not occur in cells other than hepatocytes in Alb–uPA mice or among tandem copies of any transgene in other transgenic mice. For example, transgene deletion may account for the appearance of human growth hormone (hGH)-negative clones of small intestinal epithelial cells in mice bearing a fatty acid–binding protein–hGH fusion transgene, which was expected to direct uniform expression throughout the small intestine (Sweetser et al., 1988). This mechanism may also explain the escape of a small number of differentiated cells from diphtheria toxin–induced killing in two groups of transgenic mice in which diphtheria toxin expression was targeted to pancreatic acinar cells (Palmiter et al., 1987) or pituitary somatotropes (Behringer et al., 1988). However, before deletion events can be detected by a change in organ function or gross morphology, two conditions must be met: loss of transgene expression must impart a selective advantage in growth or viability to affected cells, and the target tissue must permit amplification of these cells. In liver, most mature hepatocytes can reenter the replication cycle in response to a currently unidentified stimulus that promotes liver regeneration following hepatectomy (Fausto, 1990; Michalopoulos, 1990). This regenerative capacity coupled with the preferential growth advantage of red nodule hepatocytes fulfill both requirements. In this respect, it is interesting that hepatitis B surface antigen–negative foci and nodules develop in older hepatitis B virus transgenic mouse livers, although major transgene rearrangements were not observed in nodules (Chisari et al., 1989).

One additional line of transgenic mice has been reported to fulfill the two conditions listed above. We previously observed that expression of the herpes simplex virus thy-

midine kinase gene in postmeiotic germ cells resulted in infertile sperm (Braun et al., 1990). In the MyK-103 transgenic lineage, intrachromosomal recombination between two copies of a 5 kb sequence that was duplicated upon transgene integration results in deletion of the herpes simplex virus thymidine kinase transgene from premeiotic germ cells (Palmiter et al., 1984; Wilkie and Palmiter, 1987; Wilkie et al., 1991). Spermatozoa derived from these cells are viable and will restore male fertility if present in sufficient numbers. The frequency of rearrangement was estimated as 2×10^{-3} per cell division (Wilkie et al., 1991), 10-fold higher than our upper estimate for recombination rate in Alb–uPA mouse liver. In the DBA mouse, reversion of the dilute (*d*) coat color mutation, which resulted from retroviral insertion in the *d* locus, occurs by recombination between viral long terminal repeats and excision of intervening viral sequences (Seperack et al., 1988). The authors reported a recombination frequency in germline of about 5×10^{-6} and in somatic cells of about 1×10^{-6} (although only one of the latter events was observed). Several other examples in humans of DNA deletion or duplication following germline recombination have been reported, often resulting in disease (Nathans et al., 1986; Bakker et al., 1987; Darras and Francke, 1987; Lehrman et al., 1987; Higgs et al., 1989; Vnencak-Jones and Phillips, 1990; Yen et al., 1990).

The development in Alb–uPA mice of clonal red nodules that ultimately reconstitute the entire liver mass highlights the tremendous regenerative capacity of liver cells. An important question concerns the identity of the progenitor cells involved. A class of liver stem cells has been reported to exist among the terminal or transitional bile ductules that may proliferate in response to normal hepatocellular turnover or some forms of liver damage (reviewed in Sell, 1990). Nevertheless, several observations suggest that mature hepatocytes are capable of generating the red nodules in Alb–uPA transgenic mice. During both normal liver development and liver regeneration following partial hepatectomy new hepatocytes arise from preexisting hepatocytes (Fausto, 1990; Michalopoulos, 1990). Similarly, in [^{3}H]thymidine-labeled Alb–uPA liver most of the label in both white and red liver appears over hepatocytes. Finally, even the smallest microscopic red foci are composed of cells with characteristic hepatocyte morphology that must be capable of undergoing many additional cell doublings to yield red nodules, some of which occasionally comprise almost the entire final liver mass. Thus, a pool exists of proliferating mature cells with documented regenerative potential in which DNA rearrangements could arise; stem cells appear unnecessary to account for the phenomenon.

A second important question concerns the regulation of cell growth within white and red liver parenchyma. The lesion present in white liver apparently triggers a signal that indicates a deficit in functional liver mass, because red nodule cell populations are induced to expand. The lack of compensatory growth by white liver hepatocytes suggests that they are less able to respond to this signal. The same result follows partial hepatectomy; however, nonhepatocytes in white tissue do proliferate, indicating that their response is both unimpaired and uncoupled to hepatocyte replication. The nature of the signal that initiates liver regeneration is unknown, but our findings suggest that it is not liver weight or cell number because these values are not significantly decreased in transgenic mice. Rather, there must be some indicator of liver function involved. It is tempting to speculate that loss of steady-state secretion of a factor produced by liver stimulates regeneration, given the secretory pathway defect in uPA-expressing hepatocytes. However, other alterations in liver function could also have a role. Excess circulating uPA is present for as long as white liver tissue remains in these mice, but we have no evidence that this directly influences regeneration. Finally, once red liver nodules have replaced white tissue, proliferation ceases. This indicates that red liver tissue satisfies the demand for functional liver mass and that it can respond appropriately to the signal indicating that regeneration is complete (Fausto, 1990; Michalopoulos, 1990).

Although an unexpected finding, the sequential development of molecular and morphological changes in Alb–uPA mouse livers has provided a means to study both somatic recombination and liver regeneration. The liver phenotype demonstrates the remarkable developmental potential of liver cells, since a few cells can effectively repopulate an entire organ. We can now employ this model to study the signals involved in liver regeneration and the nature of the responsive cells.

Experimental Procedures

Production and Identification of Transgenic Mice

The Alb–uPA transgene was constructed as described previously (Heckel et al., 1990). Briefly, a 2.5 kb fragment containing juxtaposed mouse albumin enhancer and promoter elements was fused to a 6.4 kb fragment containing the mouse uPA genomic coding sequence with 3′ noncoding DNA and a poly(A) addition site provided by the hGH gene. The resulting fusion construct was introduced into fertilized mouse eggs (Brinster et al., 1985), and transgenic mice were identified as described (Heckel et al., 1990) using a probe specific for the hGH sequence. Homozygous transgenic mice were identified by quantitative dot hybridization or, in some cases, by phenotype. The two lineages described in this report have been assigned the following genetic designations: line 1353-8, Tg(Alb-1,Plau)Bri144 and line 1944-6, Tg(Alb-1,Plau)Bri145 (Heckel et al., 1990).

Tissue Collection and Microscopic Examination

Liver was fixed in 10% neutral buffered formalin, processed, embedded in paraffin, cut into 5 μm thick sections, and stained with hematoxylin and eosin according to standard methods. Some sections were osmicated prior to processing to preserve lipid. The entire liver from each of six homozygous transgenic mice was fixed and sectioned at 6 μm; every eighth section was examined microscopically, and the number of red foci per liver was counted. For electron microscopy, liver was fixed by immersion in cold 3% glutaraldehyde prepared in Millonig's buffer. The tissue was postfixed in osmium tetroxide, processed into LX-112 (Ladd) by routine techniques, stained with uranyl acetate and lead citrate, and examined on a Phillips 400 transmission electron microscope. To identify cells undergoing DNA synthesis, 80 μCi of [^{3}H]thymidine (Amersham) was injected intraperitoneally into several mice, and mice were sacrificed 1 hr later. Fixed liver sections were coated with nuclear track emulsion, developed after 22 days, and stained with hematoxylin and eosin. Dark grains were visible over nuclei that had retained [^{3}H]thymidine. Partial (two thirds) hepatectomy was performed on anesthetized mice by removing the left and median liver lobes. Liver was collected at various times after surgery and processed as described above.

Liver Perfusion and Hepatocyte Isolation

Hepatocytes were isolated using a modification of the method of Soda and Tavassoli (1984). Mice were anesthetized with tribromoethanol (Aldrich), and the portal vein was exposed through a ventral midline abdominal incision. A fluid-filled 24 gauge 3/4 inch catheter (Abbocath, Abbott) was inserted into the portal vein and held in place with a 1 inch alligator clip, then the heart was exposed and an incision made into the right atrium. Twenty milliliters of 37°C perfusion buffer containing EGTA (137 mM NaCl, 4.69 mM KCl, 1.17 mM KH_2PO_4, 0.65 mM $MgSO_4 \cdot 7H_2O$, 1.0 mM EGTA, 10 mM HEPES [pH 7.4]) followed by 10 ml of an enzyme solution (0.5 mg/ml collagenase type I [Sigma], 0.1 mg/ml hyaluronidase type IV [Sigma], 66.7 mM NaCl, 6.70 mM KCl, 4.76 mM $CaCl_2 \cdot 2H_2O$, 100 mM HEPES [pH 7.6]) were slowly introduced into the catheter and passed through the liver. Individual large red nodules were isolated from surrounding liver, minced with razor blades, placed into 10 ml of the enzyme solution that also contained 0.001% DNAase I (Worthington), and shaken gently at 37°C for 15 min. Each cell suspension was allowed to stand for 5 min in a 15 ml graduated conical tube (Falcon) to allow clumps of cells to settle, and the supernatant was centrifuged at 50 × g for 3 min. The hepatocyte-enriched pellet was resuspended in 4 ml of PBS containing 0.5% BSA and layered over a two-step metrizamide gradient (2 ml of 15% metrizamide [Sigma] in 0.25% BSA, 75 mM KCl, 1.25 mM $CaCl_2$, 10 mM HEPES [pH 7.5], layered over 2 ml of 30% metrizamide in the HEPES buffer) and centrifuged at 1500 × g for 40 min at 4°C. The large cells present at the 15%–30% metrizamide interface were rinsed in PBS containing 0.5% BSA, lysed in SET buffer (1% SDS, 5 mM EDTA, 10 mM Tris–HCl [pH 7.4]) containing 100 μg/ml proteinase K (Boehringer Mannheim), and prepared for Southern blot analysis as described below. Between 4 and 20 × 10^6 cells were obtained from individual red liver nodules with 50%–80% viability as determined by trypan blue exclusion and with less than 3% contamination by small cells (nonhepatocytes).

Flow Cytometric Analysis of Hepatic Nuclei

Samples of liver were placed in freezing medium (DMEM [Gibco] with 20% FCS and 10% dimethyl sulfoxide) and frozen over liquid nitrogen. For analysis of ploidy, samples were thawed, minced in 0.1% Nonidet P-40, 2 mM $CaCl_2$, 20 mM $MgCl_2$, 10 μg/ml 4,6-diamidino-2-phenylindole, 0.1 M Tris–HCl (pH 7.4), then passaged through a 25 gauge needle. Samples were analyzed on a Becton-Dickinson FACS analyzer, and data were collected and analyzed on a DEC LSI 11/23 computer.

Clinical Chemistry and Plasma uPA Measurement

Blood was collected from the retro-orbital sinus in heparin-coated hematocrit tubes and centrifuged to separate plasma from cells. Plasma was analyzed for total protein, albumin, total bilirubin, and alanine aminotransferase activity on a Kodak Ektrachem 700 analyzer. Urine protein concentration was determined using Bili-Labstix reagent strips (Miles). Plasma was assayed for plasminogen activator concentration by a zymographic analysis as described (Heckel et al., 1990). Briefly, plasma proteins were electrophoretically fractionated on nonreducing SDS–acrylamide gels cast with nonfat dry milk and human plasminogen. Gels were washed in Triton X-100, incubated in glycine buffer, and stained with amido black to detect caseinolytic activity.

mRNA Measurement

Transgene-derived uPA, plasminogen, albumin, and α-fetoprotein mRNA levels were measured in liver RNA extracts using a quantitative solution hybridization assay and synthetic oligonucleotide probes as described (Heckel et al., 1990), except the hybridization mixtures for albumin and α-fetoprotein assays contained 10% formamide and were incubated at 45°C. Transgene mRNA was detected using an oligonucleotide complementary to the hGH sequence (Heckel et al., 1990). Remaining mRNA species were detected using the following oligonucleotide probes: plasminogen, 5′-TGTGCTTATGTAGCCATCCAGCGAGTCCCC-3′ (Degen et al., 1990); albumin, 5′-CACCCCTGGAAAAAGCAGAGCCGG-3′; and α-fetoprotein, 5′-CTAACGTGGAAGCTATCCCAAACTC-3′. Molecules per cell were calculated as described (Heckel et al., 1990).

Southern Blot Analyses

For Southern blot analysis, samples of liver or kidney were homogenized in SET buffer containing 100 μg/ml proteinase K, and DNA was prepared as described (Palmiter et al., 1982). DNA (5 μg) was digested with restriction enzymes, electrophoresed on 0.7% agarose, and transferred to nitrocellulose. Filters were hybridized with a nick-translated BglII–EcoRI fragment from the hGH gene to detect transgene and a SstI–EcoRV fragment from the murine *Hox-1.4* locus.

Calculation of Transgene Rearrangement Frequency

Transgene rearrangement frequency was calculated using the two-mutation model for embryonal cancers developed by Hethcote and Knudson (1978). The rate of transgene rearrangement per cell division, μ, can be expressed as

$$\mu = [n/N(\ln N - 1)]^{\frac{1}{n}}$$

where n is the mean number of regenerative foci per liver in homozygous mice (carrying two copies of the transgene array), and N equals the total number of hepatocytes per liver (modified from equation 7 in Hethcote and Knudson, 1978). We assume independent transgene rearrangement events in homozygous cells and no change in cellular fitness following inactivation of the first transgene array. Three 4- to 6-week-old homozygous mouse livers were weighed, and a piece of known weight was removed from each and homogenized in SET buffer containing 100 μg/ml proteinase K. DNA concentrations were measured as described (Hammer et al., 1985). These values were used to determine the DNA content per liver and then the average number of hepatic nuclei (3.4 × 10^9), assuming 6 pg of DNA per diploid mouse nucleus. If 40% of hepatic nuclei represent nonhepatocytes (Fausto, 1990), then there were 2.1 × 10^9 hepatocyte nuclei per homozygous mouse liver. There was an average of 71 (range 11–250) red foci per liver in five 4.5- to 5-week-old line 1353-8 homozygotes. For N = 2.1 × 10^9 and n = 71, μ = 1.4 × 10^{-4} (range for variable n, 5 × 10^{-5} to 2.6 × 10^{-4}). In one 3-week-old line 1944-6 homozygote there were no apparent red liver foci, giving μ < 1.6 × 10^{-5}. Each calculated μ represents a minimum estimate, since very small red foci may not have been counted, and livers from homozygotes that did not develop edema and that appeared to contain a greater number of red foci were not sectioned for determination of red focus number.

Acknowledgments

We thank Mary Avarbock, Diane Allen, Cherie Kessler, Felicity Oram, and Carol Quaife for technical assistance; Carolyn Pope for secretarial assistance; Steven Schuster for suggestions concerning hepatocyte isolation; Carlo Pesce for processing tissues for autoradiography; Alfred Knudson, Jr. for suggesting a way to determine recombination frequency; Sandra Degen for providing the plasminogen probe; and John Bancroft, Robert Maronpot, and Tom Van Winkle for discussions of the liver pathology. This work was supported by National Institutes of Health grants to R. D. P. (HD09172), R. L. B. (CA38635), and J. L. D. (CA44611). E. P. S. is a fellow of the Veterinary Medical Scientist Training Program at the University of Pennsylvania. J. L. H. is a fellow of the William Cooper Procter Research Scholar Program at the Children's Hospital of Cincinnati and a recipient of an American Cancer Society Career Development Award (CDA89–134).

The costs of publication of this article were defrayed in part by the payment of page charges. This article must therefore be hereby marked "*advertisement*" in accordance with 18 USC Section 1734 solely to indicate this fact.

Received April 10, 1991; revised May 17, 1991.

References

Bakker, E., Van Broeckhoven, C., Bonten, E. J., van de Vooren, M. J., Veenema, H., Van Hul, W., Van Ommen, G. J. B., Vandenberghe, A., and Pearson, P. L. (1987). Germline mosaicism and Duchenne muscular dystrophy mutations. Nature *329*, 554–556.

Behringer, R. R., Mathews, L. S., Palmiter, R. D., and Brinster, R. L. (1988). Dwarf mice produced by genetic ablation of growth hormone-expressing cells. Genes Dev. *2*, 453–461.

Braun, R. E., Lo, D., Pinkert, C. A., Widera, G., Flavell, R. A., Palmiter, R. D., and Brinster, R. L. (1990). Infertility in male transgenic mice: disruption of sperm development by HSV-tk expression in post meiotic germ cells. Biol. Reprod. *43*, 684–693.

Brinster, R. L., Chen, H. Y., Trumbauer, M. E., Yagle, M. K., and Palmiter, R. D. (1985). Factors affecting the efficiency of introducing foreign DNA into mice by microinjecting eggs. Proc. Natl. Acad. Sci. USA *82*, 4438–4442.

Brodsky, W. Y., and Uryvaeva, I. V. (1977). Cell polyploidy: its relation to tissue growth and function. Int. Rev. Cytol. *50*, 275–332.

Carlson, J. A., Rogers, B. B., Sifers, R. N., Finegold, M. J., Clift, S. M., DeMayo, F. J., Bullock, D. W., and Woo, S. L. C. (1989). Accumulation of PiZ α_1-antitrypsin causes liver damage in transgenic mice. J. Clin. Invest. *83*, 1183–1190.

Chisari, F. V., Pinkert, C. A., Milich, D. R., Filippi, P., McLachlan, A., Palmiter, R. D., and Brinster, R. L. (1985). A transgenic mouse model of the chronic hepatitis B surface antigen carrier state. Science *230*, 1157–1160.

Chisari, F. V., Filippi, P., Buras, J., McLachlan, A., Popper, H., Pinkert, C. A., Palmiter, R. D., and Brinster, R. L. (1987). Structural and pathological effects of synthesis of hepatitis B virus large envelope polypeptide in transgenic mice. Proc. Natl. Acad. Sci. USA *84*, 6909–6913.

Chisari, F. V., Klopchin, K., Moriyama, T., Pasquinelli, C., Dunsford, H. A., Sell, S., Pinkert, C. A., Brinster, R. L., and Palmiter, R. D. (1989). Molecular pathogenesis of hepatocellular carcinoma in hepatitis B virus transgenic mice. Cell *59*, 1145–1156.

Collen, D., and Lijnen, H. R. (1987). Fibrinolysis and the control of hemostasis. In The Molecular Basis of Blood Diseases, G. Stamatoyannopoulos, A. W. Nienhuis, P. Leder, and P. W. Majerus, eds. (Philadelphia: W. B. Saunders Co.), pp. 662–688.

Danø, K., Andreasen, P. A., Grøndahl-Hansen, J., Kristensen, D., Nielsen, L. S., and Skriver, L. (1985). Plasminogen activators, tissue degradation, and cancer. Adv. Cancer Res. *44*, 149–265.

Darras, B. T., and Francke, U. (1987). A partial deletion of the muscular dystrophy gene transmitted twice by an unaffected male. Nature *329*, 556–558.

Degen, S. J. F., Bell, S. M., Schaefer, L. A., and Elliot, R. W. (1990). Characterization of the cDNA coding for mouse plasminogen and localization of the gene to mouse chromosome 17. Genomics *8*, 49–61.

Dycaico, M. J., Grant, S. G. N., Felts, K., Nichols, W. S., Geller, S. A., Hager, J. H., Pollard, A. J., Kohler, S. W., Short, H. P., Jirik, F. R., Hanahan, D., and Sorge, J. A. (1988). Neonatal hepatitis induced by α_1-antitrypsin: a transgenic mouse model. Science *242*, 1409–1412.

Fausto, N. (1990). Hepatic regeneration. In Hepatology, A Textbook of Liver Disease, 2nd ed., D. Zakim and T. D. Boyer, eds. (Philadelphia: W. B. Saunders Co.), pp. 49–65.

Hammer, R. E., Brinster, R. L., and Palmiter, R. D. (1985). Use of gene transfer to increase animal growth. Cold Spring Harbor Symp. Quant. Biol. *50*, 379–387.

Hanahan, D. (1989). Transgenic mice as probes into complex systems. Science *246*, 1265–1275.

Heckel, J. L., Sandgren, E. P., Degen, J. L., Palmiter, R. D., and Brinster, R. L. (1990). Neonatal bleeding in transgenic mice expressing urokinase-type plasminogen activator. Cell *62*, 447–456.

Held, W. A., Mullins, J. J., Kuhn, N. J., Gallagher, J. F., Gu, G. D., and Gross, K. W. (1989). T antigen expression and tumorigenesis in transgenic mice containing a mouse major urinary protein/SV40 T antigen hybrid gene. EMBO J. *8*, 183–191.

Hethcote, H. W., and Knudson, A. G., Jr. (1978). Model for the incidence of embryonal cancers: application to retinoblastoma. Proc. Natl. Acad. Sci. USA *75*, 2453–2457.

Higgs, D. R., Vickers, M. A., Wilkie, A. O. M., Pretorius, I. M., Jarman, A. P., and Weatherall, D. J. (1989). A review of the molecular genetics of the human globin gene cluster. Blood *73*, 1081–1104.

Jaenisch, R. (1988). Transgenic animals. Science *240*, 1468–1474.

Jhappan, C., Stahle, C., Harkins, R. N., Fausto, N., Smith, G. H., and Merlino, G. T. (1990). TGFα overexpression in transgenic mice induces liver neoplasia and abnormal development of the mammary gland and pancreas. Cell *61*, 1137–1146.

Lehrman, M. A., Goldstein, J. L., Russell, D. W., and Brown, M. S. (1987). Duplication of seven exons in LDL receptor gene caused by Alu–Alu recombination in a subject with familial hypercholesterolemia. Cell *48*, 827–835.

Liskay, R. M., Stachelek, J. L., and Letsou, A. (1984). Homologous recombination between repeated chromosomal sequences in mouse cells. Cold Spring Harbor Symp. Quant. Biol. *49*, 183–189.

Messing, A., Chen, H. Y., Palmiter, R. D., and Brinster, R. L. (1985). Peripheral neuropathies, hepatocellular carcinomas and islet cell adenomas in transgenic mice. Nature *316*, 461–463.

Michalopoulos, G. K. (1990). Liver regeneration: molecular mechanisms of growth control. FASEB J. *4*, 176–187.

Nathans, J., Piantanida, T. P., Eddy, R. L., Shows, T. B., and Hogness, D. S. (1986). Molecular genetics of inherited variation in human color vision. Science *232*, 203–210.

Palmiter, R. D., Chen, H. Y., and Brinster, R. L. (1982). Differential regulation of metallothionein-thymidine kinase fusion genes in transgenic mice and their offspring. Cell *29*, 701–710.

Palmiter, R. D., Wilkie, T. M., Chen, H. Y., and Brinster, R. L. (1984). Transmission distortion and mosaicism in an unusual transgenic mouse pedigree. Cell *36*, 869–877.

Palmiter, R. D., Behringer, R. R., Quaife, C. J., Maxwell, F., Maxwell, I. H., and Brinster, R. L. (1987). Cell lineage ablation in transgenic mice by cell-specific expression of a toxin gene. Cell *50*, 435–443.

Pittius, C. W., Hennighausen, L., Lee, E., Westphal, H., Nicols, E., Vitale, J., and Gordon, K. (1988). A milk protein gene promoter directs the expression of human tissue plasminogen activator cDNA to the mammary gland in transgenic mice. Proc. Natl. Acad. Sci. USA *85*, 5874–5878.

Quaife, C. J., Mathews, L. S., Pinkert, C. A., Hammer, R. E., Brinster, R. L., and Palmiter, R. D. (1989). Histopathology associated with elevated levels of growth hormone and insulin-like growth factor I in transgenic mice. Endocrinology *124*, 40–48.

Saksela, O., and Rifkin, D. B. (1988). Cell-associated plasminogen activation: regulation and physiological functions. Annu. Rev. Cell Biol. *4*, 93–126.

Sandgren, E. P., Quaife, C. J., Pinkert, C. A., Palmiter, R. D., and Brinster, R. L. (1989). Oncogene-induced liver neoplasia in transgenic mice. Oncogene *4*, 715–724.

Sandgren, E. P., Luetteke, N. C., Palmiter, R. D., Brinster, R. L., and Lee, D. C. (1990). Overexpression of TGFα in transgenic mice: induction of epithelial hyperplasia, pancreatic metaplasia, and carcinoma of the breast. Cell *61*, 1121–1135.

Sell, S. (1990). Is there a liver stem cell? Cancer Res. *50*, 3811–3815.

Seperack, P. K., Strobel, M. C., Corrow, D. J., Jenkins, N. A., and Copeland, N. G. (1988). Somatic and germ-line reverse mutation rates of the retrovirus-induced dilute coat-color mutation of DBA mice. Proc. Natl. Acad. Sci. USA *85*, 189–192.

Sepulveda, A. R., Finegold, M. J., Smith, B., Slagle, B. L., DeMayo, J. L., Shen, R.-F., Woo, S. L. C., and Butel, J. S. (1989). Development of a transgenic mouse system for the analysis of stages in liver carcinogenesis using tissue-specific expression of SV40 large T-antigen controlled by regulatory elements of the human α-1-antitrypsin gene. Cancer Res. *49*, 6108–6117.

Soda, R., and Tavassoli, M. (1984). Liver endothelium and not hepatocytes or Kupffer cells have transferrin receptors. Blood *63*, 270–276.

Stolz, A., and Kaplowitz, N. (1990). Biochemical tests for liver disease. In Hepatology, A Textbook of Liver Disease, 2nd ed., D. Zakim and T. D. Boyer, eds. (Philadelphia: W. B. Saunders Co.), pp. 637–667.

Sweetser, D. A., Birkenmeier, E. H., Hoppe, P. C., McKeel, D. W., and Gordon, J. I. (1988). Mechanisms underlying generation of gradients in gene expression within the intestine: an analysis using transgenic mice containing fatty acid binding protein-human growth hormone fusion genes. Genes Dev. *2*, 1318–1332.

Vnencak-Jones, C. L., and Phillips, J. A., III (1990). Hot spots for growth hormone gene deletions in homologous regions outside of *Alu* repeats. Science *250*, 1745–1748.

Wilkie, T. M., and Palmiter, R. D. (1987). Analysis of the integrant in MyK-103 transgenic mice in which males fail to transmit the integrant. Mol. Cell. Biol. 7, 1646–1655.

Wilkie, T. M., Braun, R. E., Ehrman, W. J., Palmiter, R. D., and Hammer, R. E. (1991). Germ-line intrachromosomal recombination restores fertility in transgenic MyK-103 male mice. Genes Dev. 5, 38–48.

Yen, P. H., Li, X.-M., Tsai, S.-P., Johnson, C., Mohandas, T., and Shapiro, L. J. (1990). Frequent deletions of the human X chromosome distal short arm result from recombination between low copy repetitive elements. Cell 61, 603–610.

Proc. Natl. Acad. Sci. USA
Vol. 92, pp. 4942–4946, May 1995
Medical Sciences

Complete reconstitution of mouse liver with xenogeneic hepatocytes

(liver cell transplantation/liver regeneration/xenogeneic transplantation/transgenic)

JONATHAN A. RHIM*†, ERIC P. SANDGREN*‡, RICHARD D. PALMITER§, AND RALPH L. BRINSTER*¶

*Department of Animal Biology, School of Veterinary Medicine, University of Pennsylvania, Philadelphia, PA 19104; †Department of Pathology and Laboratory Medicine, University of Pennsylvania School of Medicine, Philadelphia, PA 19104; and §Howard Hughes Medical Institute and Department of Biochemistry, University of Washington SL-15, Seattle, WA 98195

Contributed by Ralph L. Brinster, February 6, 1995

ABSTRACT **We have developed a system for studying hepatocellular growth potential in which liver cells are introduced into the diseased livers of albumin–urokinase (Alb-uPA) transgenic mice. To use this system to study xenogeneic cell transplantation, rat liver cells were introduced into immunotolerant Alb-uPA transgenic mice. In regenerated recipient livers, up to 100% of hepatocellular gene expression was of rat origin, demonstrating the creation of a functional mouse liver in which parenchyma is derived from xenogeneic (rat) hepatocytes. Immunotolerant Alb-uPA transgenic mice provide a tool for studying hepatocellular biology of any species, including humans, in a controlled experimental setting.**

We have developed a transgenic mouse system to assess the regenerative capacity of hepatocytes. In this system, albumin–urokinase (Alb-uPA) transgenic mice are recipients of donor mouse hepatocytes. The transplanted hepatocytes grow within the Alb-uPA liver (1), replacing transgene-expressing hepatocytes that are functionally compromised by transgene expression (2). Using this approach, we demonstrated that hepatocytes from adult liver have extensive replicative potential (1). The growth of the transplanted cells was nodular and clonal and occurred over several weeks. The resulting fully regenerated livers were chimeric, composed both of donor-derived cells and of host-derived cells that had deleted transgene DNA and therefore no longer expressed the transgene. Like transplanted hepatocytes, these host-derived cells also had a growth advantage relative to transgene-expressing hepatocytes and expanded in a nodular fashion (termed "red nodules"), competing with the donated hepatocytes. In hemizygous transgenic animals, transgene inactivation is a relatively frequent event, often resulting in hundreds of clonal nodules in young hemizygous mice (2); complete replacement of the transgenic liver by the clonal expansion of these nodules occurs by 8 weeks of age. By comparison, in homozygous mice, transgene inactivation is a less common event, consistent with the fact that two transgene arrays must be inactivated. Clonal nodules are rare in young homozygotes and, as a consequence, transgenic liver persists longer. Thus, hepatocyte transfer into homozygous Alb-uPA mice would be ideal for assessing liver cell growth; the lack of competition from red nodules should allow the donated cells to completely replace the recipient liver.

Because Alb-uPA transgenic mouse liver supported the growth of transplanted mouse hepatocytes (1), we hypothesized that immunotolerant mice would support the growth of transplanted hepatocytes from other species. For initial studies of xenogeneic cell transplantation, we chose to donate liver cells from the rat, the species most often used to study liver growth and development. Rat liver cells present several advantages as donor cells. Protocols exist to produce well-defined liver cell populations, which could be separately transplante into Alb-uPA transgenic mice. The ability of each populatio to repopulate diseased recipient mouse liver would indicat both the replicative and lineage potentials of each class of cel Furthermore, transplantation of nonhepatocytic cells int Alb-uPA transgenic mice might enable us to detect and t characterize hepatic stem cells, the existence of which remain controversial (3–5). Finally, if this method were feasibl Alb-uPA transgenic mouse livers repopulated with xenogene hepatocytes would be valuable tools for studying liver biolog of other species, including humans, in a controlled, *in vi* experimental setting.

MATERIALS AND METHODS

Generation of Immunotolerant Alb-uPA Transgenic Mic To generate immunotolerant Alb-uPA transgenic mice, w crossed Alb-uPA transgenic mice (2) with Swiss athymic, nuc (*nu/nu*) mice (Taconic Farms). Transgenic mice were ident fied by dot blot hybridization of tail DNA as described (2 Hemizygous transgenic *nu/nu* mice and homozygous tran genic *nu/nu* mice were generated by breeding hemizygou transgenic *nu/+* females with hemizygous transgenic *nu/n* males. Initially, homozygous mice were distinguished fro hemizygous mice by quantitative dot hybridization by measu ing the ratio of radioactive probe annealed to duplicate do after hybridization to either a transgene probe (800-bp *B* II–*Eco*RI fragment from the human growth hormone gene) a an endogenous gene (4-kb fragment from the *Hoxa* locus Subsequently, we took advantage of the observation th: insertion of the transgene resulted in a deletion of endogenou DNA at the site of integration. An easier test of homozygosit was devised in which duplicate dots were hybridized with transgene-specific probe (fragment from the human growt hormone gene) (as above) or a unique probe (550-bp *Bam*H fragment) derived from the deleted region.

Liver Cell Isolation and Transplantation. Rat liver cel were isolated from 3- to 6-week-old female Sprague–Dawle rats (Taconic Farms) by two-step EDTA/collagenase perfu sion using a protocol modified from Klaunig *et al.* (6). In th isolation procedure, liver cell suspensions were centrifuge twice at 50 × *g* to enrich for hepatocytes. Cell viability wa determined by trypan blue exclusion and ranged from 50% t 90%. After isolation, liver cells were kept on ice and tran ferred within 2 hr. Liver cells ($1–2 \times 10^5$) were transplante into recipient mice between 10 and 15 days of age by intra splenic injection as described (1).

Detection of Rat-Specific DNA and mRNA. Rat and mous DNAs were distinguished using a restriction fragment lengt

The publication costs of this article were defrayed in part by page charge payment. This article must therefore be hereby marked "*advertisement*" in accordance with 18 U.S.C. §1734 solely to indicate this fact.

Abbreviations: Alb-uPA, albumin–urokinase transgenic mice; mA monoclonal antibody.

‡Present address: Department of Pathobiological Sciences, School Veterinary Medicine, University of Wisconsin, Madison, WI 5370
¶To whom reprint requests should be addressed.

olymorphism in the phenylethanolamine *N*-methyltransferase gene. Genomic DNA (6 μg) was digested with *Pst* I, electrophoresed through a 0.7% agarose gel, transferred to nitrocellulose, and hybridized with a 449-bp probe specific to exon 3 of the mouse phenylethanolamine *N*-methyltransferase gene (7). Fragments of different sizes were seen in rat and mouse control livers. In samples containing both rat and mouse DNA, the relative amount of rat DNA was calculated from the intensity of the radioactivity hybridized (determined using a Molecular Dynamics PhosphorImager) to the rat and mouse *Pst* I fragments using a standard curve generated by mixing various amounts of mouse and rat DNA. A 10% contribution of rat DNA was detectable.

Mouse and rat transferrin mRNAs were measured by solution hybridization using ^{32}P end-labeled oligonucleotides complementary to sequences in the 3′-untranslated regions of the mRNAs (8). The mouse probe (no. 415) was 5′-AAGGCACAGCAGCGAAGACTACAC-3′, which differs in eight positions (underlined) from the rat probe (no. 422), which was 5′-AACACACAGCAGTGAAGACGGACA-3′. The rat sequence was derived from our own sequence of the 3′-untranslated region of rat transferrin cDNA, which differed substantially from the published sequence. The hybridization mixture contained 10% (vol/vol) formamide and about 10,000 cpm of either probe. After incubation for ≈20 hr at 45°C, the nonhybridized probe was eliminated with S_1 nuclease, and the protected probe was precipitated with trichloracetic acid and collected on a Whatman GF/C filter for scintillation counting. Standard curves were made from normal mouse and normal rat liver nucleic acids. There was no cross-hybridization of the mouse probe with rat transferrin mRNA or vice versa. The sensitivity of the assay was sufficient to detect a 1% contribution of rat transferrin mRNA in a mouse liver sample.

Immunohistochemistry. Indirect immunostaining of liver sections was adapted from ref. 9. Mouse monoclonal antibody (mAb) 258.26 is reactive with rat hepatocytes; mAb 18.11 is reactive with rat bile ducts (10). The secondary antiserum was affinity-purified goat anti-mouse immunoglobulin conjugated with horseradish peroxidase (Sigma). Frozen sections, 10 μm thick, were air-dried and fixed for 10 min in 100% acetone at 4°C. Sections were then washed in phosphate-buffered saline (PBS) and incubated with the primary antibody for 45 min at room temperature. The sections were then washed in PBS, incubated in 1% goat serum for 5 min, and incubated with a 1:100 dilution of the secondary antiserum for 45 min at room temperature. The sections were washed for 20 min in PBS and then incubated for 2 min with the chromogen 3,3′-diaminobenzidine. The sections were then lightly stained with Mayer's hematoxylin. Parallel sections stained only with the secondary antibody were negative (data not shown). Immunohistochemical detection of rat hepatocytes was confirmed using another rat-specific hepatocyte antibody, mAb 362.50 (11) (data not shown).

Liver was immunostained for α_{2u}-globulin protein based upon the procedure described in ref. 12 using the IgG fraction of a polyclonal rabbit antiserum to α_{2u}-globulin (a generous gift of A. Roy, University of Texas Health Science Center at San Antonio). Tissues were fixed in neutral-buffered formalin and embedded in paraffin for sectioning. Slides were deparaffinized and blocked with 3% (vol/vol) swine serum for 30 min, followed by incubation with the primary antiserum for 30 min at room temperature. Sections were washed in PBS. The primary antibody was detected using a peroxidase-antiperoxidase kit (Dako) according to the manufacturer's instructions. Treated sections were incubated with 3,3′-diaminobenzidine for 2 min and lightly counterstained in Mayer's hematoxylin. Parallel sections incubated with only secondary antibody were negative (data not shown). Control rat liver was taken from male rats ≈65 days of age.

RESULTS

Repopulation of Alb-uPA Transgenic Mouse Liver with Rat Hepatocytes. Rat liver cells were transplanted into the livers of immunotolerant (*nu/nu*) Alb-uPA transgenic mice that were either hemizygous or homozygous for the transgene. Unless otherwise specified, recipient mice were killed, and their livers were analyzed when liver regeneration was nearly complete—that is, when the liver was <10% transgenic by gross inspection. [Transgene-expressing liver had a characteristic pale white gross appearance (2), making it readily distinguishable from nontransgenic liver.] For hemizygous animals, this occurred between 6 and 8 weeks of age; for homozygous animals, this occurred between 10 and 14 weeks of age. At the time transplanted livers were examined, the recipient mice were clinically healthy (one homozygous mouse died at 10 weeks of unknown causes) and indistinguishable from nontransgenic *nu/nu* mice maintained in our colony. Serum albumin and total protein levels for both hemizygous and homozygous transgenic recipients were similar to transgenic nontransplanted and nontransgenic controls (data not shown).

Growth of transplanted rat liver cells could be detected in homozygous transgenic livers by gross inspection (Fig. 1) because of differences in color. At 8 weeks of age, homozygous transgenic livers that had not been transplanted with rat liver cells were completely pale in color, or "white" (Fig. 1*A*). In contrast, homozygous transgenic livers transplanted with rat liver cells were white and red (Fig. 1*B*); the latter resembled normal liver parenchyma (Fig. 1*C*), suggesting that these areas were composed of donor-derived rat liver cells. Red areas were multifocal and often nodular in shape, suggesting that numerous transplanted rat liver cells had engrafted and had begun to grow in the same nodular fashion as transplanted mouse liver cells (1). Completely regenerated homozygous transgenic livers resembled normal mouse livers in color, shape, and size (Fig. 1*D*). In hemizygous livers transplanted with rat liver cells, the growth of rat-derived cells was not discernible by gross

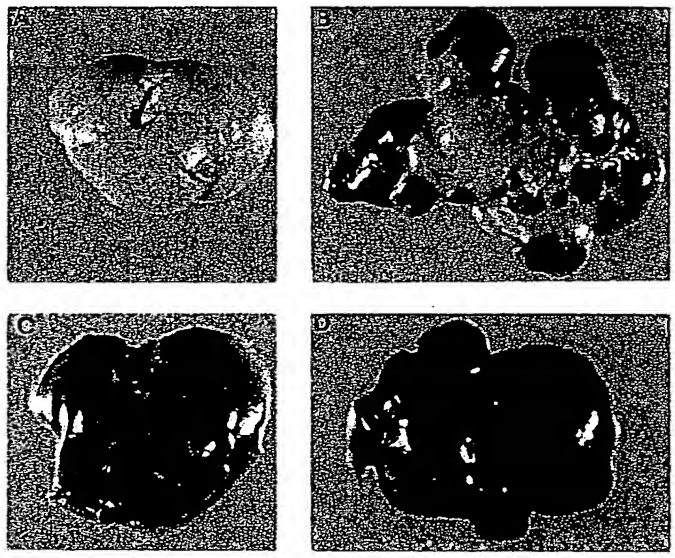

FIG. 1. Liver regeneration in homozygous transgenic *nu/nu* mice transplanted with rat liver cells. (*A*) Nontransplanted, homozygous transgenic control liver (8 weeks). The liver is uniformly pale in color, or white, due to the expression of the hepatotoxic transgene (2). (*B*) Partially regenerated homozygous transgenic *nu/nu* liver transplanted with rat liver cells (8 weeks). The partially regenerated liver contains white areas and nodular areas that are the color of normal liver (i.e., red). (*C*) Nontransgenic control mouse liver. (*D*) Completely regenerated homozygous transgenic *nu/nu* liver transplanted with rat liver cells. This liver is similar in color, shape, and size to the control mouse liver shown in *C*.

inspection (data not shown) because rat-derived liver resembled mouse liver derived from transgenic hepatocytes that had inactivated the transgene (2). The liver-to-body weight ratio of transgenic mice transplanted with rat liver cells was similar to that of nontransgenic control mice (6.8% ± 1.0%, $n = 16$; and 5.8% ± 0.6%, $n = 10$, respectively).

Rat DNA was detected in hemizygous and homozygous mouse livers by Southern blot hybridization (Fig. 2). Restriction fragments of different sizes were detected when mouse versus rat DNA was digested with *Pst* I and hybridized to a probe specific to exon 3 of the mouse phenylethanolamine *N*-methyltransferase gene. The rat-specific restriction band was detected within regenerated liver from both hemizygous and homozygous transplant recipients (Fig. 2). In hemizygous liver samples, the intensity of the rat DNA band varied considerably, ranging from undetectable to comparable to that of homozygous liver samples (Fig. 2). Quantitation of the Southern blot DNA bands demonstrated that up to 56% of the DNA in some liver samples was of rat origin.

Rat hepatocytes were detected immunohistochemically within transplanted livers using a mAb that did not stain mouse hepatocytes (Fig. 3*A*) but strongly stained rat hepatocytes (Fig. 3*B*). No staining of bile ducts or vessels was evident (Fig. 3*B*). Regenerated hemizygous livers that had been transplanted with rat liver cells showed stained and unstained areas (Fig. 3 *C* and *D*). The unstained areas, which were nodular in shape, were most likely composed of mouse hepatocytes that had inactivated the transgene (1). Regenerated homozygous liver showed extensive staining (Fig. 3 *E* and *F*), suggesting that it was composed predominantly of rat hepatocytes. Unstained areas were seen within regenerated homozygous liver around portal tracts, suggesting that these areas were composed of residual host-derived cells (Fig. 3*F*). The biliary epithelium within portal tracts did not react with a mAb specific for rat bile ducts, suggesting that the biliary tree was of mouse origin (data not shown).

Detection of Rat Gene and Protein Expression in Rat–Mouse Chimeric Livers. To detect rat gene expression in the rat–mouse chimeric livers, we analyzed transferrin gene transcripts using probes that could distinguish between rat and mouse transcripts; rat transferrin mRNA levels were expressed as a percentage of total transferrin mRNA detected (rat plus mouse). Transferrin mRNA analysis was performed on randomly selected samples of regenerated (i.e., red) liver from hemizygous and homozygous transgenic recipients. In regenerated liver samples from hemizygous recipients, the percentage of transferrin transcripts of rat origin varied considerably, ranging from <1% to 92% ($n = 12$). In regenerated liver samples from all three homozygous animals analyzed, 90–100% of the transferrin transcripts were derived from the rat ($n = 14$). The average percentages ± SD for each of the three homozygous mice were 98.5% ± 2.1%, $n = 2$; 98.5% ± 0.9%, $n = 3$; and 96.1% ± 4.7%, $n = 9$. Lower levels of rat transferrin mRNA were seen in those areas of liver containing residual white, nonregenerated liver. For example, one area of predominantly white liver from the specimen shown in Fig. 1*B* showed 70% rat transferrin mRNA. (The origin of the rat transcripts in this specimen was unclear, although they were presumably from contaminating rat hepatocytes). The reproducibly high repopulation of homozygous transgenic liver by rat liver cells is consistent with the fact that homozygous animals, unlike hemizygous animals, do not generate many mouse-derived red nodules.

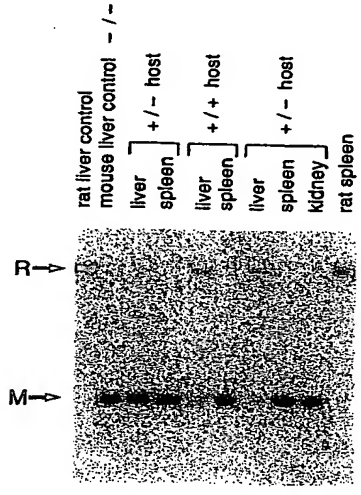

FIG. 2. Southern blot analysis of regenerated liver from transgenic *nu/nu* mice transplanted with rat liver cells demonstrating the presence of rat DNA. Liver samples were taken from regenerated areas of hemizygous (+/−) and homozygous (+/+) transgenic *nu/nu* mouse livers transplanted with rat liver cells and analyzed for rat DNA by Southern blot hybridization. Fragments of different sizes were detected in rat (R) and mouse (M) control livers. In transgenic liver samples containing both mouse and rat fragments, note the diminished intensity of the mouse liver fragment relative to spleen. −/−, Nontransgenic; +/−, hemizygous for the transgene; +/+, homozygous for the transgene.

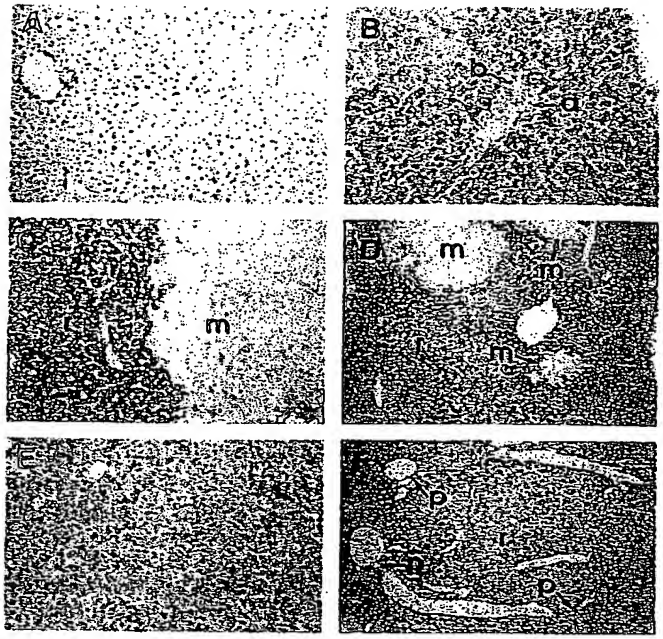

FIG. 3. Immunohistochemical detection of rat hepatocytes in regenerated hemizygous and homozygous transgenic *nu/nu* mouse livers transplanted with rat liver cells. (*A–F*) Frozen sections of liver immunostained with a mAb against rat hepatocytes and counterstained with hematoxylin. (*A*) Control nontransgenic mouse liver. Occasional hepatocytes are lightly stained. (*B*) Control rat liver. All hepatocytes are strongly stained. An arteriole (a) and bile duct (b) within a portal tract are not stained. (*C*) Hemizygous transgenic *nu/nu* mouse transplanted with rat liver cells. Rat-derived (r) stained areas and mouse-derived (m) unstained areas are evident. At the boundary between the two areas, stained and unstained hepatocytes intermingle, without a sharp boundary. No compression of cells, as is often seen in expanding tumors, is evident. (*D*) Hemizygous transgenic *nu/nu* mouse transplanted with rat liver cells. The unstained, mouse-derived (m) areas are nodular in configuration and are separated from one another by areas of rat (r) cells. (*E*) Homozygous transgenic *nu/nu* mouse transplanted with rat liver cells. All cells are stained. (*F*) Homozygous transgenic *nu/nu* mouse transplanted with rat liver cells. Unstained portal areas (p) are grouped around large areas composed of rat hepatocytes (r). (*A–C* and *E*, ×75; *D* and *F*, ×40.)

The percentage of rat mRNA detected in recipient livers showed a linear correlation ($r = 0.9757$) with the percentage of rat DNA detected (Fig. 4). As the rat transferrin mRNA detected in liver samples approached 100%, the rat DNA approached 60%, the percentage of hepatocytes in normal liver. No rat transferrin mRNA was detected with the rat probe in either nontransgenic *nu/nu* livers or in nonimmunosuppressed (non-*nu/nu*) transgenic livers transplanted with rat liver cells (data not shown).

Rat protein expression was detected by immunohistochemistry using antiserum to the rat liver protein, α_{2u}-globulin (12). In the rat, α_{2u}-globulin is synthesized by hepatocytes, secreted into the blood, freely filtered by the kidney, and reabsorbed by renal tubular epithelial cells (13, 14). In normal rat liver, α_{2u}-globulin was detected within the hepatocytes around the central vein (Fig. 5*A*) in a pattern consistent with previous observations (12). In rat–mouse chimeric livers, α_{2u}-globulin was detected in rat-derived areas (Fig. 5*B*) in a pattern similar to that of normal rat liver (Fig. 5*A*). While no α_{2u}-globulin was detected in control mouse kidneys (Fig. 5*C*), it was detected in the renal tubular epithelial cells of a transgenic mouse transplanted with rat liver cells (Fig. 5*D*).

DISCUSSION

To extend the usefulness of the Alb-uPA transgenic mouse model for studying liver cell growth, we introduced the Alb-uPA transgene into immunotolerant *nu/nu* mice. Transplantation of rat liver cells into these mice resulted in the complete reconstitution of mouse liver with rat hepatocytes. This is a remarkable demonstration that a functional liver can be formed from transplanted xenogeneic hepatocytes and suggests that Alb-uPA mouse livers can be reconstituted with hepatocytes from a range of species.

Transplanted rat hepatocytes responded to the Alb-uPA mouse liver environment and divided, replacing the transgenic parenchyma. Rat hepatocytes also responded to mouse modulatory influences, since the rat–mouse chimeric livers were of similar size to mouse control livers. These observations suggest that rat hepatocytes produced surface proteins that could interact appropriately with soluble mouse factors, with extracellular matrix, and with surface proteins on other mouse liver cells.

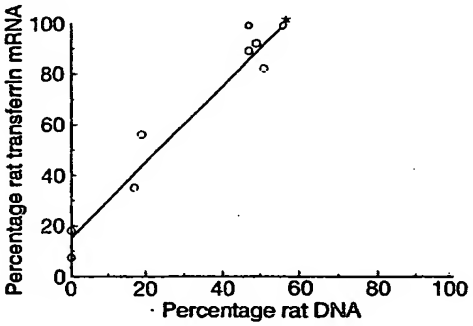

FIG. 4. Rat gene expression versus rat DNA in regenerated liver. Samples of regenerated liver from hemizygous (○) and homozygous (●) transgenic *nu/nu* mice transplanted with rat liver cells were analyzed for rat and mouse transferrin mRNA and for rat DNA. The percentage of rat transferrin mRNA was plotted as a function of rat DNA detected in the same sample. There was a linear correlation between the proportion of rat transferrin mRNA and rat DNA detected ($r = 0.9747$). The line ($y = 1.55x + 14.90$) represents the best fit as determined by regression analysis. Note that as the level of transferrin approaches 100%, the proportion of rat DNA approaches 60%, the estimated percentage of hepatocytes in mouse liver. *, The DNA of a third homozygous mouse liver was too degraded for analysis; mRNA from the same liver showed that 100% of the transferrin mRNA was rat derived (solution hybridization does not require full-length message).

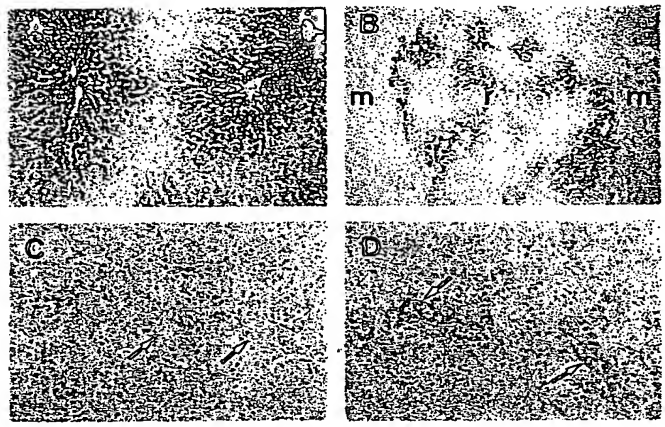

FIG. 5. Immunohistochemical detection of rat α_{2u}-globulin protein expression in transgenic mice. Formalin-fixed, paraffin-embedded sections of liver or kidney were immunostained with a polyclonal antiserum against rat α_{2u}-globulin and counterstained with hematoxylin. (*A*) Control rat liver. Central veins (v) are designated. (*B*) Liver of hemizygous transgenic *nu/nu* mouse transplanted with rat liver cells. Shown is a rat-derived area (r) in between two mouse-derived areas (m). In the rat-derived area, note the perivenous distribution of α_{2u}-globulin protein expression. This distribution is similar to that of the control rat liver shown in *A*. (*C*) Control mouse kidney. Renal tubules are indicated with arrows. (*D*) Kidney of hemizygous transgenic *nu/nu* mouse shown in *B*. Renal tubules are indicated with arrows. (*A* and *B*, ×40; *C* and *D*, ×75.)

Liver function was normal in both hemizygous and homozygous transgenic mice transplanted with rat liver cells. In some hemizygous animals, analysis of transferrin transcripts suggested that the majority of liver function was supplied by mouse hepatocytes. In homozygous animals, on the other hand, over 90% of hepatocellular gene expression was rat derived. Rat hepatocytes must therefore be supplying the liver function of these animals. Since total serum protein and serum albumin levels in animals with rat–mouse chimeric livers were similar to levels in mouse controls, it follows that synthesis of serum proteins by rat cells was appropriately regulated. Finally, the clinical health of the animals suggested that rat hepatocytes were performing other important hepatocellular functions, such as intermediate metabolism and detoxification of organic wastes, at a level appropriate to the mouse, and that the secreted rat hepatocellular proteins were functional in the mouse.

Transplanted rat hepatocytes appeared to grow between the existing portal tracts of the recipient livers, just as did transplanted mouse liver cells in previous transplantation experiments (1). In regenerating livers, portal triads were found not within nodules of donor-derived hepatocytes but on the periphery of the regenerating nodules, in host liver areas. In fully regenerated livers, portal tracts appeared to contain vestiges of host-derived parenchyma (Fig. 3*F*), suggesting that these portal tracts were those of the recipient liver. Further support that portal tracts were derived from the recipient mouse comes from the observation that the biliary ducts, a component of portal tracts, did not react with a rat-specific bile duct antibody (data not shown). It follows that other portal tract components, including vessels and associated connective tissue cells, are also most likely of mouse derivation. This is consistent with the observation that only 56% of DNA was rat-derived in livers showing nearly 100% rat hepatocellular gene expression. Presumably the mouse-derived DNA comes from nonhepatocytes including endothelial cells, biliary epithelial cells, and fibroblasts. Thus we have derived livers in which hepatocytes are derived from one species, the rat, and biliary epithelial cells

and presumably other accessory cells are derived from a second species, the mouse.

The generation of mice with livers composed of rat hepatocytes provides an approach for understanding differences in the biology of rat and mouse liver. For example, after partial hepatectomy, peak mitotic activity of hepatocytes is delayed by 24 hr in mouse liver compared to rat liver (15). It is unclear whether this difference in growth response is due to intrinsic differences between mouse and rat hepatocytes or due to differences in the liver environments in the two species. If the growth response to partial hepatectomy of mouse livers reconstituted with rat hepatocytes resembles that of rat livers, this would suggest that rat hepatocytes have some intrinsic differences from mouse hepatocytes that persist even in a mouse environment. Finally, the demonstration that Alb-uPA mouse livers can be reconstituted with rat hepatocytes raises the exciting possibility that they also can be reconstituted with human liver cells. These human–mouse livers could potentially be used as a repository for human hepatocytes, as reagents for human carcinogenicity studies, or as models for human liver disease.

We thank Douglas Hixson and Ronald Faris for generously providing mAbs to rat hepatocytes and bile duct cells, Arun Roy for rabbit antiserum to rat α_{2u}-globulin, Stan McKnight for a plasmid containing rat transferrin 3′-untranslated region, Jay Degen for assistance in developing the probe used to determine transgene homozygosity, Mary Avarbock for technical assistance, and Carolyn Pope for secretarial assistance. This work was supported by National Institutes of Health Grants HD-23657 and CA-38635 (to R.L.B.) and HD-09172 (to R.D.P.). J.A.R. is a resident in pathology at the University of Pennsylvania School of Medicine.

1. Rhim, J. A., Sandgren, E. P., Degen, J. L., Palmiter, R. D. Brinster, R. L. (1994) *Science* **263**, 1149–1152.
2. Sandgren, E. P., Palmiter, R. D., Heckel, J. L., Daugherty, C. C Brinster, R. L. & Degen, J. L. (1991) *Cell* **66**, 245–256.
3. Fausto, N. (1992) in *The Role of Cell Types in Hepatocarcinogen esis*, ed. Sirica, A. E. (CRC, Boca Raton, FL), pp. 89–108.
4. Sigal, S. H., Brill, S., Fiorino, A. S. & Reid, L. M. (1992) *Am. Physiol.* **263**, G139–G148.
5. Sell, S. (1990) *Cancer Res.* **50**, 3811–3815.
6. Klaunig, J. E., Goldblatt, P. J., Hinton, D. E., Lipsky, M. M Chacko, J. & Trump, B. F. (1981) *In Vitro* **17**, 913–925.
7. Quaife, C. J., Hoyle, G. W., Froelick, G. J., Findley, S. D Baetge, E. E., Behringer, R. R., Hammang, J. P., Brinster, R. L & Palmiter, R. D. (1994) *Transgene Res.* **3**, 388–400.
8. Townes, T. M., Lingrel, J. B., Chen, H. Y., Brinster, R. L. & Palmiter, R. D. (1985) *EMBO J.* **4**, 1715–1723.
9. Hixson, D. C., Allison, J. P., Chesner, J. E., Leger, M. J. & Walborg, E. F. (1983) *Cancer Res.* **43**, 3874–3884.
10. Hixson, D. C. & Allison, J. P. (1985) *Cancer Res.* **45**, 3750–376(
11. Hixson, D. C. & McEntire, K. D. (1985) in *Molecular Determi nants of Animal Form*, ed. Edelman, G. M. (Liss, New York), pp 253–270.
12. Sarkar, F. H., Mancini, M. A., Nag, A. C. & Roy, A. K. (1986) *Endocrinol.* **111**, 205–208.
13. Olson, M. J., Garg, B. D., Murty, C. V. R. & Roy, A. K. (1987 *Toxicol. Appl. Pharmacol.* **90**, 43–51.
14. Roy, A. K., Chatterjee, B., Demyan, W. F., Miliff, B. S., Motwani N. M., Nath, T. S. & Schiop, M. J. (1983) *Rec. Prog. Horm. Res* **39**, 425–461.
15. Fausto, N. (1990) in *Hepatology, A Textbook of Liver Disease*, eds Zakim, D. & Boyer, T. D. (Saunders, Philadelphia), 3rd Ed., pp 49–65.

Woodchuck Hepatocytes Remain Permissive for Hepadnavirus Infection and Mouse Liver Repopulation After Cryopreservation

MAURA DANDRI,[1] MARTIN R. BURDA,[1] ANDREAS GOCHT,[2] EVA TÖRÖK,[3] JÖRG M. POLLOK,[3] CHARLES E. ROGLER,[4] HANS WILL,[1] AND JÖRG PETERSEN[1,5]

Isolated hepatocytes represent a relevant model of the liver and are highly required both for research and therapeutic applications. However, sources of primary liver cells from human beings and from some animal species are limited. Therefore, cryopreservation of hepatocytes could greatly facilitate advances in various research areas. The aim of this study was to evaluate whether cryopreserved primary woodchuck hepatocytes could be used for woodchuck hepatitis B virus (WHV) infection studies, and whether they could maintain their regenerative potential *in vivo* after thawing. Critical steps for good quality of cryopreserved hepatocytes included the use of University of Wisconsin (UW) solution as a main component of the freezing medium, stepwise reduction of dimethylsulfoxide (DMSO) to avoid osmotic shock, and maintenance of low concentrations of DMSO in the culture medium. After cryopreservation, cell viability was still high (70% to 80%), and 50% to 60% of thawed cells attached to the plates. The appearance of covalently closed circular (ccc)DNA and of WHV-replicative forms a few days after *in vitro* infection demonstrated that thawed woodchuck hepatocytes were still susceptible to viral infection, thus proving maintenance of a very high hepatocyte-specific differentiation status. Furthermore, transplantation of woodchuck hepatocytes into the liver of urokinase-type plasminogen activator (uPA)/recombination activation gene-2 (RAG-2) mice, a model of liver regeneration, demonstrated that cryopreserved cells retained the ability to divide and to extensively repopulate a xenogenic liver. Notably, *in vivo* susceptibility to infection with WHV and proliferative capacity of frozen/thawed woodchuck hepatocytes in recipient mice were identical to those observed by transplanting fresh hepatocytes. (HEPATOLOGY 2001;34:824-833.)

Liver transplantation is a successful and well-established treatment for end-stage liver disease and liver failure. However, donor-organ scarcity is a fundamental limitation of this therapy. The availability of highly differentiated primary liver cells to be used for cell-based therapies, such as hepatocyte transplantation, tissue-engineered organs, or for extracorporeal liver support systems, represents an attractive alternative to whole-organ transplantation.[1,2] Freshly isolated normal adult hepatocytes are already widely used in various research areas of hepatology, pharmacology, and toxicology, and initial clinical trials have also shown their potential for therapeutic applications.[3] Essential prerequisites for therapeutic use of hepatocyte transplantation in humans is that primary liver cells must be promptly available, remain highly differentiated, and maintain their proliferative capabilities within the host liver, because only a limited number of cells can be infused into a patient.[4]

In past years, numerous research laboratories established procedures for the isolation of primary hepatocytes from commonly used laboratory animals, rat hepatocytes being the most studied. However, only a few laboratories have the possibility to procure livers and perform the isolation of highly viable hepatocytes from humans and animal species that are scarcely available. Therefore, efficient cryopreservation and banking of hepatocytes would greatly expand and facilitate the use of primary liver cells both for research and therapeutic applications, while decreasing the need of freshly procured livers for the preparation of hepatocytes both from animal species and humans.

Persistent infection with hepatitis B virus (HBV) is one of the major causes of liver disease in humans, being associated with various degrees of chronic hepatitis, cirrhosis, and the development of hepatocellular carcinoma.[5,6] Replication of HBV can be successfully achieved by transfecting hepatoma cell lines with cloned HBV-DNA genomes. These systems have significantly contributed to elucidating various aspects of viral replication[5] and are very useful for production and functional analysis of mutant HBV.[7,8] However, the currently available hepatoma cell lines are not permissive for infection with any of the known HBVs. Therefore, the narrow host range of HBV and the lack of culture systems permissive for hepadnaviral infection have hampered our understanding of some crucial events of the hepadnavirus life cycle. These steps concern identification of the specific cellular receptor(s) involved in the process of attachment of virions to the hepato-

Abbreviations: HBV, hepatitis B virus; ccc, covalently closed circular; WHV, woodchuck hepatitis virus; UPA, urokinase-type plasminogen activator; RAG-2, recombination activation gene-2; FBS, fetal bovine serum; UW, University of Wisconsin; DMSO, dimethylsulfoxide; WHcAg, woodchuck hepatitis core antigen.

From the [1]Heinrich-Pette-Institute for Experimental Virology and Immunology, University of Hamburg, Hamburg, Germany; the Departments of [2]Pathology, [3]Hepatobiliary Surgery and Transplantation, and [5]Medicine, University Hospital Eppendorf, University of Hamburg, Hamburg, Germany; and [4]Albert Einstein College of Medicine, Marion Bessin Liver Research Center, Bronx, NY.

Received April 20, 2001; accepted July 27, 2001.

Supported by a grant from the Deutsche Forschungsgemeinschaft to J.P. (PE /608 2-3). M.D. was supported by an EMBO long-term fellowship. C.E.R. is a recipient of awards from the Irma T. Hirschl-Weiler trust, with additional support from NIH grants. The Heinrich-Pette-Institute is supported by the Freie und Hansestadt Hamburg and the Bundesministerium für Gesundheit, Germany.

Address reprint requests to: Dr. Jörg Petersen, M.D., Medizinische Kernklinik und Poliklinik, Universitätsklinikum Hamburg Eppendorf, Martinistr. 52, D-20246, Hamburg, Germany. E-mail: petersen@hpi.uni-hamburg.de; fax: (49) 40-42803-8065.

0270-9139/01/3404-0029$35.00/0
doi:10.1053/jhep.2001.28189

cyte-membrane (I); characterization of penetration and uncoating steps (II); as well as of the mechanisms of nuclear entry, synthesis, and amplification of the covalently-closed-circular (ccc) DNA, the natural template of viral transcription. To address these important questions, highly viable and readily available primary hepatocytes susceptible to hepadnaviral infection are needed.

Woodchuck hepatitis virus (WHV) is one of the closest-related animal viruses for human HBV-infection studies, and primary woodchuck hepatocytes have been successfully used to investigate specific features of the mammalian hepadnaviruses and for antiviral studies.[9-14] Using a two-step collagenase perfusion method,[15] high yields (about 10^9) of intact primary woodchuck hepatocytes are usually obtained, and freshly isolated hepatocytes are amenable to hepadnaviral infection in culture.[16] However, woodchucks are relatively large animals of outbred origins that can be found in wilderness only in a limited area of the United States, and are difficult to handle in many laboratories. Consequently, sources of primary liver cells from adult woodchucks are limited, though more cells are isolated than can be used immediately after the isolation process. Successful cryopreservation and recovery of primary hepatocytes permissive for hepadnaviral infection would offer the great advantage of performing a larger number of infection studies at different time points, using hepatocytes isolated from a single donor.

Previous studies have shown that adult hepatocytes isolated from various species can be preserved in liquid nitrogen for prolonged periods.[17,18] Experiments with rat hepatocytes have demonstrated that thawed cells retain various functions, such as drug-metabolizing enzyme activities, when cultured under specific conditions. In this report, we present a protocol that allows cryopreservation and efficient recovery of primary hepatocytes isolated from adult woodchucks. In particular, we show that frozen/thawed hepatocytes retain susceptibility to hepadnaviral infection *in vitro* and *in vivo* when transplanted into immunodeficient urokinase-type plasminogen activator (uPA)/recombination activation gene-2 (RAG-2) mice.[20,21] In this system, hepatocyte-targeted expression of uPA leads to cumulative cellular dysfunction and subsequent death of transgene-carrying hepatocytes. This provides a proliferative stimulus for cell growth lasting approximately 2 to 3 months after birth, thereby allowing clonal expansion of transplanted hepatocytes within the diseased host liver.[22,23] We previously reported repopulation of uPA mouse livers with freshly isolated woodchuck hepatocytes, followed by establishment of WHV infection in mice. Here, we demonstrate that cryopreserved woodchuck hepatocytes are able to extensively repopulate a xenogenic liver and that their proliferative capacity is comparable with that observed after transplantation of fresh hepatocytes.

MATERIALS AND METHODS

Isolation of Woodchuck Hepatocytes

Adult woodchucks negative for all WHV serologic markers and WHV chronic carriers were purchased from Northeastern Wildlife (South Plymouth, NY) and housed in the animal facility of the University Hospital Eppendorf in accordance with institutional guidelines and approved protocols. Primary woodchuck hepatocytes were isolated by a two-step *in situ* collagenase perfusion method as previously reported.[20] Briefly, the liver was initially perfused with a preperfusion solution (1× Leffert's buffer: HEPES 10 mmol/L, KCl 3 mmol/L, NaCl 130 mmol/L, NaH_2PO_4-H_2O 1 mmol/L, glucose 10 mmol/L [pH 7.4]) containing 5 mmol/L ethylene glycol-bis(β-aminoethyl ether)-*N,N*-tetraacetic acid (EGTA); then, Leffert's buffer not containing EGTA was allowed to run briefly through the liver; and finally the tissue was perfused with Leffert's buffer containing 5 mmol/L $CaCl_2$ and 0.025% (wt/vol) collagenase type II (Worthington Biochemical Corp., Lakewood, NJ). The flow rate of the perfusate was 60 mL/min. After the perfusion, the digested liver tissue was explanted and placed in cold Leffert's buffer supplemented with 5 mmol/L $CaCl_2$. The liver capsule was cut, and cells were dissociated and then filtered through 100-μm nylon filters. Afterward, cell suspensions were centrifuged 3 times (50*g*, 5 minutes) to separate hepatocytes from nonparenchymal cells, and hepatocyte viability was determined by the Trypan blue exclusion test. Freshly isolated woodchuck hepatocytes were either prepared for cryopreservation or resuspended in a previously described[16] Leibovitz L-15–modified (GibcoBRL, Karlsruhe, Germany) medium containing 10% fetal bovine serum (FBS) (Gemini, Calabasas, CA), and seeded onto 10-cm tissue culture plates (4×10^6 cells/dish) precoated with rat tail collagen type 1 (Becton Dickinson, Bedford, MA). Cells were maintained at 37°C in 5% CO_2 atmosphere, and the culture medium was renewed daily.

Hepatocyte Cryopreservation

Two different freezing procedures were performed in this study to assess the optimal conditions for freezing woodchuck hepatocytes.

One-Step Addition of Dimethylsulfoxide. Freshly isolated hepatocytes were directly suspended at a density of 5×10^6 cells per milliliter in an ice-cold suspension buffer containing 70% University of Wisconsin (UW) solution or various cell culture media, 20% FBS, and 10% dimethylsulfoxide (DMSO) (Sigma, St. Louis, MO). Cells were gently mixed, and after 5 minutes on ice, aliquots of 1-mL cell suspension were transferred to prechilled freezing vials.

Stepwise Addition of DMSO. After centrifugation (50*g*, 5 minutes, 4°C) of freshly isolated hepatocytes, cells were resuspended and gently mixed in 50% of the final volume in a medium containing 76% UW solution, 20% FBS, and only 4% DMSO. After 5 minutes on ice, another volume of medium containing 64% UW, 20% FBS, and 16% DMSO was added to the cell suspension. The final concentration of the cryoprotective agent, DMSO, was 10%. After 5 minutes on ice, hepatocytes were gently pipetted and distributed in freezing vials.

In both cases, the vials were transferred directly to a −70°C freezer, where they remained for 12 to 16 hours before being plunged into liquid nitrogen. In some experiments, primary woodchuck hepatocytes had also been frozen using a computer-controlled freezing machine, in which temperature was reduced at a rate of 1°C/min to −80°C. Hepatocytes were stored for a few days to several months in liquid nitrogen.

Hepatocyte Thawing

For cell thawing, frozen vials were placed directly in a 37°C water bath until the ice disappeared. Immediately after thawing, the vials were put on ice and the efficacy of two thawing procedures was evaluated.

One-Step Reduction of DMSO. Hepatocyte suspensions were transferred into ice-cold Falcon tubes, 4 mL of ice-cold RPMI culture medium was added per milliliter of cell suspension, and cells were gently pipetted.

Stepwise Reduction of DMSO. To gradually reduce the cryoprotectant, ice-cold RPMI culture medium was added to the thawed hepatocyte suspensions as follows: 0.5 mL, 1.5 mL, and 2 mL of medium were added per milliliter of cell suspension at 5-minute intervals. By both procedures, the final concentration of DMSO was 2%. Viability of thawed cells was determined by Trypan blue exclusion. Afterward, the cells were centrifuged (50*g* for 5 minutes, 4°C), the supernatant discarded, and the cell pellet resuspended in culture medium containing 2% DMSO as described below.

Hepatocyte Cultures

Woodchuck hepatocytes were seeded on rat tail collagen type I precoated plates. The plating medium was always supplemented with 10% FBS and 2% DMSO when thawed hepatocytes were used. Four hours after plating, cell culture medium was removed and used to count the number of nonattached cells. Viable plated cells were washed gently and maintained in culture with medium also supplemented with 20 ng /mL of mouse epidermal growth factor (Sigma). To evaluate attachment efficiency, cells were trypsinyzed and counted.

WHV Infection Studies

Twenty-four hours after plating of freshly isolated or cryopreserved woodchuck hepatocytes, 20 μL of serum from a WHV chronically infected woodchuck (1×10^{10} virions per milliliter) was added to each plate, and incubation was performed overnight in the absence of FBS. After WHV-containing medium was removed, plates were washed twice with culture medium and hepatocytes were maintained in L-15 medium containing reduced amounts of FBS (5%). Medium was renewed daily.

Viral DNA Analysis

cccDNA was isolated and analyzed by Southern blot technique according to the method described by Wu et al.[24] To extract genomic DNA, hepatocytes from one 10-cm dish were lysed in 1 mL of a solution containing 0.1% sodium dodecyl sulfate, 150 mmol/L NaCl, 20 mmol/L Tris-HCl (pH 7.5), 20 mmol/L EDTA, and 0.6 mg of proteinase K per milliliter, and incubated at 45°C for 5 hours. After phenol chloroform extraction, the nucleic acids were collected by ethanol precipitation. Pellets were resuspended in TE (10 mmol/L Tris [pH 7.5], 1mmol/L EDTA) buffer, digested with *Pvu II* restriction endonuclease, which is a WHV-DNA noncutter, and then subjected to 1.5% agarose gel electrophoresis and Southern blot analysis as described previously.[14]

To extract viral DNA from cytoplasmic fractions, cultured hepatocytes were incubated in 1 mL lysis buffer (50 mmol/L Tris-HCl [pH 7.5], 0.2% NP40) per dish. After the nuclei were removed by centrifugation (1 minute at 14,000 rpm), sodium dodecyl sulfate and proteinase K (final concentration, 0.1% and 0.5 mg/mL, respectively) were added to the supernatant, and samples were incubated for 2 hours at 37°C. Thereafter, the nucleic acids were phenol chloroform–extracted and ethanol-precipitated as previously described. Pellets were resuspended in TE buffer and directly analyzed by electrophoresis.

To assay for the release of virus, culture medium was first precleared (8,000 rpm; HB-4 Sorvall rotor, 20 minutes, 4°C), and then centrifuged (50,000 rpm; Beckman SW60 rotor, 4 hours, 4°C) through a 20% sucrose cushion. Nucleic acids were extracted from pelleted virions by proteinase K digestion and phenol purification,[25] precipitated by ethanol, and subjected to Southern blot analysis using a 3.3-Kbp Dig-labeled or P^{32}-labeled WHV-DNA probe as previously reported.[14]

To estimate WHV titers in uPA/RAG-2–transplanted mice, 20 μL of mouse serum was dot-blotted onto a nylon membrane according to the procedure described by Scotto[26] and hybridized under high-stringency conditions overnight with a WHV-DNA P^{32}-labeled probe. Serum samples from nontransplanted mice that had been previously injected with WHV-positive serum (see below) served as negative controls. Serial dilutions of woodchuck serum obtained from a WHV carrier (1×10^9 WHV genome equivalent/mL) were loaded in parallel on the blots and served as a standard. Hybridization signals were quantitated by scanning densitometry using a FujiX/2000 laser densitometer (Fuji, Düsseldorf, Germany).

Transplantation of Woodchuck Hepatocytes Into uPA/RAG-2 Mice

Alb-uPA transgenic mice and RAG-2 knockout mice were purchased from Jackson Laboratories (Bar Harbor, ME) and Taconic Farms (Germantown, NY), respectively. Alb-uPA transgenic mice were crossed with RAG-2 knockout mice (RAG-2), and hemizygous uPA/RAG-2 mice were used for transplantation experiments. All animals were housed and maintained under specific pathogen-free conditions in accordance with national and institutional guidelines under approved protocols. A fraction of freshly isolated woodchuck hepatocytes was resuspended in precold RPMI medium and used for transplantation within 3 hours. For freezing, some woodchuck hepatocytes were resuspended in precold UW solution containing 20% FBS and 10% DMSO (1×10^6 viable hepatocytes/mL), placed in a 70°C freezer overnight, and then transferred to liquid nitrogen. After 4 weeks, cells were thawed by rapid immersion in a 37°C water bath, and DMSO was stepwise-reduced as described above. After removal of the freezing medium by centrifugation, thawed hepatocytes were resuspended in precold RPMI medium, and viability was determined by the Trypan blue exclusion test. Five $\times 10^5$ fresh viable or frozen /thawed viable woodchuck hepatocytes were transplanted into 2- to 3-week-old uPA/RAG-2 mice by intrasplenic injection, as previously reported.[20] Two days after transplantation, hepatocyte-recipient and nontransplanted uPA/RAG-2 littermates received a 10-μL intramuscular injection of a WHV-positive woodchuck serum containing approximately 1×10^9 virions/mL.

Histologic Analyses

Three months after hepatocyte transplantation, mice were killed and the livers harvested. Serial cryostat sections of uPA/RAG-2 mouse livers were examined by hematoxylin-eosin staining and immunohistochemistry with a rabbit antiserum (WHc antiserum) against woodchuck hepatitis core antigen (WHcAg). For immunostaining, liver tissue sections were fixed with acetic acid–ethanol (1:3) and paraffin-embedded. Deparaffinized and rehydrated sections were pretreated with 10 mmol/L citrate buffer (pH 6.0). Unspecific binding of antibody was blocked with 10% normal goat serum (Jackson/Dianova, West Grove, PA), and sections were then incubated with WHc antiserum (diluted 1:500). Specifically bound antibody was visualized by incubation with a biotinylated goat anti-rabbit IgG F(ab') antibody (Jackson/Dianova), followed by incubation with peroxidase-conjugated streptavidin-biotin complex (Jackson/Dianova). The peroxidase was developed with 3,3'-diaminobenzidine tetrahydrochloride (Sigma). All washing buffers and antibody solutions contained 0.05 mol/L Tris-buffered saline (pH 7.4) + 0.1% Triton X-100 (Serva, Heidelberg, Germany). To evaluate the extent to which woodchuck hepatocytes repopulated mouse livers, 6 sections per liver lobe were cut from 5 lobes of each of the analyzed mice (30 sections total) and immunostained with WHc antiserum. Ten random fields per section were examined microscopically, and the percentage of hepatitis B core antigen (HbcAg)-positive–stained hepatocytes was calculated.

RESULTS

Freezing Conditions. To determine the optimal components of the freezing medium, preliminary experiments were performed using various culture media (Leibowitz L-15, RPMI, Williams' E medium) or UW solution, which is used for organ preservation before transplantation. We observed that the highest viability and the most reproducible results were obtained when hepatocytes isolated either from woodchucks or rats were preserved in UW solution (Table 1). Furthermore, previous studies performed in other laboratories and by us showed that DMSO has better cryoprotective capacities than glycerol, 1,2-propanediol, or dextrans, because this cryoprotective agent very efficiently reduces ice-crystal formation during the freezing process.[27,28] Therefore, to cryopreserve primary hepatocytes, freshly isolated cells were resuspended in freezing medium containing 70% UW solution, 20% FBS, and 10% DMSO. In agreement with other studies,[18] we also observed that hepatocytes were best preserved with a 10%

TABLE 1. Viability of Hepatocytes Cryopreserved Using Various Freezing Media

Species	Freezing Medium (70:20:10)	Hepatocyte Viability: Freshly Isolated	Cryopreserved Addition of DMSO: One-step	Cryopreserved Addition of DMSO: Stepwise
Woodchuck				
WHV⁻	L-15/FBS/DMSO		62%	64%
	RPMI/FBS/DMSO	95%	59%	ND
	UW/FBS/DMSO		74%	71%
Rat	Williams' E/FBS/DMSO		57%	ND
	RPMI/FBS/DMSO	83%	55%	ND
	UW/FBS/DMSO		79.5%	ND

DMSO concentration, while higher FBS concentrations (20%) did not improve cell viability (data not shown).

To determine whether slow addition of DMSO was a critical step for hepatocyte cryopreservation, cell pellets were either resuspended directly in freezing medium containing 10% DMSO or, alternatively, the concentration of the cryoprotectant was gradually increased (see Materials and Methods). We observed that stepwise addition of DMSO did not significantly increase cell viability after thawing (Table 1). Therefore, one-step addition of DMSO was chosen for further experiments.

The cooling rates are considered very critical parameters for successful cryopreservation of primary hepatocytes. In our studies, hepatocytes were resuspended at a final concentration of 5×10^6 cells per milliliter of freezing medium, distributed into freezing vials, and immediately transferred to −70°C, where they were maintained for 16 to 24 hours before being plunged into liquid nitrogen. In contrast with previous cryopreservation protocols that have favored the use of an intermediate step at −20°C,[17,18] we observed that viability of thawed woodchuck hepatocytes was further reduced by 10% to 25% when the vials were preincubated for 20 minutes at room temperature and/or placed for 20 minutes at −20°C, before being transferred to −70°C (data not shown). In some experiments, hepatocytes were also frozen using a computer-controlled freezing machine. As shown in Table 2, the results obtained by freezing the cells with the machine were comparable but not generally better than those achieved by placing the cells first at −70°C and then into liquid nitrogen.

Viability and Attachment Efficiency of Thawed Woodchuck Hepatocytes. As shown in Tables 1 and 2, high cell viability (70% to 80%) was estimated by the Trypan blue exclusion test when primary woodchuck hepatocytes were rapidly thawed and the cryoprotectant was gradually reduced to 2% to limit the osmotic shock caused by the outflow of DMSO. Concerning the culture medium composition, it has been shown that low concentrations of DMSO improved hepatocyte survival and function *in vitro*.[29] Therefore, after a short centrifugation to remove the freezing medium, cell pellets were resuspended in cell culture medium supplemented with 10% FBS and 2% DMSO. About 56% of the thawed uninfected woodchuck hepatocytes (approximately 77% of the thawed viable cells) were able to attach to the collagen-precoated dishes when DMSO concentration was reduced stepwise to 2% and maintained in the culture medium. As shown in Table 2, the percentage of attached hepatocytes was markedly lower (45% vs. 56%) when the cryoprotectant was removed at once. Moreover, we observed that, regardless of the thawing procedure used, addition of 2% DMSO in the culture medium not only increased attachment efficiency, but also improved survival of thawed hepatocytes in culture, because thawed cells plated in the absence of DMSO showed signs of degeneration within a few days (data not shown).

As shown in Fig. 1, phase-contrast microscopy indicated that the morphology of cultured cells prepared from fresh and frozen/thawed woodchuck hepatocytes was very similar for at least 1 week. However, after 10 days in culture, some signs of degeneration with increased cytoplasmic granularity became evident in all the cultures prepared from frozen cells. Hepatocytes isolated from WHV chronically infected woodchucks could also be successfully cryopreserved, although viability of thawed WHV-positive cells was generally lower (approximately 50% vs. 70%) than values obtained with uninfected hepatocytes (see Table 2).

Temporary Storage of Cryopreserved Hepatocytes on Dry Ice Drastically Reduces Attachment Efficiency. To test whether liquid nitrogen–cryopreserved woodchuck hepatocytes could be conveniently transported to a different location by maintaining the cells on dry ice for a certain time before being thawed and used, viability and attachment of uninfected woodchuck hepatocytes was determined. Hepatocytes were either rapidly thawed by taking them from the liquid nitrogen tank to a 37°C water bath as described above, or, alternatively, the frozen vials were placed on dry ice for various periods before thawing

TABLE 2. Viability and Attachment Efficiency of Woodchuck Hepatocytes Freshly Isolated and Cryopreserved by Using Different Freezing and Thawing Conditions

Hepatocyte Source	Fresh Hepatocytes: Viability (%)	Fresh Hepatocytes: Attachment (%)	Cryopreserved Hepatocytes (−70°C/N_2): One-step Removal of DMSO: Viability (%)	One-step Removal of DMSO: Attachment (%)	Stepwise Removal of DMSO: Viability (%)	Stepwise Removal of DMSO: Attachment (%)
WHV⁻ woodchuck	94 ± 3 (n = 8)	77 ± 3 (n = 8)	64 ± 3 (n = 4)	45 ± 4 (n = 4)	73 ± 7 (n = 6)	56 ± 4 (n = 6)
WHV⁺ woodchuck	90 ± 3 (n = 4)	74 ± 2 (n = 4)	50 ± 4 (n = 3)	38 ± 2 (n = 3)	60; 43	40; 31
			Cryopreserved Hepatocytes (machine/N_2)			
	Fresh Hepatocytes: Viability (%)	Fresh Hepatocytes: Attachment (%)	One-step Removal of DMSO: Viability (%)	One-step Removal of DMSO: Attachment (%)	Stepwise Removal of DMSO: Viability (%)	Stepwise Removal of DMSO: Attachment (%)
WHV⁻ woodchuck	90; 95	76; 80	63; 65	45; 46	71; 76	56; 58

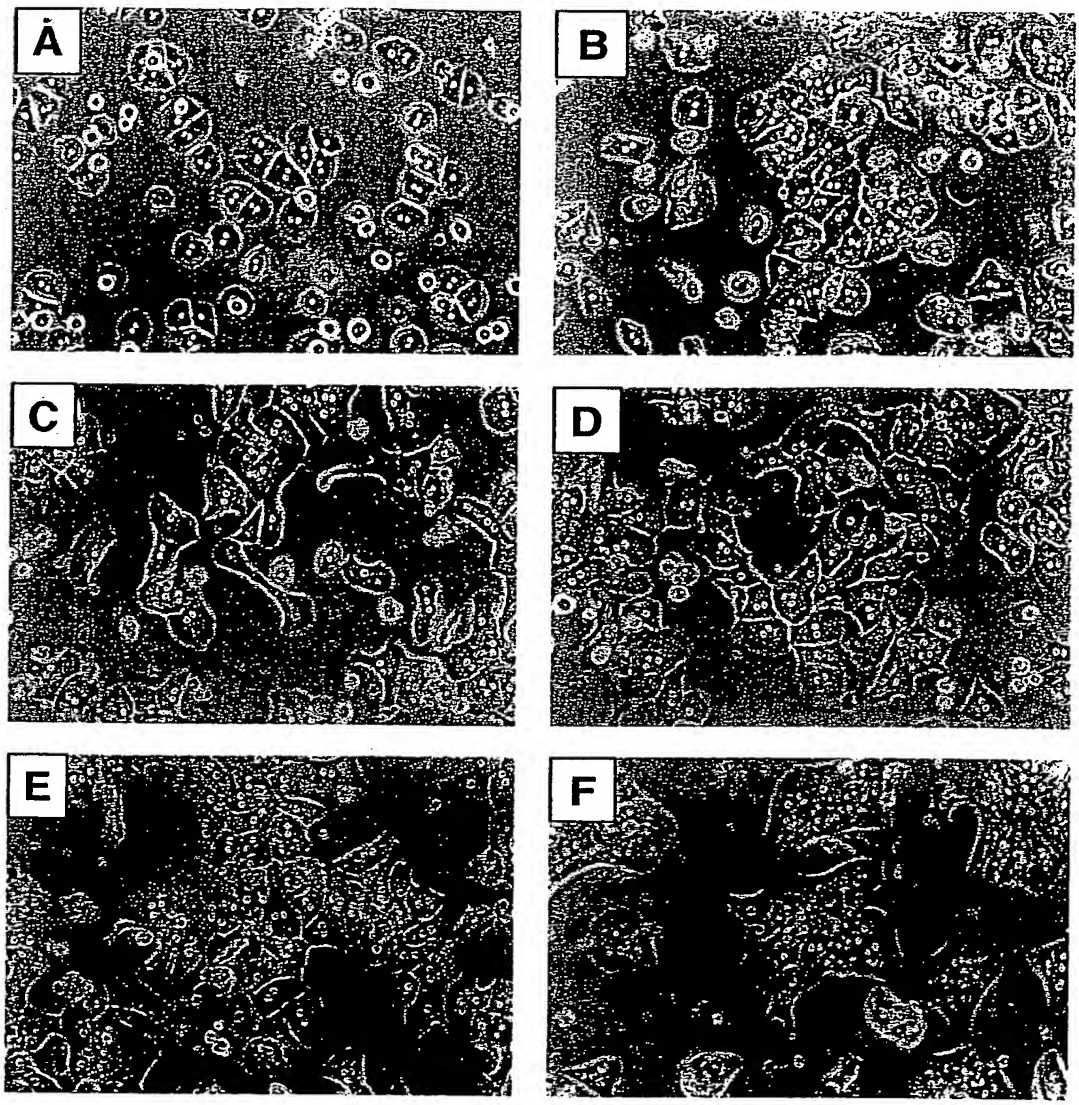

FIG. 1. Light-microscopic appearance of woodchuck hepatocyte cultures prepared from cryopreserved cells. Thawed cells were cultured for 4 hours (A), 24 hours (B), 2 days (C and D), and 4 days (E). (F) Freshly isolated woodchuck hepatocytes cultured for 4 days (original magnification ×200). When attached and maintained in culture in the presence of DMSO, thawed woodchuck hepatocytes were morphologically identical to unpreserved hepatocytes.

the cells. In all cases, DMSO concentration was reduced stepwise to 2%, the freezing medium was removed, cells were resuspended in complete plating medium, and viability was determined by the Trypan blue exclusion test. As shown in Fig. 2, the percentage of viable cells remained almost unchanged for at least 24 hours of storage on dry ice. However, we observed that incubation on dry ice dramatically impaired the attachment capability of cryopreserved hepatocytes on collagen-coated plates. Six hours after plating the cells, the medium was removed and the number of both attached and nonattached cells was determined. After 24 hours of storage of frozen vials on dry ice, attachment was reduced by 50%, while after 48 hours, no hepatocytes attached to the plate.

In Vitro *Infection of Cryopreserved Woodchuck Hepatocytes With WHV.* Successful *in vitro* infection of primary hepatocytes with HBVs requires maintenance of a very high hepatocyte-specific differentiation status, and usually freshly isolated hepatocytes become nonpermissive for hepadnaviral infection shortly after plating.[13,30] To determine whether cultured hepatocytes were still permissive for hepadnaviral infection after cryopreservation, plates containing either freshly isolated or thawed woodchuck hepatocytes were incubated overnight with infectious WHV serum (see Materials and Methods). To determine whether WHV virions were taken up by the cells, and whether viral DNA was uncoated and converted to cccDNA into the nucleus of newly infected hepatocytes, we first investigated the time course of cccDNA synthesis in freshly isolated hepatocyte cultures. Cells were harvested 1, 2, 4, and 6 days after infection and analyzed for the presence of cccDNA.

As shown in Fig. 3A, formation of cccDNA was first detected 48 hours after the virus was added to the cultures of freshly isolated cells. cccDNA levels increased rapidly in the following days, until day 6, when cccDNA appeared to have reached a steady-state level.[13,14] As shown in Fig. 3B, 6 days after infection of thawed cells with WHV-positive serum, high levels of cccDNA could be demonstrated by Southern blot analysis, indicating successful uptake of viral particles by frozen and thawed woodchuck hepatocytes.

To evaluate whether *in vitro* experimental infection of cryopreserved hepatocytes led to the production of WHV viral particles, DNA (genomic and cytoplasmic) was isolated from thawed hepatocytes infected 24 hours after seeding and har-

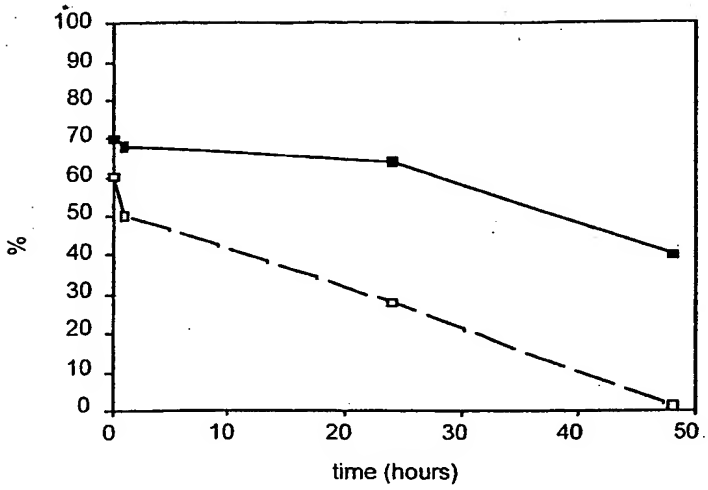

FIG. 2. Cryopreserved hepatocytes are very sensitive to temperature changes. Viability (■) and attachment (□) efficiency of cryopreserved hepatocytes after thawing is highest when frozen cells are immediately warmed to 37°C and plated. Any storage of the cells on dry ice before plating drastically reduces attachment efficiency. After 48 hours, no hepatocytes attached to the plate. Viability and attachment rates are expressed in percentage (%) on the *vertical* axis. Time is expressed in hours on the *horizontal* axis.

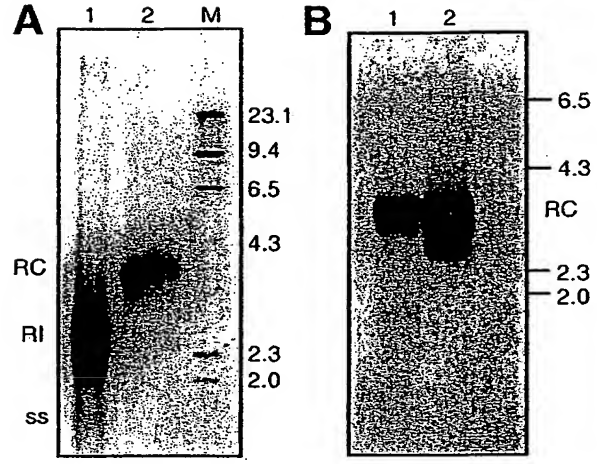

FIG. 4. Productive WHV infection of woodchuck hepatocytes after cryopreservation. (A) WHV DNA from intracellular core particles (*lane 1*) was isolated from thawed hepatocytes infected 24 hours after seeding and harvested 7 days after infection. Culture fluids were also collected and virus particles from 3 mL of medium were pelletted, and the nucleic acids extracted and analyzed by Southern blotting (*lane 2*). Relaxed circular (RC), replicative intermediates (RI), and single-stranded (SS) forms are indicated. M, Dig-labeled λ-*Hind* III marker. (B) Southern blot analysis of virus particles released into the culture medium. *Lane 1*, 7 days after infection, 6 mL of culture medium from thawed hepatocytes was ultracentrifuged and the extracted DNA was analyzed. *Lane 2*, viral DNA was directly extracted from 10 μL of serum from a WHV-chronic carrier (1×10^{10} virions per milliliter) and loaded onto the gel. Migration positions of the molecular-weight marker are indicated. All samples were loaded onto a 1.5% agrose gel.

vested 7 days after infection. WHV-replicative intermediates and single-strand DNA, indicative of new viral DNA synthesis, were detected by Southern blotting (Fig. 4A), demonstrating that after infection and conversion of infectious viral DNA to cccDNA, new WHV-DNA molecules were synthesized in cultures from those cryopreserved hepatocytes. Finally, to assess whether viral particles were actively secreted into the culture medium, 7 days after infection of cryopreserved liver cells, WHV-DNA–containing particles were precipitated from the medium, which was maintained in culture for only 24 hours, and analyzed by Southern blotting. Virus secretion was observed in cultures of thawed hepatocytes. Virus titers reached a level of approximately 5×10^7 WHV genome equivalents per milliliters of medium, as determined by scanning densitometry (Fig. 4B).

Proliferative Capacity of Cryopreserved Woodchuck Hepatocytes In Vivo. To assess whether cryopreserved hepatocytes could engraft a xenogenic liver and could retain the capacity to proliferate after cryopreservation, naive frozen/thawed woodchuck hepatocytes were transplanted into immunodeficient uPA/RAG-2 transgenic mice. Transplantation experiments were performed using fresh and frozen/thawed hepatocytes isolated from the same woodchuck, and their ability to repopulate diseased mouse liver was compared. Frozen hepatocytes were kept in liquid nitrogen for 4 weeks before thawing and transplantation. Viability of fresh versus frozen cells was 95% and 70%, respectively. The same number (5×10^5) of viable fresh or viable frozen/thawed hepatocytes were injected into 9 recipient mice. Five recipient mice received cryopreserved cells and 4 mice received freshly isolated hepatocytes. Two mice, 1 from each group, died shortly after the transplantation procedure because of bleeding complications, which is a common problem in these mice.[20,21]

To determine whether transplanted woodchuck hepatocytes survived and remained highly differentiated in mouse

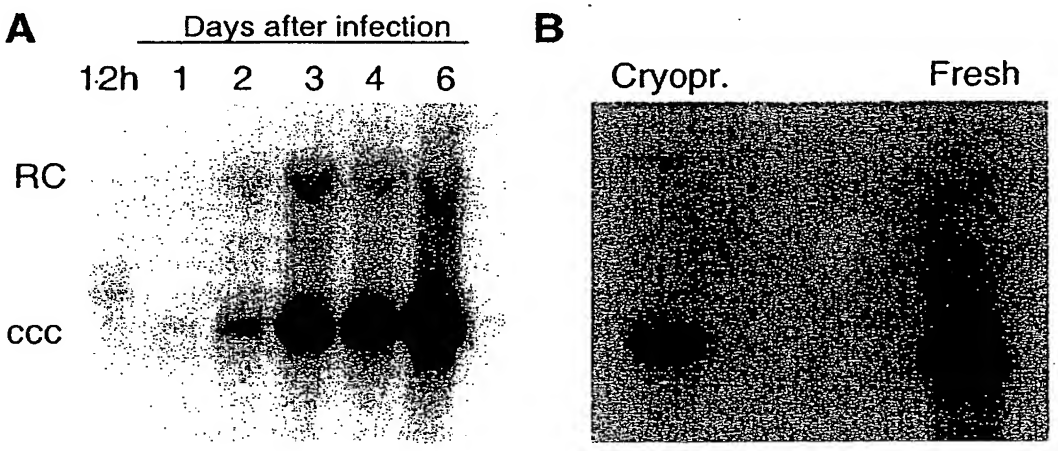

FIG. 3. Detection of cccDNA in the nucleus of thawed woodchuck hepatocytes infected with WHV+ serum 1 day after plating. cccDNA was extracted either from freshly isolated or cryopreserved primary woodchuck hepatocytes at different times after plating and infection. (A) Time course of cccDNA synthesis in freshly isolated hepatocyte cultures (days are indicated). Approximately 3×10^6 cells were used for each time point. (B) Six days after infection, cccDNA was extracted from approximately 2×10^6 cryopreserved and 1×10^6 fresh woodchuck hepatocytes and loaded onto a 2% agarose gel. RC, relaxed circular DNA; ccc, cccDNA.

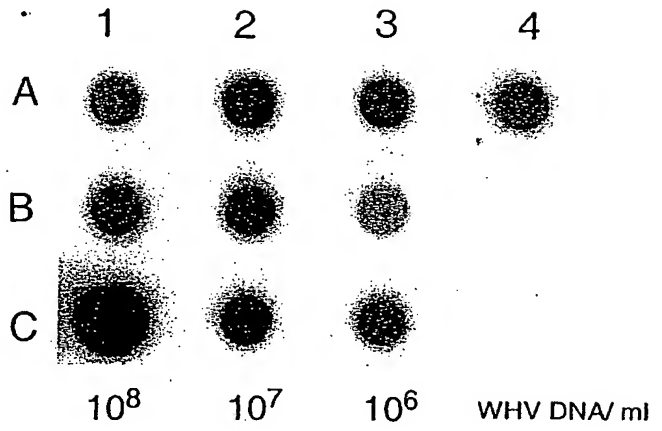

FIG. 5. Establishment of WHV infection in uPA/RAG-2 mice transplanted with cryopreserved naive woodchuck hepatocytes. Serum samples from mice repopulated with thawed (A) or fresh (B) woodchuck hepatocytes and infected with WHV 2 days after transplantation were analyzed by dot-blot using a P^{32}-labeled genome-length WHV-DNA probe. (C) Test mixtures of untransplanted mouse serum containing serial dilutions of WHV^+ woodchuck serum (WHV genome equivalent/mL serum are indicated) were used as standard. All sera were taken 3 months after infection.

livers, a few days after transplantation, all 7 transplanted mice and 3 nontransplanted littermates were inoculated with WHV-infectious serum (see Materials and Methods). Three months after hepatocyte transplantation, when liver repopulation was complete, mice were killed, serum samples collected, and livers analyzed. Serum samples were analyzed by dot-blot hybridyzation for the presence of WHV DNA. As shown in Fig. 5, viral titers ranged between 1×10^5 to 1×10^7 WHV genomes per milliliter in mice transplanted either with fresh or cryopreserved woodchuck hepatocytes, while WHV DNA was not detected in serum of untransplanted mice that also had been inoculated with WHV-infectious serum (*i.e.*, Fig. 5, sample 4B). There was no significant difference in the virus titers from uPA/RAG-2 mice containing fresh or frozen hepatocytes, demonstrating that mouse livers had been engrafted both with fresh and with frozen woodchuck hepatocytes, and that thawed cells remained permissive for WHV infection.

To roughly estimate the level of repopulation, and therefore to determine whether cryopreserved woodchuck hepatocytes maintained their ability to proliferate and replace damaged parenchyma, immunohistochemistry was performed using a WHc antiserum, which is an unequivocal marker to distinguish between mouse host and transplanted woodchuck hepatocytes (Fig. 6A). Sections of mouse liver tissues repopulated either with fresh or cryopreserved woodchuck hepatocytes were also analyzed by HE staining. As observed in earlier transplantation studies and shown in Fig. 6B, large portions of the mouse liver were repopulated with woodchuck hepatocytes, which showed a more intense eosin staining. Histologic analysis of randomly chosen mouse liver sections showed that both frozen and fresh woodchuck hepatocytes were present in abundance in all liver lobes and in all animals, replacing approximately 30% to 60% of damaged livers. As observed in previous transplantation studies with uPA/RAG-2 mice, the degree of repopulation varied among mice within each group, but there was no significant difference in the amount of woodchuck hepatocytes observed in mice that contained hepatocytes of frozen origin compared with those harboring cells of fresh origin.

DISCUSSION

Studies on the early events of the hepadnavirus life cycle require the use of highly differentiated primary hepatocyte cultures that are competent for HBV infection. Cryopreservation of woodchuck hepatocytes has been previously reported, although only a small fraction of those frozen cells were able to attach to the plates after thawing, and there was no indication of *in vitro* infection of those cells with WHV.[32] Our findings indicate that cryopreserved primary woodchuck hepatocytes, properly thawed and cultured, are suitable for infection studies with woodchuck hepatitis B virus. Various freezing-thawing procedures, as well as culturing conditions, were analyzed here.

We chose to use UW solution as the main component of the freezing medium and to directly suspend the hepatocytes in a freezing medium containing 10% DMSO and 20% FBS, because stepwise addition of the cryoprotectant, DMSO, did not significantly increase cell viability after thawing. The transition from liquid to solid phase is considered a very critical step in the freezing process; therefore, intracellular ice-crystal formation, which occurs between −15°C and −20°C, should be minimized. We observed that cell viability was better preserved when the hepatocytes were directly transferred to −70°C, without an intermediate step at −20°C, as suggested by others.[17,18] Furthermore, the use of a programmable freezing chamber did not appear to give better results than the use of a −70°C freezer (73.5% vs. 73 ± 7% viability, respectively) before plunging the cells into liquid nitrogen. Thus, our observations imply that cryopreservation of woodchuck liver cells can be efficiently performed in most laboratories, without the need of specific cooling machines.

Previous studies suggested that the cryoprotectant should be removed from thawed cells as soon as possible to avoid potential toxicity.[33] However, low concentrations of DMSO (1% to 2%) in the culture medium have been shown to support cell differentiation[34-36] and to increase infectivity of freshly isolated hepatocytes.[37] Here, we provide evidence that after stepwise reduction of DMSO, maintenance of 2% DMSO in culture not only improved attachment rates of thawed hepatocytes, but it allowed establishment of WHV infection *in vitro*. In fact, regardless of the thawing procedure used (one-step or stepwise reduction of DMSO), we failed to demonstrate WHV infection of thawed cells cultured in the absence of DMSO (data not shown).

The cccDNA analysis by Southern blot revealed that infectivity of cryopreserved hepatocytes was reduced by only approximately 50% compared with values obtained with freshly isolated cells. Thus, these data demonstrate that the most critical and hepatocyte-specific steps of the virus life cycle, such as receptor recognition, cell and nuclear entry, as well as conversion of the viral genome into the covalently closed circular form (cccDNA), can be investigated using cryopreserved hepatocytes. Furthermore, the presence of WHV-replicative intermediates and single-strand DNA in the cytoplasm of infected cells, as well as the release of progeny virus 1 week after infection, indicated that the replication cycle of WHV in cryopreserved liver cells was complete. Although we cannot rule out the possibility that input virus had contributed to the intensity of the signals corresponding to replicative intermediates and single-stranded DNA, we consider this unlikely. In

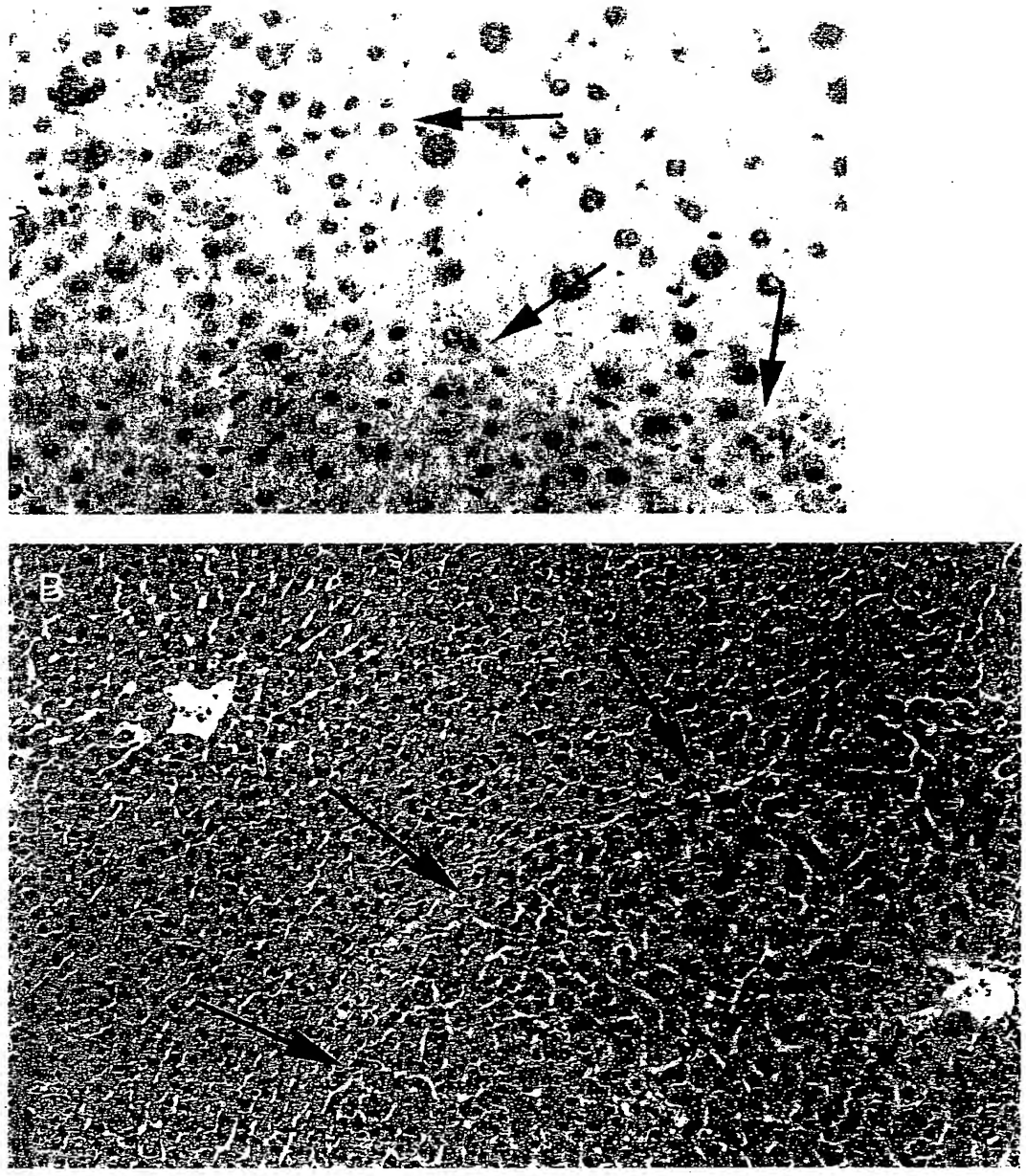

FIG. 6. Histologic analysis of uPA/RAG-2 mouse livers transplanted with cryopreserved woodchuck hepatocytes, infected with WHV, and killed after 3 months. (A) Detection of $WHcAg^+$ woodchuck hepatocytes in mouse livers by immunostaining with a WHc antiserum. Transplanted woodchuck hepatocytes had seeded the liver and grown in a nodular pattern, replacing large portions of the mouse liver. (B) Hematoxylin-eosin staining of frozen liver sections from uPA/RAG-2 mice. Woodchuck hepatocytes show a more intense eosin staining. *Arrows* mark borders. (Original magnification [A] ×100; [B] ×50.)

previous infection studies performed with noninfectious, UV-inactivated virus, we failed to detect viral DNA 1 week after infection[38] (Dandri M, Will H, May, 1998, unpublished data).

Banking and shipment of cryopreserved cells would not only reduce the number of animals needed for research, but it would also offer a larger number of laboratories the opportunity to perform specific studies without the need to set up and perform the isolation process. Our results with woodchuck liver cells showed that cryopreserved primary hepatocytes could be efficiently recovered and used both for *in vitro* and *in vivo* studies, provided that the cells were kept in liquid nitrogen until use. In fact, temporary storage of frozen hepatocytes at higher temperatures, like on dry ice, appeared to induce irreversible damage to the cells, and, consequently, attachment efficiency was drastically reduced.

Because of the scarcity of fresh human livers, cryopreservation and effective recovery of primary human hepatocytes are greatly needed for various therapeutic applications. For instance, feasibility of hepatocyte transplantation in humans has been demonstrated,[3] and it may offer an attractive therapeutic alternative to whole-liver transplantation to treat some metabolic liver diseases, such as familial hypercholesterolemia, Wilson's disease, and α_1-antitrypsin deficiency.[2,39] However, because only a limited number of cells can be safely injected into a patient,[40] transplanted hepatocytes must retain their ability to grow to become a significant hepatocyte mass in the host liver. To determine whether cryopreserved woodchuck hepatocytes retain their proliferative potential *in vivo*, we performed transplantation experiments in immunodeficient uPA/RAG-2 mice, using either fresh or cryopreserved cells. The expression of WHV-specific markers, such as WHcAg, permits a rough estimate of the magnitude of liver repopulation. Moreover, productive infection with WHV is an unequivocal marker in determining survival and differentia-

tion status of primary woodchuck hepatocytes in transplanted mice.[20] As observed in earlier studies,[20] productive infection with WHV was achieved in all transplanted mice engrafted with naive woodchuck hepatocytes. Furthermore, our *in vivo* infection studies indicate that susceptibility for infection with WHV in mice harboring cryopreserved cells was comparable with that observed by infecting animals containing fresh woodchuck hepatocytes.

Although we used 5×10^5 viable woodchuck hepatocytes for all our transplantation experiments, which represents only 0.5% of the hepatocyte mass present in a mouse liver, the number of hepatocytes visible by immunohistochemistry was always well above 30%, regardless of whether freshly isolated or cryopreserved hepatocytes were used. Thus, these findings demonstrate that even if all transplanted cells would have reached the liver, which is known not to be the case,[4,41] cryopreserved hepatocytes were able to extensively repopulate diseased mouse liver. uPA transgenic mice are an elegant model of liver regeneration, and they have been recently used by Sandgren et al.[31] to examine the regenerative capacity of thawed mouse hepatocytes. Together, these findings indicate that cryopreserved hepatocytes from various species retain their regenerative capacity after thawing, which is a fundamental requirement for potential therapeutic applications in the future.

Our data using pure cultures of thawed woodchuck hepatocytes showed that cell survival *in vitro* was limited to 1 to 2 weeks. Although this time frame was sufficient to infect the cells and to investigate the early steps of viral replication, it appears that thawed cells are not well suited for long-term investigations, as may be required for some antiviral studies. However, our *in vivo* results have shown that when thawed hepatocytes were transplanted into uPA/RAG-2 mice, the cells could recover completely and viral titers were similar to those found using fresh hepatocytes. Together, these observations indicate that in the proper environment, cryopreserved hepatocytes are able to survive for prolonged periods, and that conditions of incubation after thawing are critical for maintenance of functional activities. Preliminary studies showed that a similar freeze-thaw protocol permitted long-term preservation of hepatocytes also isolated from humans. Therefore, it will be important to determine whether human hepatocytes can also efficiently recover and retain their proliferative potential after cryopreservation.

In conclusion, the preservation of highly specific hepatocyte functions, such as permissiveness for HBV infection and proliferative capacity after thawing, suggests that properly cryopreserved hepatocytes are suitable not only for various *in vitro* studies, but possibly also for studying the potential of therapeutic hepatocyte transplantation in humans.

Acknowledgment: The authors are grateful to D. Zuckerman, S. Schnöger, and R. Reusch for excellent technical assistance.

REFERENCES

1. Gupta S, Rajvanshi P, Bhargava KK, Kerr A. Hepatocyte transplantation: progress toward liver repopulation. Prog Liver Dis 1996;14:199-222.
2. Lake JR. Hepatocyte transplantation [Editorial; Comment]. N Engl J Med 1998;338:1463-1465.
3. Fox IJ, Chowdhury JR, Kaufman SS, Goertzen TC, Chowdhury NR, Warkentin PI, Dorko K, et al. Treatment of the Crigler-Najjar syndrome type I with hepatocyte transplantation [Comments]. N Engl J Med 1998; 338:1422-1426.
4. Gupta S, Bhargava KK, Novikoff PM. Mechanisms of cell engraftment during liver repopulation with hepatocyte transplantation. Semin Liver Dis 1999;19:15-26.
5. Ganem D. Hepadnaviridae and their replication. In: Fields BN, Knipe DN, Howley PM, eds. Virology. Vol 2, 3rd ed. Philadelphia: Lippincott-Raven, 1996:2703-2739.
6. Buendia MA. Hepatitis B viruses and cancerogenesis. Biomed Pharmacother 1998;52:34-43.
7. Gunther S, Piwon N, Iwanska A, Schilling R, Meisel H, Will H. Type, prevalence, and significance of core promoter/enhancer II mutations in hepatitis B viruses from immunosuppressed patients with severe liver disease. J Virol 1996;70:8318-8331.
8. Sterneck M, Kalinina T, Gunther S, Fischer L, Santantonio T, Greten H, Will H. Functional analysis of HBV genomes from patients with fulminant hepatitis. HEPATOLOGY 1998;28:1390-1397.
9. Roggendorf M, Tolle TK. The woodchuck: an animal model for hepatitis B virus infection in man. Intervirology 1995;38:100-112.
10. Zoulim F, Saputelli J, Seeger C. Woodchuck hepatitis virus X protein is required for viral infection in vivo. J Virol 1994;68:2026-2030.
11. Dandri M, Petersen J, Stockert RJ, Harris TM, Rogler CE. Metabolic labeling of woodchuck hepatitis B virus X protein in naturally infected hepatocytes reveals a bimodal half-life and association with the nuclear framework. J Virol 1998;72:9359-9364.
12. Tennant BC, Baldwin BH, Graham LA, Ascenzi MA, Hornbuckle WE, Rowland PH, Tochkov IA, et al. Antiviral activity and toxicity of fialuridine in the woodchuck model of hepatitis B virus infection. HEPATOLOGY 1998;28:179-191.
13. Moraleda G, Saputelli J, Aldrich CE, Averett D, Condreay L, Mason WS. Lack of effect of antiviral therapy in nondividing hepatocyte cultures on the closed circular DNA of woodchuck hepatitis virus. J Virol 1997;71: 9392-9399.
14. Dandri M, Burda MR, Will H, Petersen J. Increased hepatocyte turnover and inhibition of woodchuck hepatitis B virus replication by adefovir in vitro do not lead to reduction of the closed circular DNA. HEPATOLOGY 2000;32:139-146.
15. Seglen PO. Preparation of isolated rat liver cells. Methods Cell Biol 1976; 13:29-83.
16. Aldrich CE, Coates L, Wu TT, Newbold J, Tennant BC, Summers J, Seeger C, et al. In vitro infection of woodchuck hepatocytes with woodchuck hepatitis virus and ground squirrel hepatitis virus. Virology 1989; 172:247-252.
17. Chesne C, Guyomard C, Fautrel A, Poullain MG, Fremond B, De Jong H, Guillouzo A. Viability and function in primary culture of adult hepatocytes from various animal species and human beings after cryopreservation. HEPATOLOGY 1993;18:406-414.
18. Guillouzo A, Rialland L, Fautrel A, Guyomard C. Survival and function of isolated hepatocytes after cryopreservation. Chem Biol Interact 1999; 121:7-16.
19. Fautrel A, Joly B, Guyomard C, Guillouzo A. Long-term maintenance of drug-metabolizing enzyme activities in rat hepatocytes after cryopreservation. Toxicol Appl Pharmacol 1997;147:110-114.
20. Petersen J, Dandri M, Gupta S, Rogler CE. Liver repopulation with xenogenic hepatocytes in B and T cell–deficient mice leads to chronic hepadnavirus infection and clonal growth of hepatocellular carcinoma. Proc Natl Acad Sci U S A 1998;95:310-315.
21. Dandri M, Burda MR, Torok E, Pollok JM, Iwanska A, Sommer G, Rogiers X, et al. Repopulation of mouse liver with human hepatocytes and in vivo infection with hepatitis B virus. HEPATOLOGY 2001;33:981-988.
22. Sandgren EP, Palmiter RD, Heckel JL, Daugherty CC, Brinster RL, Degen JL. Complete hepatic regeneration after somatic deletion of an albumin-plasminogen activator transgene. Cell 1991;66:245-256.
23. Rhim JA, Sandgren EP, Degen JL, Palmiter RD, Brinster RL. Replacement of diseased mouse liver by hepatic cell transplantation. Science 1994;263: 1149-1152.
24. Wu TT, Coates L, Aldrich CE, Summers J, Mason WS. In hepatocytes infected with duck hepatitis B virus, the template for viral RNA synthesis is amplified by an intracellular pathway. Virology 1990;175:255-261.
25. Gunther S, Li BC, Miska S, Kruger DH, Meisel H, Will H. A novel method for efficient amplification of whole hepatitis B virus genomes permits rapid functional analysis and reveals deletion mutants in immunosuppressed patients. J Virol 1995;69:5437-5444.
26. Scotto J, Hadchouel M, Hery C, Yvart J, Tiollais P, Brechot C. Detection of hepatitis B virus DNA in serum by a simple spot hybridization technique: comparison with results for other viral markers. HEPATOLOGY 1983;3: 279-284.

27. Chesne C, Guillouzo A. Cryopreservation of isolated rat hepatocytes: a critical evaluation of freezing and thawing conditions. Cryobiology 1988; 25:323-330.
28. Koebe HG, Muhling B, Deglmann CJ, Schildberg FW. Cryopreserved porcine hepatocyte cultures. Chem Biol Interact 1999;121:99-115.
29. Isom HC, Secott T, Georgoff I, Woodworth C, Mummaw J. Maintenance of differentiated rat hepatocytes in primary culture. Proc Natl Acad Sci U S A 1985;82:3252-3256.
30. Galle PR, Hagelstein J, Kommerell B, Volkmann M, Schranz P, Zentgraf H. In vitro experimental infection of primary human hepatocytes with hepatitis B virus. Gastroenterology 1994;106:664-673.
31. Jamal HZ, Weglarz TC, Sandgren EP. Cryopreserved mouse hepatocytes retain regenerative capacity in vivo [Comments]. Gastroenterology 2000;118:390-394.
32. Taylor J, Mason W, Summers J, Goldberg J, Aldrich C, Coates L, Gerin J, et al. Replication of human hepatitis delta virus in primary cultures of woodchuck hepatocytes. J Virol 1987;61:2891-2895.
33. Li AP, Gorycki PD, Hengstler JG, Kedderis GL, Koebe HG, Rahmani R, de Sousas G, et al. Present status of the application of cryopreserved hepatocytes in the evaluation of xenobiotics: consensus of an international expert panel. Chem Biol Interact 1999;121:117-123.
34. Rogler LE. Selective bipotential differentiation of mouse embryonic hepatoblasts in vitro. Am J Pathol 1997;150:591-602.
35. Cable EE, Isom HC. Exposure of primary rat hepatocytes in long-term DMSO culture to selected transition metals induces hepatocyte proliferation and formation of duct-like structures. HEPATOLOGY 1997;26:1444-1457.
36. Kojima T, Yamamoto M, Mochizuki C, Mitaka T, Sawada N, Mochizuki Y. Different changes in expression and function of connexin 26 and connexin 32 during DNA synthesis and redifferentiation in primary rat hepatocytes using a DMSO culture system. HEPATOLOGY 1997;26:585-597.
37. Gripon P, Diot C, Theze N, Fourel I, Loreal O, Brechot C, Guguen-Guillouzo C. Hepatitis B virus infection of adult human hepatocytes cultured in the presence of dimethyl sulfoxide. J Virol 1988;62:4136-4143.
38. Bruns M, Miska S, Chassot S, Will H. Enhancement of hepatitis B virus infection by noninfectious subviral particles. J Virol 1998;72:1462-1468.
39. Overturf K, Al-Dhalimy M, Tanguay R, Brantly M, Ou CN, Finegold M, Grompe M. Hepatocytes corrected by gene therapy are selected in vivo in a murine model of hereditary tyrosinaemia type I [Comments] [published erratum appears in Nat Genet 1996 Apr;12(4):458]. Nat Genet 1996;12:266-273.
40. Rajvanshi P, Kerr A, Bhargava KK, Burk RD, Gupta S. Efficacy and safety of repeated hepatocyte transplantation for significant liver repopulation in rodents. Gastroenterology 1996;111:1092-1102.
41. Gupta S, Rajvanshi P, Aragona E, Lee CD, Yerneni PR, Burk RD. Transplanted hepatocytes proliferate differently after CC14 treatment and hepatocyte growth factor infusion. Am J Physiol 1999;276:G629-G638.

Repopulation of Mouse Liver With Human Hepatocytes and *In Vivo* Infection With Hepatitis B Virus

MAURA DANDRI,[1] MARTIN R. BURDA,[1] EVA TÖRÖK,[2] JOERG M. POLLOK,[2] ALICJA IWANSKA,[1] GUNHILD SOMMER,[1] XAVIER ROGIERS,[2] CHARLES E. ROGLER,[3] SANJEEV GUPTA,[3] HANS WILL,[1] HEINER GRETEN,[4] AND JOERG PETERSEN[1,4]

SEE EDITORIAL ON PAGE 1005

Mice containing livers repopulated with human hepatocytes would provide excellent *in vivo* models for studies on human liver diseases and hepatotropic viruses, for which no permissive cell lines exist. Here, we report partial repopulation of the liver of immunodeficient urokinase-type plasminogen activator (uPA)/recombinant activation gene-2 (RAG-2) mice with normal human hepatocytes isolated from the adult liver. In the transplanted mice, the production of human albumin was demonstrated, indicating that human hepatocytes remained functional in the mouse liver for at least 2 months after transplantation. Inoculation of transplanted mice with human hepatitis B virus (HBV) led to the establishment of productive HBV infection. According to human-specific genomic DNA analysis and immunostaining of cryostat liver sections, human hepatocytes were estimated to constitute up to 15% of the uPA/RAG-2 mouse liver. This is proof that normal human hepatocytes can integrate into the mouse hepatic parenchyma, undergo multiple cell divisions, and remain permissive for a human hepatotropic virus in a xenogenic liver. This system will provide new opportunities for studies on etiology and therapy of viral and nonviral human liver diseases, as well as on hepatocyte biology and hepatocellular transplantation. (HEPATOLOGY 2001;33:981-988.)

Abbreviations: HBV, hepatitis B virus; uPA, urokinase-type plasminogen activator; RAG-2, recombination activation gene-2; PCR, polymerase chain reaction; PH, partial hepatectomy; EGTA, ethylene glycol-bis(β-aminoethyl ether)-*N,N*-tetraacetic acid; SDS-PAGE, sodium dodecyl sulfate–polyacrylamide gel electrophoresis; Mab, monoclonal antibody; HSA, human serum albumin; HBsAg, hepatitis B surface antigen; HBcAg, hepatitis B core antigen.

From the [1]Heinrich-Pette-Institut for Experimental Virology and Immunology, [2]Department of Hepatobiliary Surgery and Transplantation, and [4]Department of Medicine, University Hospital Eppendorf, University of Hamburg, Hamburg, Germany; and [3]Albert Einstein College of Medicine, Marion Bessin Liver Research Center, Bronx, NY.

Received November 1, 2000; accepted January 22, 2001.

Drs. Dandri and Burda contributed equally to this work.

Supported by a grant from the Deutsche Forschungsgemeinschaft to J.P. (PE/608 2-1). M.D. was supported by an EMBO long-term fellowship. C.E.R. and S.G. are recipients of awards from the Irma T. Hirschl-Weiler trust, with additional support from NIH grants. The Heinrich-Pette-Institut is supported by the Freie und Hansestadt Hamburg and the Bundesministerium für Gesundheit, Germany.

Address reprint requests to: Dr. Joerg Petersen, M.D., Klinik und Poliklinik für Innere Medizin Universitätsklinikum Hamburg-Eppendorf, Martinistr. 52, D-20246 Hamburg, Germany. E-mail: petersen@hpi.uni-hamburg.de; fax: (49) 40-42803-8065.

0270-9139/01/3304-0028$35.00/0

doi:10.1053/jhep.2001.23314

Persistent infection with hepatitis B virus (HBV) is a major worldwide health problem, and chronically infected individuals are at high risk for developing cirrhosis and hepatocellular carcinoma.[1,2] Despite the availability of an HBV vaccine, there are still more than 350 million chronically infected people worldwide, and the few antiviral treatments currently available have a limited rate of efficacy. The narrow host range of HBV and the lack of both *in vitro* systems and of convenient animal models have greatly hampered our understanding of the complete virus life cycle, as well as the development of more effective antiviral drugs aimed at eradicating the virus from chronic carriers.[3] Chimpanzees are the only animal species infectable with HBV,[4,5] but studies with these animals and evaluation of antiviral therapies are severely restricted because of their limited availability and high costs. Animal models based on HBV-related hepadnaviruses, such as woodchuck and Pekin duck hepatitis B viruses, are often used for assessment of antiviral drugs[6-8] and have provided important information about factors involved in establishment of virus infection, viral persistence, and hepatocarcinogenesis.[9-14] However, woodchucks are relatively large animals of outbred origins that are difficult to handle in many laboratories, and chronic hepadnavirus infection in birds does not lead to cancer. The development of HBV-expressing transgenic mice has also provided important insights regarding viral pathobiology and the role of HBV gene products in hepatocellular injury.[12,15-19] Although infectious virus can be produced in transgenic mice, their hepatocytes are not permissive for infection. Therefore, the still-unknown early steps of viral infection, such as virus receptor recognition and mechanism of entry, cannot be addressed in these systems.

Furthermore, unlike in HBV-infected human hepatocytes, all viral RNAs are synthesized from a chromosomally integrated copy of the virus, and no cccDNA, the natural template of viral transcription *in vivo*, is produced. This implies for instance that complete abrogation of virus production by antiviral drugs, which requires elimination of covalently closed circular DNA, cannot be studied in transgenic mice. Taken together, elucidation of the early steps of HBV infection and more meaningful testing of new antivirals would greatly profit from an animal system with HBV-permissive human hepatocytes incorporated into the liver parenchyma.

Although techniques for the isolation of hepatocytes from human livers are continuing to improve, primary human hepatocytes are difficult to maintain in culture and become nonpermissive for HBV very quickly after plating. In addition, they are never identical in function and gene expression to hepatocytes integrated in the liver architecture. Therefore, any technique that would allow human hepatocytes to remain

in an environment that supports both cell growth and liver-specific differentiation would offer unique opportunities to study human hepatotropic viral infections and to evaluate the efficacy of novel antiviral drugs in a system closely mimicking the *in vivo* situation.

Liver repopulation with hepatocyte transplantation has significant potential for gene therapy applications and analysis of fundamental biological mechanisms in metabolic and viral diseases.[20-22] Previous studies documented that transplanted hepatocytes can integrate into the host liver parenchyma[23-25]; however, transplanted hepatocytes show very limited proliferative activity in the normal liver.[26] Studies in transgenic mice have shown that the liver can be repopulated by genetically engineered rodent hepatocytes harboring a selective growth advantage over resident hepatocytes.[27-30] The discovery of a liver-toxic phenotype in urokinase-type plasminogen activator (uPA) transgenic mice led to the development of a novel liver repopulation model, in which hepatocyte-targeted expression of the albumin-uPA transgene depletes host hepatocytes progressively. Cell damage appears to be caused by intracellular activation of the uPA substrate plasminogen, which in turn would activate plasmin and induce proteolytic damage within the rough endoplasmic reticulum. Therefore, uPA transgene expression leads to the death of transgene-carrying hepatocytes, and this results in a growth advantage for transplanted cells that are amplified in a polyclonal pattern. However, transgene deletion takes place in some endogenous mouse hepatocytes, and those cells are competitively growing with transplanted hepatocytes.[27,28] In this mouse model, hepatocyte-proliferative stimulus lasts approximately 8 weeks after birth, until the transplanted hepatocyte mass becomes comparable with the hepatocyte mass in the liver of nontransgenic normal mice.[27,31]

To develop a novel hepatitis B mouse model, we recently crossed uPA transgenic mice with recombinant activation gene-2 (RAG-2) mice, which lack mature T and B lymphocytes as a result of a deletion in the RAG-2.[32] As a result, transplantation of woodchuck hepatocytes allowed extensive proliferation of xenografted cells in the mouse liver and permitted establishment of productive woodchuck hepatitis virus infection with indefinite viral replication in mice.[31]

To further investigate whether the uPA/RAG-2 mouse model could be extended to human hepatocyte–based systems, mice were transplanted with primary human hepatocytes isolated from the normal adult liver. Transplanted human hepatocytes became integrated in the uPA/RAG-2 liver parenchyma and were estimated to constitute up to 15% of the mouse liver. When UPA/RAG-2 mice were inoculated with HBV-infectious serum, HBV-specific markers were specifically found in the liver and in the peripheral blood of hepatocyte recipients. The ability to establish productive HBV infection in mice transplanted with human hepatocytes indicates that such a system will allow analysis of viral biology in a convenient small-animal model.

MATERIALS AND METHODS

Animals. uPA transgenic mice and RAG-2 knockout mice were purchased from Jackson Laboratories (Bar Harbor, ME) and Taconic Farms (Germantown, NY), respectively. Animals were housed and maintained under specific pathogen-free conditions in accordance with institutional guidelines under approved protocols. uPA transgenic mice were crossed with RAG-2 knockout mice, and chimeric mice were characterized by polymerase chain reaction (PCR) as previously reported.[31] Only hemizygous uPA mice were used for transplantation experiments.

Isolation and Transplantation of Human Hepatocytes. Donor human livers that were reduced in size for transplantations into children or were rejected for transplantation because of traumatic lesions, as well as liver tissues obtained from patients undergoing partial hepatectomies (PH) because of metastases of colorectal carcinoma, were used for cell isolation and transplantation procedures in accordance with institutional guidelines. In all cases, patients were negative for HBV, hepatitis C virus, and human immunodeficiency virus serologic markers; liver biopsies were negative for HBV markers; and isolated hepatocytes were checked for the absence of specific HBV-DNA sequences by PCR. The donor livers were perfused *in situ* with cold University of Wisconsin solution (Du Pont, Wilmington, DE) before explantation and kept on ice until use. In the case of tumor resections, a wedge from the resected liver lobe was cut at a distance of at least 3 cm from the metastasis. Warm ischemia time, defined as the time after clamping of the branches of the hepatic artery and portal vein until excision of the piece of tissue, varied from 90 minutes to 4 hours. Immediately after excision, the liver tissue was placed on ice and immediately perfused with ice-cold University of Wisconsin solution by means of multiple catheters inserted into the vessels on the cut surface of the resected fragment.

Thereafter, human hepatocytes were isolated using a 2-step collagenase perfusion method. Briefly, a branch of the portal vein was cannulated, the liver or liver segment was placed on a sterile glass plate, in a 37°C water bath, half-submersed in prewarmed isotonic solution, and perfused for 5 minutes with the preperfusion solution (1× Leffert's buffer: 10 mmol/L HEPES, 3 mmol/L KCl, 130 mmol/L NaCl, 1 mmol/L NaH_2PO_4-H_2O, 10 mmol/L glucose [pH 7.4]) containing 5 mmol/L ethylene glycol-bis(β-aminoethyl ether)-*N*,*N*-tetraacetic acid (EGTA). The flow rate of the perfusate was 100 mL/min, and all the solutions were prewarmed at 38°C. Thereafter, Leffert's buffer not containing EGTA was allowed to run through the liver for 3 to 5 minutes, and then the tissue was perfused with the collagenase buffer (1× Leffert's buffer containing 5 mmol/L $CaCl_2$ and 0.05% [wt/vol] collagenase type I [Worthington Biochemical Corp., NJ]). Perfusion time with collagenase varied between 10 to 30 minutes according to the size of the tissue. Subsequently, the digested liver tissue was placed in cold Leffert's buffer supplemented with 5 mmol/L $CaCl_2$, the liver capsule was cut, cells were dissociated, and then filtered through 100-μm nylon filters. Cell suspensions were centrifuged 3 times (50*g*, 5 minutes) to separate hepatocytes from nonparenchymal cells. Hepatocyte viability was assessed by Trypan blue exclusion. Immediately after isolation, 5×10^5 viable human hepatocytes were resuspended in a volume of 50 μL phosphate-buffered saline and transplanted into 13- to 21-day-old recipient uPA/RAG-2 mice by intrasplenic injection.[31]

HBV Infection Studies. Human serum containing high-titer HBV DNA (5×10^8 virus genome equivalents/mL serum) was obtained from a HBV chronic carrier, and samples were aliquotted and kept at −70°C until use. For HBV infection studies, 2 days after hepatocyte transplantation, 2 transplanted and 2 nontransplanted mice were injected subcutaneously with 20 μL of HBV-positive human serum.

Detection of Human Serum Albumin and Viral Envelope Proteins by Immunoblotting. Samples of mouse and human sera were subjected to sodium dodecyl sulfate–polyacrylamide gel electrophoresis (SDS-PAGE) and blotted onto polyvinylidene difluoride (PVDF)-membranes. The blots were probed either with a commercially available mouse monoclonal antibody (Mab) against human serum albumin (HSA) (1: 10,000 dilution; Sigma, St. Louis, MO), which does not cross-react with the mouse proteins, or with a mixture of Mabs specific for HBs (Mab H 166, courtesy of R. Decker, Abbott Diagnostika, Wiesbaden, Germany; dilution 1:10,000) and PreS1 (Mab 18/7, kindly provided by W. Gerlich, University Giessen, Germany; dilution 1:4,000). Specific binding was detected by using peroxidase-coupled anti-mouse IgG antibodies and an enhanced chemiluminescence system (Pierce, Rockford, IL). For semiquantitative determination of the relative amount of HSA in transplanted mouse

sera, the mouse serum samples to be quantified plus a set of artificial mixtures composed of known ratios of human and mouse sera were used to prepare Western blots. A series of exposures were made, and the film on which the lowest concentration of HSA was just detectable was used for densitometric analysis. Each mouse serum sample was analyzed by ECL Western blot, and HSA levels were quantified using scanning densitometry at least twice.

Detection of Human Genomic DNA in Mouse Liver. Genomic DNA was extracted from frozen liver tissues by proteinase K digestion, phenol extraction, and ethanol precipitation as described.[33] Human genomic DNA in transplanted uPA/RAG-2 mouse livers was detected both by PCR and by dot-blot hybridization. A computer search using the MAC Vector/gene bank BLAST search program was performed to identify short nucleotide sequences specific for human *Alu* DNA repeats. Several oligonucleotides were selected and used as PCR primers to test their specificity on human and mouse genome DNAs (data not shown). The following primers specific for the human *Alu* sequences: Primer 1, 5′-GCT TCC TGA GTA ACT GGA CAA CAG C-3′, and Primer 2, 5′-TGC GAT GGC ATG TTT CCA AG-3′, were chosen for PCR amplification, because they produce a specific band of 440 bp that is not detectable using mouse tissue as the template. To estimate the percentage of human versus mouse genomic DNA in transplanted mice, 2 μg of DNA extracted from liver tissues was dot-blotted onto a nylon membrane[34] and hybridized under high-stringency conditions overnight with a 440-bp *Alu* DNA P^{32}-labeled probe, which was obtained by PCR using the above-mentioned *Alu* primers and human genomic DNA as the template. Test mixtures of known amounts of human and mouse genomic DNAs were loaded in parallel on the blots and served as a standard. Hybridization signals were quantitated by scanning densitometry using the TINA program from Raytest (Straubenhardt, Germany) and a FujiX/2000 laser densitometer (Fuji, Düsseldorf, Germany).

Detection and Quantification of HBV in uPA/RAG-2 Mouse Sera. Viral DNA was extracted from mouse and human sera using the QIAamp Blood Kit (Qiagen, Hilden, Germany) and amplified by PCR with the following primers: Primer 1-1823 (+): 5′-TTTTTCACCTCTGCCTAATCATC-3′; Primer 2-2121 (−): 5′-ACCCACCCAGGTAGCTAGAGTCAT-3′. To determine the HBV-DNA titer in mouse and human sera, samples were also analyzed using the LightCycler system (Roche, Basel, Switzerland) in a quantitative real-time PCR reaction using the same primers as above and the fluorescent-labeled hybridization probes: LCRed640 1877 (−): 5′-TTGGAGGCTTGAACAGTAGGACATGA-3′, FITC 1899 (−): 5′-CCAAAGCCACCCAAGGCAC-3′. As a control, known amounts of cloned HBV DNA were amplified in parallel to establish a standard curve for quantification.

Blood Chemistry and Enzyme-Linked Immunosorbent Assay for Hepatitis B Surface Antigen. Sera were analyzed for total protein, albumin, bilirubin, and alanine transaminase and aspartate transaminase activity in a standard automated clinical analyzer (Siemens, München, Germany). Human hepatitis B surface antigen (HBsAg) was measured using the HBsAg Axsym Test (Abbott, Wiesbaden, Germany) using 1:100 dilution of the mouse sera.

Histologic Studies. Serial cryostat sections of transplanted and nontransplanted uPA/RAG-2 mouse livers were examined by hematoxylin-eosin staining, and by immunohistochemistry with a rabbit antiserum (hepatitis B core [HBc] antiserum) (DAKO Diagnostika, Hamburg, Germany) against human hepatitis B core antigen (HBcAg). For immunohistochemical staining, sections were fixed in acetone and incubated with HBc antiserum (diluted 1:250 in phosphate-buffered saline containing 5% goat serum) for 1 hour at room temperature. Endogenous peroxidase activity was blocked with 0.3% H_2O_2 and methanol. Specifically bound antibody was visualized by incubation with a biotinylated goat anti-rabbit IgG antibody, followed by incubation with streptavidin–horseradish peroxidase and diaminobenzidene as substrate (Vectastain ABC kit, Burlingame, CA). To estimate the percentage of donor human hepatocytes in recipient livers, 10 sections per liver lobe were cut from 5 lobes of each of the analyzed mice (50 sections total) and immunostained with HBc antiserum. Twenty-five random fields per section were examined microscopically (>2,000 cells), and the percentage of HBcAg-positive stained hepatocytes was calculated.

TABLE 1. Transplantation of Primary Human Hepatocytes in uPA/RA6-2 Transgenic Mice

Human Liver Specimens	Hepatocyte Viability* (%)	No. of Transplanted uPA/RAG-2 Mice	Survival Ratio	Mice With HSA ≥ 1%
A (donor liver)	81	3	2/3	2/2
B (donor liver)	85	5	5/5	4/5
C (donor liver)	83	4	3/4	1/3
D-H (PH livers)†	40-80	29	26/29	0/26

*Trypan blue exclusion test was used to determine hepatocyte viability shortly before transplantation into uPA/RAG-2 mice.

†PH livers, human liver specimens obtained after partial hepatectomy.

RESULTS

Transplantation of uPA/RAG-2 Mouse Liver With Xenogenic Human Hepatocytes. To isolate primary human hepatocytes, we used both donor liver specimens that were not used for human liver transplantation, and surgical liver tissues remaining after PH. Immediately after cell isolation, human hepatocytes were transplanted into multiple uPA/RAG-2 mice by intrasplenic injection. So far, we succeeded in transplantation of human hepatocytes only by perfusing donor liver specimens (n = 3), not by using surrounding tissues from tumor resections (n = 5). Viability of hepatocytes isolated from healthy livers was high (≥80%), and approximately 80% of transplanted mice (10 of 12) survived the procedure (see Table 1). The most common reason for death of transplanted young mice was a diffuse bleeding complication caused by the overexpression of uroplasminogen. By screening of the mice for the production of HSA (see below), we estimated that engraftment of human hepatocytes was successful (HSA ≥1%) in 70% (7 of 10) of the transplanted mice. Viable hepatocytes could be isolated from PH livers that underwent a considerable time of warm ischemia before perfusion (90 minutes to 4 hours), but cell viability was lower (40% to 80%) and transplantation into mice was not successful (0 of 29). Hepatocytes that had been liberated from cirrhotic livers or from healthy donors in other liver centers, and were sent to us as cell solutions, were also not successfully transplanted.

Evaluation of Human Hepatocyte Engraftment in Mice. To screen for survival and engraftment of transplanted human hepatocytes, 8 weeks after transplantation, serum albumin profiles were analyzed by immunoblotting using a specific Mab that does not cross-react with any mouse serum protein. Human albumin was specifically found in uPA/RAG-2 mice sera containing human hepatocytes (Fig. 1A, lanes 1 and 2), while no positive signals were detected in sera of nontransplanted mice (Fig. 1A, lanes 3 and 4), which had been inoculated with human serum 2 days after hepatocyte transplantation.

To evaluate the ratio of human versus mouse serum albumin in transplanted mice, test mixtures of human and mouse sera were loaded in parallel onto the gel, and signal intensities on the blots were quantified by densitometry. As shown in Fig. 1A and 1B, 2 months after transplantation, levels of human albumin ranged between approximately 1% to 10% (mean of 5%) in the sera of 5 successfully transplanted mice, and in 2 cases (mouse #226 and #273). HSA levels appeared to be even higher (15% and 13%, respectively), strongly indicat-

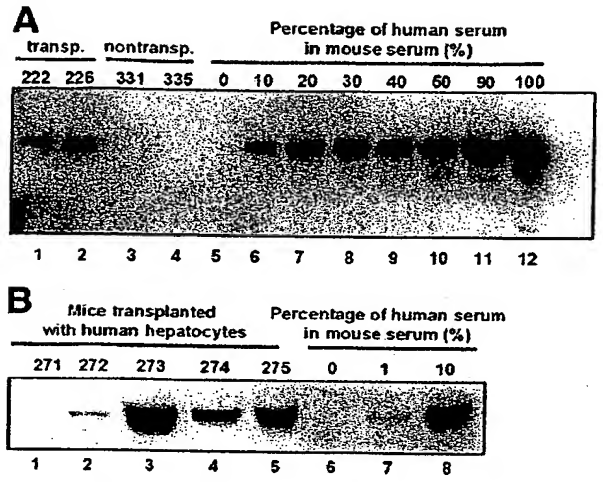

FIG. 1. Secretion of HSA in the serum of uPA/RAG-2 mice 8 weeks after hepatocyte transplantation. Human albumin was specifically detected in the serum of transplanted mice by SDS-PAGE (10%) and immunoblotting with a specific antibody raised against human albumin. (A) Serum samples of 2 uPA/RAG-2 mice transplanted with normal human hepatocytes (*lanes 1* and 2) and from 2 nontransplanted uPA/RAG-2 mice (*lanes* 3 and 4), which had been previously injected with human serum (see text). (B) Levels of human albumin detected in different mice (*lanes 1-5*) transplanted with human hepatocytes (5×10^5 cells) liberated from donor liver B (see Table 1). Mouse #271 (*lane 1*) was not successfully transplanted (HSA < 1%). The amount of human albumin in mouse sera was quantified by loading in parallel defined mixtures of a human and a mouse serum; percentage of human serum is given. All serum samples were diluted 1:1,000 before loading.

ing that transplanted human hepatocytes engrafted and survived in the uPA/RAG-2 livers.

To directly demonstrate human hepatocyte engraftment into the liver of uPA/RAG-2 mice, animals were killed 2 months after transplantation, and the livers were screened for the presence of human specific genome sequences both by PCR and dot-blot hybridization. Genomic DNAs were extracted both from human and mouse liver specimens and amplified by PCR using primers specific for a fraction of highly repeated human *Alu* sequences (see Materials and Methods). A single band of the expected size (440 bp) was exclusively amplified when DNAs extracted either from human or uPA/RAG-2 mouse livers transplanted with human hepatocytes were used (Fig. 2A). To obtain a rough estimation of the amount of human hepatocytes present in transplanted livers, we hybridized DNAs extracted from mouse livers (Fig. 2B, lanes 1 and 2), as well as test mixtures of human and mouse genomic DNAs (Fig. 2B, lanes 3 to 5), with a DNA probe specific for human *Alu* sequences. Positive PCR and dot-blot hybridization signals were clearly detected only in the livers of transplanted mice that were also positive for the presence of HSA (i.e., mouse #275), thus proving that detection of human albumin by immunoblotting is a suitable screening assay to estimate transplantation efficacy. Furthermore, scanning densitometry revealed that the percentage of human genomic DNA in the mouse liver specimens analyzed ranged between 2% to 10%, suggesting that a certain degree of repopulation may have occurred, because only 5×10^5 human hepatocytes were transplanted in each animal (which is approximately 0.5% of the hepatocyte number present in a mouse liver). We did not detect human DNA in tissues other than the liver, demonstrating that normal adult human hepatocytes did not survive in spleen, pancreas, mesenterium, or lung (data not shown).

UPA/RAG-2 mice containing human hepatocytes were clinically healthy, and the livers appeared normal in respect to color, size, and liver-to-body-weight ratios at killing. Serum concentrations of total protein, albumin, bilirubin, and transaminases were similar in uPA/RAG-2 mice containing human hepatocytes compared with control nontransplanted littermates (data not shown).

Establishment of Productive HBV Infection in Transplanted uPA/RAG-2 Mice. Provided transplanted human hepatocytes remain highly differentiated, they should be permissive for HBV infection and replication, because HBV infection is one of the most sensitive markers for the differentiation status of hepatocytes. Thus, the successful infection of transplanted hepatocytes in mice would indicate the retention of a highly hepatocyte-specific differentiation status of the transplanted cells, and imply that these mice represent a very useful animal system for HBV infection studies *in vivo*. Therefore, 2 days after transplantation, 2 uPA/RAG-2 mice and 2 control nontransplanted littermates were injected with HBV-infectious human serum. Eight weeks after infection, HBV viremia was determined by measuring HBV-DNA levels using a real-time quantitative PCR assay. High levels of HBV DNA (4.5 and 10×10^8 genome equivalent/mL serum) were found in sera of uPA/RAG-2 mice transplanted with human hepatocytes, whereas no viral DNA was detectable in nontransplanted but HBV-injected mice. The absence of HBV-DNA in nontransplanted mice demonstrated that positive signals could not have resulted from the original injection and, as expected, that mice not containing human hepatocytes are not susceptible to HBV infection. Agarose gel electrophoretic analysis of the amplified DNA showed a single band of the expected size, demonstrating the specificity of the PCR assay (Fig. 3A).

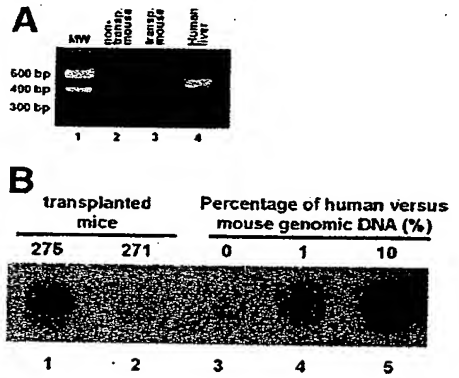

FIG. 2. Detection of human hepatocytes in the liver of transplanted mice. Genomic DNA was extracted from the liver of mice transplanted with human hepatocytes and analyzed both by PCR and by dot blot using a P^{32}-labeled DNA probe specific for the human *Alu* sequences. (A) A specific band of 440 bp was amplified using human tissue DNA (*lane 4*), but not mouse liver DNA (*lane 2*). Specific DNA amplification was exclusively visible in the liver of transplanted mice (*lane 3*). *Lane 1*, molecular-weight standard. (B) *Lanes 1* and 2, representative example of mice successfully (#275) and unsuccessfully (#271) transplanted with hepatocytes isolated from the same donor liver. *Lanes* 3-5 present mixtures of genomic DNAs extracted from human livers and untransplanted uPA/RAG-2 mouse livers. Percentage of human hepatocyte DNA is given.

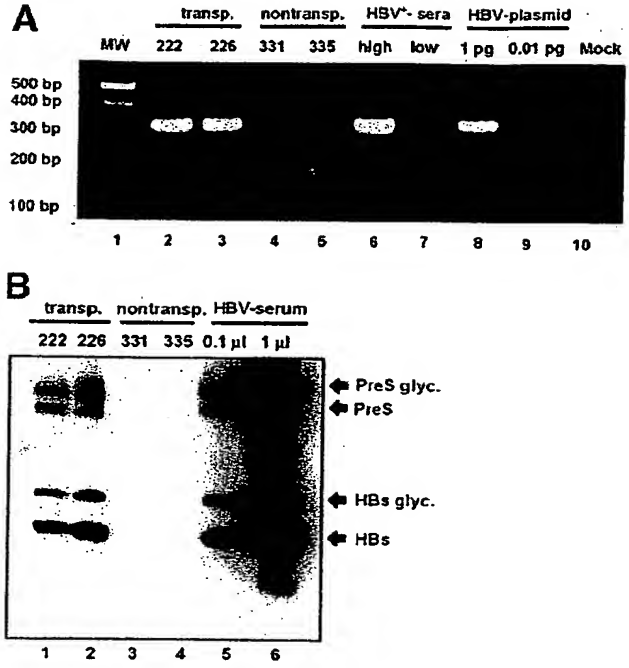

FIG. 3. Establishment of HBV infection in mice transplanted with human hepatocytes. (A) Agarose gel analysis of HBV DNA amplified by PCR from mouse and human sera . *Lane 1*, molecular-weight standard; *lanes 2* and 3, serum samples from uPA/RAG-2 transplanted mice 2 months after injection of HBV-infectious serum; *lanes 4* and 5, nontransplanted, but HBV-injected, uPA/RAG-2 mice; HBV DNA from serum of a high-titered (*lane 6*) and a low-titered (*lane 7*) HBV patient; *lanes 8* and *9*, 1 pg and 0.01 pg of an HBV plasmid used in a control PCR reaction, respectively; *lane 10*, mock control. HBV-DNA titers were quantified by using a real-time quantitative PCR assay as described. (B) Detection of viral envelope proteins in mouse sera by immunoblotting. Human and mouse sera were resolved on a 15% SDS-PAGE gel, and viral envelope proteins were detected with a mixture of monoclonal anti-S and anti-preS1 antibodies. Serum samples (1 µL) from uPA/RAG-2 mice transplanted with adult human hepatocytes and infected with HBV (*lanes 1* and 2); serum samples from HBV-injected, but nontransplanted, littermates (*lanes 3* and *4*); *lanes 5* and *6*, 0.1 and 1 µL of human serum from a highly viremic carrier (1×10^{10} HBV genome equivalents/mL serum), respectively.

As independent evidence for the establishment of productive HBV infection in transplanted uPA/RAG-2 mice, we analyzed the presence of viral envelope proteins in the mouse sera both by enzyme-linked immunosorbent assay and by immunoblotting. In the enzyme-linked immunosorbent assay, mice sera resulted in positive-versus-negative (S/N) sample ratios of 74 and 114, which is in the same range as signals routinely obtained with highly viremic human sera. As expected, sera from mice that received HBV-infectious serum without previous hepatocyte transplantation were negative in this assay. Analysis of the viral envelope proteins by immunoblotting using a mixture of 2 Mabs against small (HBs) and large S (preS1) envelope proteins revealed the presence of specific bands in transplanted mouse sera (Fig. 3B, lanes 1 and 2). These bands comigrated with the glycosylated and nonglycosylated forms of HBs and preS1 from a highly viremic human serum (1×10^{10} HBV genome equivalents/mL serum) loaded in parallel on the blot (Fig. 3B, lanes 5 and 6). The intensity of the bands obtained with serum samples from transplanted mice (Fig. 3B, lanes 1 and 2) indicated an approximately 10-fold lower level of viral envelope proteins in mice compared with the HBV-positive human serum used. Because the viremia in the transplanted mice was also 10-fold lower than in the highly viremic human serum used as control, these data strongly suggest the presence of a similar excess of subviral particles versus virions in sera of transplanted mice as known for humans.

Human Hepatocytes Can Partially Repopulate the uPA/RAG-2 Mouse Liver. The expression of HBV-specific genes represents an unequivocal marker to distinguish between mouse host and transplanted human hepatocytes, and permits a rough estimation of the number of successfully transplanted and functional hepatocytes in mouse livers.[31,36] Therefore, mouse liver sections randomly chosen from different lobes were immunohistochemically stained for HBcAg. Eight weeks after HBV infection of mice transplanted with human hepatocytes, HBcAg-positive hepatocytes were found as clusters throughout the uPA/RAG-2 mouse livers and, as expected,[31] grouped around portal veins and in adjacent areas (Fig. 4A-C). Inspection of multiple cryostat sections for each of the transplanted and infected mice (recipients #222 and #226) revealed HBcAg-positive staining in 5% ± 2% and in 15% ± 4% of all hepatocytes, respectively (mean ± SD), whereas none were positive in nontransplanted but HBV-injected mice (Fig. 4D).

Histologic examination of various extrahepatic tissues of transplanted mice, such as spleen, lungs, and peritoneum, failed to identify surviving hepatocytes in those organs 8 weeks after transplantation (data not shown). These observations are in agreement with previous reports showing that intrasplenic injection of normal hepatocytes in mice does not favor persisting cell engraftment in tissues other than the liver.[31,37] Furthermore, no tumor formation was observed in uPA/RAG-2 transplanted mice, strongly arguing for the presence of only normal hepatocytes in our donor sources. Because we did not detect any inflammatory response 8 weeks after transplantation of human hepatocytes, it is very likely that persistent HBV replication beyond our observation period can be established in this model, similar to that reported for woodchuck hepatitis virus in the woodchuck hepatocyte transplantation model.[31]

Previous studies indicated that only approximately 20% of splenically injected cells reaches the liver and survives (that corresponds in our experiments to about 1×10^5 cells), while a mouse liver contains about 1×10^8 hepatocytes.[38,39] In this case, engraftment without repopulation could result in only 0.1% to 0.5% human hepatocytes in transplanted mice. The presence of 1% to 15% human hepatocytes in mouse livers, as indicated by the levels of human albumin in the serum, human genomic DNA in the liver, as well as by the number of HBcAg-positive hepatocytes, strongly suggests that each transplanted human hepatocyte may have undergone up to 6 to 7 cell doublings, provided that all transplanted cells proliferated equally. Based on these data and considerations, human hepatocytes have significantly proliferated in the uPA/RAG-2 mouse liver environment, and their growth pattern appears to have restored a normal cord structure of the liver. To assess whether a significant human hepatocyte engraftment is feasible when using RAG-2 mice that were not crossed with uPA transgenic mice, transplantation experiments were performed in parallel with such animals, including infecting them with HBV posttransplantation. No evidence for success-

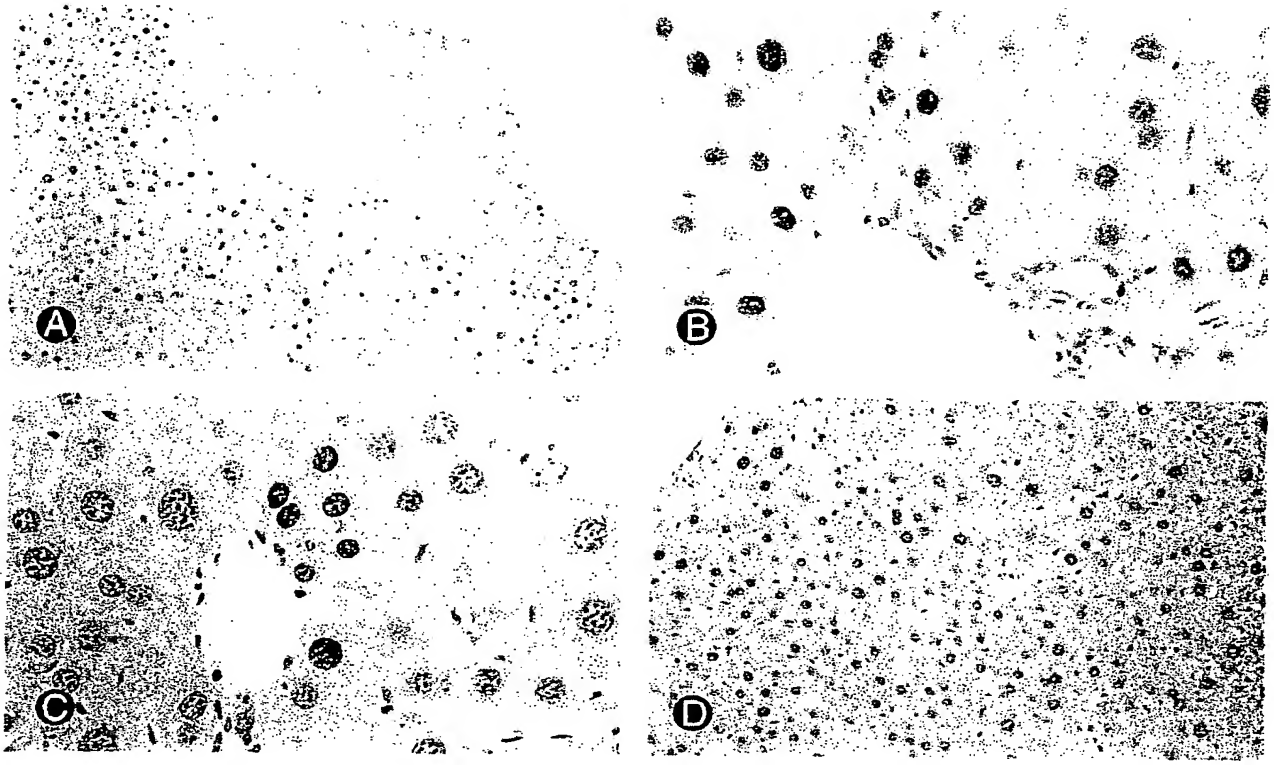

FIG. 4. Histologic localization of HBV-infected human hepatocytes in uPA/RAG-2 mice 8 weeks after transplantation. Detection of HBcAg in 2 uPA/RAG-2 mouse livers (A-C) by staining with an HBc antiserum. Strong nuclear and occasionally some cytoplasmic (A) staining in periportal and adjacent areas. (D) Liver tissue from a nontransplanted, but HBV-injected, uPA/RAG-2 mouse showed no HBcAg reactivity. (Original magnification [A, D] ×100; [B, C] ×200.)

ful engraftment of human hepatocytes in RAG-2 mice was obtained, as was evident from the failure to detect HSA (limit of detection 0.1%) or HBV DNA in the sera 8 weeks after transplantation. In addition, histochemistry was negative for HBcAg (data not shown).

DISCUSSION

This is the first report that highly differentiated normal human hepatocytes are able to engraft a xenogenic liver. Furthermore, our data demonstrate that the use of immunotolerant RAG-2 knock-out mice crossed with uPA transgenic mice allows not only integration, but also partial repopulation of the mouse liver with these hepatocytes. The highest degree of liver repopulation achieved so far by transplanting human hepatocytes isolated from the adult liver, according to serologic and histologic values, was estimated to be up to 15%. Although that is clearly below the repopulation level reached by transplanting hepatocytes isolated from woodchucks (up to 90%)[31] or from other rodents,[40] our results demonstrate that even partial repopulation allows to reach virus titers comparable with those generally found in many HBV carriers. The lower degree of cell growth achieved by transplanting human liver cells may be the result of differences in the quality of hepatocytes recovered from human livers compared with those routinely obtained by *in vivo* perfusion of animals. Moreover, evolutionary differences between human and rodent hepatocyte-specific proteins involved in cell/cell interactions or in other functions may also impair the repopulation efficacy of human hepatocytes. However, the production of HSA and HBV circulating virions 8 weeks after transplantation indicate that function and differentiation status of repopulating human hepatocytes are well maintained in adult uPA/RAG-2 mice. Therefore, it will be important to determine whether the system is also suitable for studying infection of other hepatotropic viruses, such as hepatitis C virus, and hepatotropic microorganisms for which no permissive cell lines exist.

We are aware that in recent years, several other groups tried to repopulate mouse livers with human hepatocytes, with limited success. From our experience, it appears that the most critical and limiting factor to succeed in transplantation of normal human hepatocytes in these mice is the scarce availability of healthy liver tissues that underwent a very short ischemia time before perfusion. Under these circumstances, our transplantation efficacy was 70%. All other experiments, as described above, failed in our hands. Interestingly, fractions of hepatocytes isolated after a warm ischemia time of more than 1 hour were successfully plated in culture on collagen layers, but were not successfully transplanted in mice, indicating that common markers of cell viability and attachment efficiency may not be sensitive enough to predict the fate of transplanted hepatocytes. Further improvements of human hepatocyte isolation and cryopreservation techniques, as well as the attractive possibility of performing serial transplanta-

tion of human hepatocytes from mouse to mouse, would greatly facilitate advances in the field of human hepatocyte transplantation. Although it is clear that a larger number of independent hepatocyte preparations and successfully transplanted animals are needed to better define the best parameters as well as the limits of this system, our data provide proof that partial repopulation of the mouse liver with normal human liver cells is feasible. Unfortunately, we were not able to detect human hepatocytes in RAG-2 knock-out mice after transplantation, which may imply that a liver deficit, and possibly also ongoing mouse liver regeneration, is a prerequisite for successful engraftment.

The experimental system reported herein has some unique features and advantages compared with previous animal models used for studies of hepadnaviral infection and pathogenesis.[6,15,41] In fact, such chimeric animals are likely to allow studies of the full HBV replication cycle in a liver containing normal human hepatocytes. Furthermore, hepatocytes isolated from a single human liver can be transplanted into multiple recipients, which will all contain human hepatocytes harboring the same genetic information. This will be of particular value for *in vivo* testing of antivirals and other therapeutic drugs using rather small amounts of compounds. Moreover, we demonstrated that uPA/RAG-2 mice transplanted with human hepatocytes can be infected with HBV *in vivo*. With further modifications of our model, therapeutic approaches aimed at modulation of the immune response may be possible. Clearly, our system will offer the possibility to test antivirals that interfere not only with viral replication, but also with viral spread. In 2 other recently reported xenotransplantation models, cell engraftment was achieved by implanting human liver slices[42] or hepatocyte suspensions[43] extrahepatically, under the kidney capsule of immunodeficient mice. Although production of HBV was demonstrated, both these systems allowed survival, but not growth, of human hepatocytes in mice. Transplantation of human hepatocytes in a system that allows cell growth in the liver, as shown here, will also open new opportunities to study the regenerative potential of human liver cell populations,[44] as well as mechanisms of cell differentiation and hepatocarcinogenesis. Human hepatocytes at different stages of tumor progression may be transplanted into uPA/RAG-2 mice to characterize the cellular and molecular phenotype of precancerous cells, as well as factors that promote tumor progression. Furthermore, the efficacy of anticancer compounds and vectors for gene therapy aimed at correcting various metabolic liver diseases could be evaluated directly in these chimeric mice.

In conclusion, the knowledge that human hepatocytes can engraft and partially repopulate a xenogenic liver opens new, exciting possibilities to develop novel experimental models for studies on human liver diseases and hepatotropic viruses. Furthermore, it provides new tools to characterize the biology of human hepatocytes and to improve hepatocyte transplantation techniques, the latter being a possible alternative to whole-organ transplantation in humans.

Acknowledgment: The authors thank W. Gerlich and R. Decker for providing preS1 and HBs monoclonal antibodies, respectively, and R. Reusch for excellent technical assistance.

REFERENCES

1. Blumberg BS. Hepatitis B virus, the vaccine, and the control of primary cancer of the liver. Proc Natl Acad Sci U S A 1997;94:7121-7125.
2. Rogler CE. Cellular and molecular mechanisms of hepatocarcinogenesis associated with hepadnavirus infection. Curr Top Microbiol Immunol 1991;168:103-140.
3. Ganem D. Hepadnaviridae and their replication. In: Fields BN, Knipe DN, Howley PM, eds. Virology: Vol. 2, ed 3. Philadelphia: Lippincott-Raven, 1996:2703-2739.
4. Guidotti LG, Rochford R, Chung J, Shapiro M, Purcell R, Chisari FV. Viral clearance without destruction of infected cells during acute HBV infection. Science 1999;284:825-829.
5. Ogata N, Cote PJ, Zanetti AR, Miller RH, Shapiro M, Gerin J, Purcell RH. Licensed recombinant hepatitis B vaccines protect chimpanzees against infection with the prototype surface gene mutant of hepatitis B virus. HEPATOLOGY 1999;30:779-786.
6. Tennant JGaB. The woodchuck model of hepatitis B virus infection. In: Arias IM BJ, Fausto N, Jakoby WB, Schachter DA, Shafritz DA, eds. The Liver: Biology and Pathobiology. Ed 3. New York: Raven, 1994:1455-1466.
7. Mason WS, Cullen J, Moraleda G, Saputelli J, Aldrich CE, Miller DS, Tennant B, et al. Lamivudine therapy of WHV-infected woodchucks. Virology 1998;245(1):18-32.
8. Luscombe C, Pedersen J, Uren E, Locarnini S. Long-term ganciclovir chemotherapy for congenital duck hepatitis B virus infection in vivo: effect on intrahepatic-viral DNA, RNA, and protein expression. HEPATOLOGY 1996;24:766-773.
9. Breiner KM, Urban S, Schaller H. Carboxypeptidase D (gp180), a Golgi-resident protein, functions in the attachment and entry of avian hepatitis B viruses. J Virol 1998;72:8098-8104.
10. Chen HS, Kaneko S, Girones R, Anderson RW, Hornbuckle WE, Tennant B, Cote PJ, et al. The woodchuck hepatitis virus X gene is important for establishment of virus infection in woodchucks. J Virol 1993;67:1218-1226.
11. Dandri M, Schirmacher P, Rogler CE. Woodchuck hepatitis virus X protein is present in chronically infected woodchuck liver and woodchuck hepatocellular carcinomas which are permissive for viral replication. J Virol 1996;70:5246-5254.
12. Fourel G, Trepo C, Bougueleret L, Henglein B, Ponzetto A, Tiollais P, Buendia MA, et al. Frequent activation of N-myc genes by hepadnavirus insertion in woodchuck liver tumours [Comments]. Nature 1990;347:294-298.
13. Bruns M, Miska S, Chassot S, Will H. Enhancement of hepatitis B virus infection by noninfectious subviral particles. J Virol 1998;72:1462-1468.
14. Jilbert AR, Wu TT, England JM, Hall PM, Carp NZ, O'Connell AP, Mason WS, et al. Rapid resolution of duck hepatitis B virus infections occurs after massive hepatocellular involvement. J Virol 1992;66:1377-1388.
15. Chisari FV, Ferrari C. Hepatitis B virus immunopathogenesis. Annu Rev Immunol 1995;13:29-60.
16. Guidotti LG, Ishikawa T, Hobbs MV, Matzke B, Schreiber R, Chisari FV. Intracellular inactivation of the hepatitis B virus by cytotoxic T lymphocytes. Immunity 1996;4(1):25-36.
17. Kim CM, Koike K, Saito I, Miyamura T, Jay G. HBx gene of hepatitis B virus induces liver cancer in transgenic mice. Nature 1991;351:317-320.
18. Guidotti LG, Ando K, Hobbs MV, Ishikawa T, Runkel L, Schreiber RD, Chisari FV, et al. Cytotoxic T lymphocytes inhibit hepatitis B virus gene expression by a noncytolytic mechanism in transgenic mice. Proc Natl Acad Sci U S A 1994;91:3764-3768.
19. Chisari FV, Filippi P, Buras J, McLachlan A, Popper H, Pinkert CA, Palmiter RD, et al. Structural and pathological effects of synthesis of hepatitis B virus large envelope polypeptide in transgenic mice. Proc Natl Acad Sci U S A 1987;84:6909-6913.
20. Lake JR. Hepatocyte transplantation [Editorial; Comment]. N Engl J Med 1998;338:1463-1465.
21. Fox IJ, Chowdhury JR, Kaufman SS, Goertzen TC, Chowdhury NR, Warkentin PI, Dorko K, et al. Treatment of the Crigler-Najjar syndrome type I with hepatocyte transplantation [Comments]. N Engl J Med 1998;338:1422-1426.
22. Vemuru RP, Aragona E, Gupta S. Analysis of hepatocellular proliferation: study of archival liver tissue is facilitated by an endogenous marker of DNA replication. HEPATOLOGY 1992;16:968-973.
23. Gupta S, Rajvanshi P, Bhargava KK, Kerr A. Hepatocyte transplantation: progress toward liver repopulation. Prog Liver Dis 1996;14:199-222.
24. Gunsalus JR, Brady DA, Coulter SM, Gray BM, Edge AS. Reduction of serum cholesterol in Watanabe rabbits by xenogeneic hepatocellular transplantation [Comments]. Nat Med 1997;3(1):48-53.
25. Brown JJ, Parashar B, Moshage H, Tanaka KE, Engelhardt D, Rabbani E, Roy-Chowdhury N, et al. A long-term hepatitis B viremia model gener-

Proc. Natl. Acad. Sci. USA
Vol. 95, pp. 310–315, January 1998
Microbiology

Liver repopulation with xenogenic hepatocytes in B and T cell-deficient mice leads to chronic hepadnavirus infection and clonal growth of hepatocellular carcinoma

JOERG PETERSEN*, MAURA DANDRI†, SANJEEV GUPTA, AND CHARLES E. ROGLER‡

Marion Bessin Liver Research Center, Department of Medicine, Albert Einstein College of Medicine, Bronx, NY 10461

Edited by Robert H. Purcell, National Institutes of Health, Bethesda, MD, and approved November 5, 1997 (received for review August 22, 1997)

ABSTRACT **To investigate host and viral mechanisms determining hepadnaviral persistence and hepatocarcinogenesis, we developed a mouse model by transplanting woodchuck hepatocytes into the liver of mice that contain the urokinase-type plasminogen activator transgene (uPA) and lack mature B and T lymphocytes due to a recombination activation gene 2 (RAG-2) gene knockout. The woodchuck hepatocytes were transplanted via intrasplenic injection and were found to integrate into the recipient mouse liver cord structure. Normal adult woodchuck hepatocytes proliferated and reconstituted up to 90% of the uPA/RAG-2 mouse liver. uPA/RAG-2 mice containing woodchuck hepatocytes were infectable with woodchuck hepatitis virus (WHV) and showed WHV replication for at least 10 months with titers up to 1×10^{11} virions per ml in the peripheral blood. WHV-infected hepatocytes from chronic carrier woodchucks also established a persistent infection in uPA/RAG-2 mice after an 8- to 12-week lag period of viremia. Although WHV envelope, core, and X proteins were produced in the uPA/RAG-2 mice, no inflammatory host immune response was observed in the liver of WHV-replicating mice. A first antiviral test demonstrated a greater than four orders of magnitude drop in WHV titer in response to interferon α treatment. WHV replication was up-regulated by dexamethasone treatment. Comparison of precancerous lesions in donor woodchucks versus recipient uPA/RAG-2 mice revealed an enrichment of dysplastic precancerous hepatocytes in transplanted mice. Clonal amplification of hepatocytes from a woodchuck with hepatocellular carcinomas was demonstrated by the detection of unique WHV DNA integration patterns in hepatocellular carcinomas that arose in uPA/RAG-2 mice. In the absence of B or T cell-mediated immune responses, WHV establishes a persistent noncytotoxic infection of woodchuck hepatocytes in uPA/RAG-2 chimeric mouse livers. Further studies of the kinetics of hepadnavirus infection and replication in quiescent and proliferating hepatocytes should increase our understanding of hepadnavirus spread and aid in the design of therapies to block or cure persistent infection.**

Hepatitis B virus (HBV) infection remains a major health problem with more than 350 million chronic HBV carriers worldwide, who are at risk for developing liver cirrhosis and hepatocellular carcinoma (HCC) (1–4). The development of effective therapies for eradicating HBV in chronic carriers has been limited by our incomplete understanding of mechanisms of viral persistence (5).

Both humoral and cellular elements of the host immune response are important for HBV clearance. The humoral response to HBV antigens (i.e., antibodies to hepatitis B surface antigen) helps clear circulating virions and confers protection against reinfection, whereas T cell-mediated responses eliminate infected cells (6, 7). Recent work using HBV transgenic mice has shown that this process can be mediated by cytokines, such as tumor necrosis factor α and interferon γ. These cytokines have the capacity to down-regulate HBV replication in a noncytopathic manner (8, 9).

Our aims were to determine whether hepadnavirus replication will become persistent in the absence of B and T cells in the host and whether acute infection of hepatocytes in such an environment would effect the course of hepadnaviral persistence. To analyze this, we took advantage of recent advances in liver repopulation with transplanted hepatocytes (10). The discovery of a hepatocyte-lethal phenotype in urokinase-type plasminogen activator (uPA) transgenic mice and the replacement of livers from those mice with xenografted hepatocytes (11–13) suggested to us that if the mouse liver could be replaced by hepatocytes amenable to hepadnaviral infection, a variety of studies would be possible in mice containing hepatocytes from a single donor. Furthermore, the potential proliferation of hepadnavirus-infected transplanted xenogenic hepatocytes would allow us to study hepadnaviral replication and persistence in proliferating hepatocytes during liver regeneration and in quiescent hepatocytes after completion of liver regeneration. uPA-transgene-expressing hepatocytes are at a growth disadvantage compared with nontransgenic hepatocytes, because transgene expression compromises their function (11), and thus transplanted hepatocytes are selectively amplified in a mixed polyclonal pattern.

To generate the uPA/recombination activation gene 2 (RAG-2) mice, we crossed uPA transgenic mice with RAG-2 knockout mice, which lack mature B and T lymphocytes (14). Woodchuck hepatocytes, transplanted via splenic injection (10) into the liver of uPA/RAG-2 mice, became integrated in the uPA/RAG-2 liver parenchyma, replacing up to 90% of the uPA/RAG-2 mouse hepatocytes, and supported woodchuck hepatitis virus (WHV) replication indefinitely. WHV replication in uPA/RAG-2 mice could be manipulated by up-regulatory (dexamethasone) or down-regulatory (interferon α) pharmacological interventions. In addition, clonal potential of liver tumor cells derived from chronic WHV carrier woodchucks could be tested in the uPA/RAG-2 mice.

The publication costs of this article were defrayed in part by page charge payment. This article must therefore be hereby marked "*advertisement*" in accordance with 18 U.S.C. §1734 solely to indicate this fact.

This paper was submitted directly (Track II) to the *Proceedings* office. Abbreviations: WHV, woodchuck hepatitis virus; WHsAg, woodchuck hepatitis virus surface antigen; WHcAg, woodchuck hepatitis virus core antigen; WHx, woodchuck hepatitis virus X protein; uPA, urokinase-type plasminogen activator; RAG-2, recombination activation gene 2; HCC, hepatocellular carcinoma; HBV, hepatitis B virus; DPPIV, dipeptidyl peptidase IV; CCC, covalently closed circular; AHF, altered hepatic focus.

*Present address: Medizinische Kernklinik und Poliklinik des Universitätskrankenhauses Eppendorf, Universität Hamburg, Germany.
†Present address: Allgemeine Virologie, Heinrich Pette Institut für Experimentelle Virologie und Immunologie an der Universität Hamburg, Germany.
‡To whom reprint requests should be addressed at: Albert Einstein College of Medicine, Marion Bessin Liver Research Center, Ullmann 625, 1300 Morris Park Avenue, Bronx, NY 10461. e-mail: crogler@aecom.yu.edu.

METHODS

Animals. UPA mice were purchased from The Jackson Laboratories, RAG-2 knockout mice were from Taconic Farms, and adult woodchucks were from North Eastern Wildlife (South Plymouth, NY) or Cornell University (Ithaca, NY). Animals were housed and maintained under specific pathogen-free conditions in accordance with institutional guidelines under approved protocols. We used one uninfected woodchuck, which was negative for all WHV markers, and three woodchucks (nos. 2765, 3543, and 4940) with persistent WHV infections that were woodchuck hepatitis virus surface antigen (WHsAg)-positive and anti-woodchuck hepatitis virus core antibody (anti-WHc)-positive. The results from nine randomly chosen uPA/RAG-2 mice containing transplanted cells are shown in detail. Partial hepatectomies in mice were performed under tribromoethanol anesthesia (Aldrich) with approved protocols (15).

Generation of Tolerant uPA/RAG-2 Mice. uPA transgenic mice were crossed with RAG-2 knockout mice. The uPA transgene was identified by PCR of mouse-tail DNA with the following nucleotide sequences: primer 1, 5′-CATCCCTGTGACCCCTCC-3′, and primer 2, 5′-CTCCAAACCACCCCCCTC-3′. Homozygous uPA transgenic mice were distinguished from hemizygous mice by PCR as reported (13). For the experiments described, only hemizygous uPA mice were used. The RAG-2 knockout mutant gene was identified by PCR of tail DNA as described (16).

Isolation and Transplantation of Woodchuck Hepatocytes. Woodchuck hepatocytes were isolated by the two-step *in situ* collagenase perfusion method followed by differential centrifugation (17). Hepatocyte viability was >95%, as measured by trypan blue dye exclusion. From 5×10^5 to 1×10^6 hepatocytes were transplanted into a number of 10- to 18-day-old uPA/RAG-2 mice by intrasplenic injection (17).

Histological Studies. Serial cryostat sections of woodchuck and uPA/RAG-2 mouse livers were examined by hematoxylin/eosin staining, dipeptidyl peptidase IV (DPPIV) enzyme activity (18) and immunohistochemistry with a rabbit antiserum (WHc antiserum) against woodchuck hepatitis core antigen (WHcAg). For immunolabeling, sections were fixed in 4% paraformaldehyde, incubated with WHc antiserum (diluted 1:250 in PBS containing 5% sheep serum) at room temperature, and subsequently incubated with the Cy3-conjugated sheep anti-rabbit IgG antibody (Sigma) diluted 1:200 in PBS with 5% sheep serum at room temperature. Finally, slides were mounted in 40 mg of *n*-propyl gallate per ml in 90% glycerol/10% 0.5 M sodium carbonate, pH 8, for viewing under a fluorescence microscope.

Immunoprecipitation and Immunoblot Analyses. The woodchuck hepatitis virus X (WHx) protein was immunoprecipitated from cell extracts with a rabbit WHx antiserum and subjected to SDS/PAGE as described (19). For the detection of WHV core protein, 20 μg of total cell extracts was solubilized (20), boiled, and separated by SDS/PAGE. The transblots were probed with either WHx antiserum (1:1,000 dilution) or WHc antiserum (1:5,000 dilution), and binding was detected by the enhanced chemiluminescence (ECL) system (19) (Amersham).

DNA Analysis. Genomic DNAs were extracted from frozen liver and used for Southern blot analysis as described (21, 22). For detecting woodchuck genomic DNA in transplanted uPA/RAG-2 mouse livers, 150 ng of *Pvu*II-digested woodchuck DNA was used for a ^{32}P-labeled random genomic probe. Blots were hybridized under high-stringency conditions (23) at 45°C for 2 h. WHV DNA in woodchuck and uPA/RAG-2 mouse liver tissues was detected with a genome-length 3.3-kb WHV DNA ^{32}P-labeled probe (23).

Detection of WHV DNA, Woodchuck Albumin, and WHsAg in Woodchuck and uPA/RAG-2 Mouse Sera. Woodchucks were anesthetized with ketamine (Fort Dodge Laboratories, Fort Dodge, IA) and xylazine (Bayer, Shawnee Mission, KS) and blood was collected from the femoral vein. Blood was drawn from the tail vein in mice, both woodchuck and mouse sera were dot-blotted onto a nylon membrane (24) and hybridized with a ^{32}P-labeled WHV DNA probe (23), and the number of WHV DNA molecules was quantitated by scanning densitometry. Serial dilutions of known amounts of a plasmid containing one copy of WHV DNA served as a standard. For woodchuck serum albumin, 5 μg of total serum proteins was solubilized (20), boiled, and subjected to SDS/PAGE. Proteins resolved in 7.5% gels were fixed and stained with Coomassie blue. For immunoblotting of WHsAg, proteins were resolved in SDS/PAGE, electrotransferred, probed with a rabbit antiserum against WHsAg (WHs antiserum; 1:1,000 dilution), and visualized by ECL.

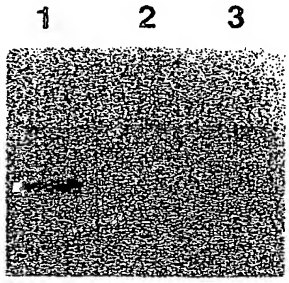

FIG. 1. Migration pattern of mouse (lane 1) and woodchuck (lane 2) serum albumin in a Coomassie blue-stained gel. The migration pattern of serum albumin from a representative uPA/RAG-2 mouse containing woodchuck hepatocytes shows both mouse and woodchuck serum albumin (lane 3).

Blood Chemistry in uPA/RAG-2 Mice. Sera were analyzed for total protein, albumin, bilirubin, alanine aminotransferase activity, and aspartate aminotransferase activity in a standard automated clinical analyzer (Technicon).

Drugs. Interferon α-2b (Schering) at 135 international units/g (body weight) and dexamethasone (Fujisawa, Deerfield, IL) at 27 ng/g (body weight) were given to mice intramuscularly daily for 15 consecutive days.

RESULTS

Repopulation of uPA/RAG-2 Mouse Liver with Xenogenic Woodchuck Hepatocytes. To screen for survival and growth of transplanted woodchuck hepatocytes in uPA/RAG-2 mice, we analyzed serum albumin profiles from all recipients. SDS/PAGE showed that mouse and woodchuck serum albumin migrated differently (Fig. 1). In uPA/RAG-2 mice, 3 months after woodchuck hepatocyte transplantation, this assay demonstrated the presence of both woodchuck and mouse serum albumin (Fig. 1). uPA/RAG-2 mice containing woodchuck hepatocytes were clinically healthy and the livers appeared normal in respect to color, size, and liver weight to body weight ratios at sacrifice. Serum concentrations of total protein, albumin, bilirubin, and transaminases were similar in uPA/RAG-2 mice containing woodchuck hepatocytes compared with control uPA/RAG-2 mice (Table 1).

Table 1. Serum parameters in representative uPA/RAG-2 mice

Parameter	Animal			
	351	457	496	969
Woodchuck hepatocytes	−	−	+	+
Total protein, g/dl	4.4	4.0	4.6	4.2
Albumin, g/dl	2.6	2.4	2.8	2.6
ALT, units/liter	118	104	112	124
AST, units/liter	140	174	139	154
Total bilirubin, mg/dl	0.2	0.2	0.3	0.2

uPA/RAG-2 mice containing woodchuck hepatocytes (no. 496 and 969) were compared with untransplanted uPA/RAG-2 mice (no. 351 and 457). ALT, alanine aminotransferase; AST, aspartate aminotransferase.

To directly demonstrate the presence of woodchuck hepatocytes in transplanted uPA/RAG-2 mouse livers, we hybridized DNAs extracted from recipients with a total woodchuck genome probe, which detects highly repeated sequences in the woodchuck genome (Fig. 2*A*). To estimate uPA/RAG-2 mouse liver repopulation with woodchuck hepatocytes, we hybridized test mixtures of woodchuck and mouse genomic DNAs in various proportions (Fig. 2*A*, lanes 1–5) and DNAs from five liver lobes of a uPA/RAG-2 mouse transplanted with WHV-positive woodchuck hepatocytes (no. 496; Fig. 2*A*, lanes 7–11). Woodchuck hepatocytes were present in abundance in all liver lobes from approximately 30% to >95% (Fig. 2*A*). Because intrasplenic injection results in uniform cell distribution to the liver in normal rats (25), our finding could have indicated differences in the proliferative ratios and development of clonally derived islands of woodchuck hepatocytes in uPA/RAG-2 mouse liver. Alternatively, in the disrupted microenvironment of the diseased uPA liver, cell distributions may not have been uniform.

Demonstration of WHV Replication and Persistence in uPA/RAG-2 Mice. We tested whether transplanted WHV-positive woodchuck hepatocytes supported WHV replication. Genomic liver DNA of a representative woodchuck hepatocyte recipient (no. 496) showed open circular WHV DNA, replicative DNA forms, and covalently closed circular (CCC) WHV DNA that matched the profile of WHV DNA from the donor woodchuck (no. 2765; Fig. 2*B*, lanes 2 and 3). Also, WHx and WHV core proteins were present in this liver (Fig. 2 *C* and *D*, respectively) and the serum contained WHsAg (Fig. 2*E*). WHV DNA in the serum of uPA/RAG-2 mice became detectable only after completion of liver regeneration with a lag period of viremia of 8–12 weeks after transplantation. WHV DNA titers stabilized at a level of approximately 5×10^8 viral genomes per ml in transplanted mouse 496 as compared with 1×10^9 WHV genomes per ml in the donor woodchuck (data not shown). In other transplanted uPA/RAG-2 mice, WHV titers of up to 1×10^{11} virions per ml of mouse serum were detected (see Fig. 4). In Dane particles isolated from the serum of transplanted uPA/RAG-2 mice, viral DNA migrated on Southern blots similar to the WHV DNA from the donor woodchuck. Analysis of WHV RNA in mouse 496 liver revealed the expected major mRNA species corresponding to the pregenome mRNA and the major envelope protein mRNAs (data not shown).

To investigate the growth pattern of woodchuck hepatocytes in uPA/RAG-2 mouse liver, we performed immunohistochemistry with a WHc antiserum. WHV-positive woodchuck hepatocytes had seeded the liver and grown in a nodular pattern within the framework of the preexisting liver with maintenance of the liver cord structure (Fig. 3*A*). Untransplanted mice did not show any specific staining. Integration of the woodchuck hepatocytes into the liver architecture was evaluated by histochemistry for the enzyme DPPIV, which is localized in bile canaliculi of hepatocytes (18). Mouse hepatocytes appeared smaller and DPPIV-positive areas were, therefore, more compact. In contrast, areas containing woodchuck cells showed greater spacing between DPPIV-positive domains due to larger cell sizes. In chimeric uPA/RAG-2 mouse livers containing woodchuck and mouse hepatocytes, we observed networks of DPPIV-positive bile canaliculi between adjacent mouse and woodchuck hepatocytes (Fig. 3*B*). The presence of woodchuck hepatocytes in those sections was confirmed by performing immunohistochemistry using a WHc antiserum in serial sections from uPA/RAG-2 mouse liver tissues. Interestingly, despite expression of WHV proteins in transplanted woodchuck hepatocytes, we did not observe any hepatocellular infiltration with inflammatory cells. The uPA/RAG-2 mice are of course deficient in T and B lymphocytes;

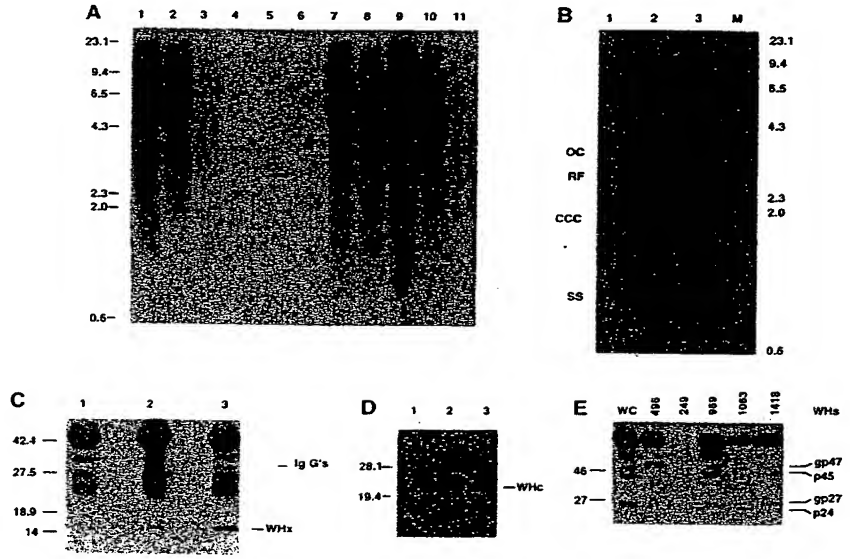

FIG. 2. Woodchuck DNA and WHx, WHc, and WHs proteins in uPA/RAG-2 mice transplanted with WHV-positive woodchuck hepatocytes. (*A*) A Southern blot of genomic DNAs, hybridized with a woodchuck genome DNA probe. Lanes 1–4 present mixtures of genomic woodchuck liver DNA and untransplanted uPA/RAG-2 mouse genomic liver DNA with signals reflecting 100%, 50%, 20%, and 1%, woodchuck hepatocyte DNA, respectively. Lane 5 presents 100% untransplanted uPA/RAG-2 mouse DNA. Woodchuck DNA is undetectable in the spleen of transplanted uPA/RAG-2 mice (lane 6) but present in various amounts in all lobes of the liver of the uPA/RAG-2 mouse transplanted with WHV-positive woodchuck hepatocytes (lanes 7–11). (*B*) WHV DNA forms, detectable in uPA/RAG-2 mouse genomic liver DNA, hybridized with a WHV DNA probe. Lanes: 1, uPA/RAG-2 mouse liver; 2, uPA/RAG-2 mouse liver transplanted with WHV-positive woodchuck hepatocytes; 3, donor woodchuck genomic liver DNA. OC, open circular DNA; RF, replicative WHV DNA forms: CCC, covalently closed circular DNA; SS, single-stranded DNA. Lane M contains molecular size markers. (*C*) Immunoprecipitates with WHx antiserum from uPA/RAG-2 mouse liver (lane 1), from uPA/RAG-2 mouse transplanted with WHV-positive woodchuck hepatocytes (lane 2), and from donor woodchuck liver (lane 3). (*D*) Immunoblotting with WHc antiserum of hepatocyte extracts from uPA/RAG-2 mouse (lane 1), from uPA/RAG-2 mouse transplanted with WHV-positive woodchuck hepatocytes (lane 2), and from donor woodchuck (lane 3). (*E*) WHs proteins in uPA/RAG-2 mice serum. Immunoblotting with WHs antiserum of uPA/RAG-2 mouse 249 and uPA/RAG-2 mouse sera transplanted with WHV-positive woodchuck hepatocytes (uPA/RAG-2 mice 496, 969, 1063, and 1418). Lane WC was probed with WHV-positive woodchuck serum.

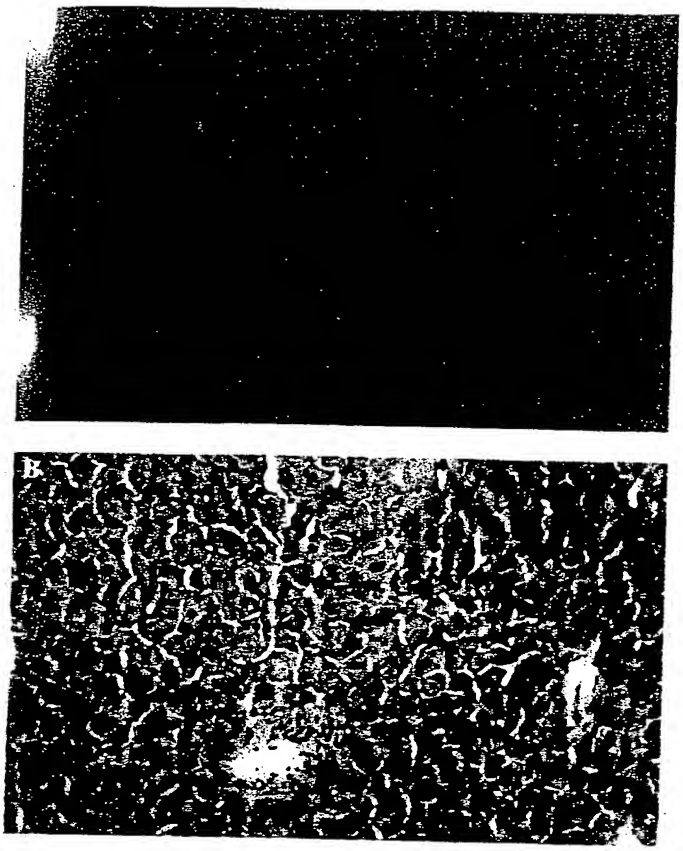

FIG. 3. (*A*) Detection of WHcAg in a uPA/RAG-2 mouse liver containing WHV-positive woodchuck hepatocytes by immunostaining with a WHc antiserum. A nodule containing transplanted WHV-positive woodchuck hepatocytes (lighter area, rhodamine light) and host mouse hepatocytes that presumably deleted the uPA transgene (darker stained area). (×200.) (*B*) DPPIV staining of bile canaliculi in uPA/RAG-2 mouse liver containing woodchuck hepatocytes. (×200.) Bile canaliculi are visible between mouse hepatocytes (darker staining) and transplanted woodchuck hepatocytes (lighter staining). Nuclei are counterstained with hematoxylin.

however, no evidence was found of infiltration with granulocytes or macrophages.

Infection of Woodchuck Hepatocytes in uPA/RAG-2 Mice. To investigate whether naive woodchuck hepatocytes could be infected with WHV in uPA/RAG-2 mice, hepatocytes from an adult uninfected woodchuck were transplanted into the liver of uPA/RAG-2 mice as described above. After completion of liver regeneration 3 months after transplantation, four uPA/RAG-2 mice were subjected to a liver biopsy and the presence of woodchuck hepatocytes was confirmed by Southern blot analysis as described above. Subsequently, these uPA/RAG-2 mice were infected intramuscularly with either 10 μl of a WHV-positive woodchuck serum, containing approximately 1×10^9 virions per ml or with 10 μl of WHV-containing serum from uPA/RAG-2 mouse 496 (5×10^8 virions per ml). The establishment of productive infection was monitored by serum dot blot analysis for WHV DNA. In quiescent hepatocytes after completion of liver regeneration 3 months after transplantation, WHV DNA became detectable at 4 weeks after infection. Southern blot analysis of uPA/RAG-2 mouse liver DNAs hybridized with WHV DNA demonstrated the presence of open circular and replicative WHV DNA forms. The serum WHV virion levels have remained stable for an additional 10 months in the infected animals (analysis currently ongoing), confirming the persistence of WHV infection in uPA/RAG-2 mice containing woodchuck hepatocytes.

Antiviral Studies in WHV Replicating uPA/RAG-2 Mice. To confirm the usefulness of the chimeric uPA/RAG-2 mouse model for studying hepadnaviral replication, we investigated modulation of WHV replication with either interferon α or dexamethasone treatment. Three uPA/RAG-2 mice were chosen for this experiment, mouse 1418 containing hepatocytes from a chronic WHV carrier and mice 1063 and 1098 that were transplanted with naive woodchuck hepatocytes and infected with WHV-containing serum as described above. All mice showed a constant level of viral replication before drug administration (Fig. 4). Dexamethasone significantly up-regulated viral replication. After withdrawal of dexamethasone, the level of WHV replication remained at higher levels compared with pretreatment levels. In contrast, treatment with interferon α down-regulated WHV replication in mouse 1063 by greater than four orders of magnitude to nondetectable levels in serum dot blots after 15 days. However, upon withdrawal of interferon α, WHV replication rebounded to levels higher than pretreatment WHV levels. Mouse 1418, with higher WHV pretreatment levels than mouse 1063, showed only a limited response to interferon α treatment but had a rebound effect upon viral replication similar to mouse 1063 after drug withdrawal.

Heterogeneous Precancerous and Malignant Phenotypes of Transplanted Woodchuck Hepatocytes in uPA/RAG-2 Mice. According to multistep models of carcinogenesis, cells undergo successive cycles of mutation and selection on their path toward malignancy (4). These models predict that a WHV carrier liver will contain hepatocytes that have experienced initiating mutations that predispose them to oncogenic transformation. We reasoned that the regeneration of WHV-positive hepatocytes after transplantation might cause (*i*) selection of precancerous hepatocytes, (*ii*) enhanced oncogenic progression of precancerous hepatocytes, or (*iii*) both.

Therefore, we compared the phenotypes of transplanted woodchuck hepatocytes in relation to hepatocytes present in the donor woodchuck. In chronic carrier woodchuck 2765, precancerous altered hepatic foci (AHFs) were very rare according to hematoxylin/eosin staining of liver sections (Fig. 5*A*). In contrast, nearly all of the transplanted woodchuck hepatocyte nodules in the corresponding uPA/RAG-2 mouse livers had a distinct AHF phenotype (Fig. 5*B*, cells to the right of the arrows) that was absent in control nontransplanted uPA/RAG-2 mouse livers. A close up of the border between mouse hepatocytes and woodchuck hepatocytes in the AHFs from Fig. 5*B* is shown in Fig. 5*D*. The woodchuck hepatocytes to the right of the arrows in Fig. 5*D*

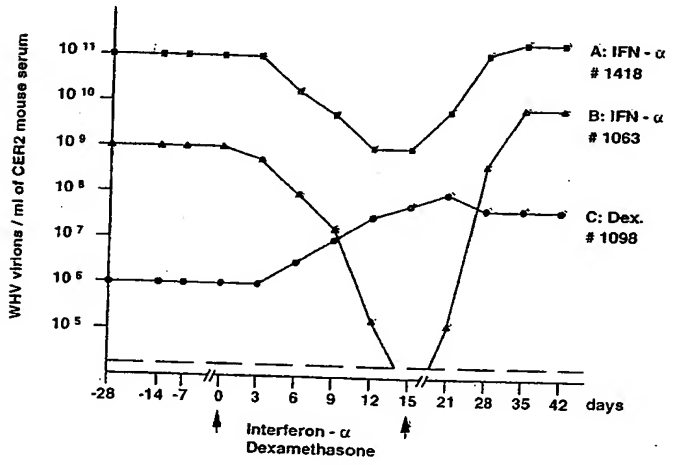

FIG. 4. Effect of interferon α and dexamethasone upon WHV secretion in uPA/RAG-2 mice. Each trace shows data from individual uPA/RAG-2 mice containing WHV-secreting woodchuck hepatocytes. Arrows mark starting point and withdrawal of agents. Time points mark the collection of serum samples. The dashed line represents the threshold of sensitivity for the dot blot analysis.

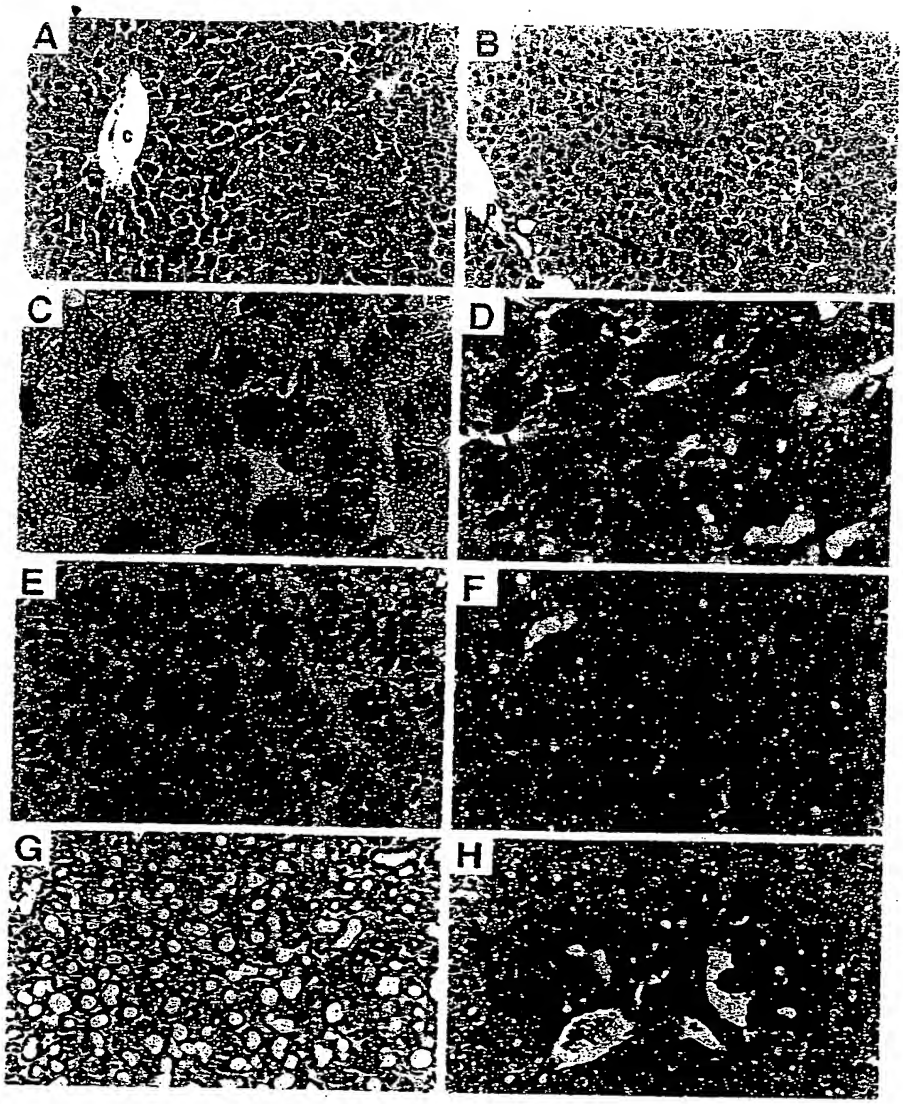

FIG. 5. Hematoxylin/eosin staining of frozen liver sections from donor woodchucks (*A*, *C*, *E*, and *G*) and uPA/RAG-2 mice recipients (*B*, *D*, *F*, and *H*) after transplantation of WHV-positive woodchuck hepatocytes. A woodchuck liver (no. 2765) contained altered hepatic foci (*A*, ×200; *C*, ×1,000; right side of arrows marks border), with large nuclei and prominent nucleoli that appear similar to transplanted woodchuck hepatocytes in uPA/RAG-2 mouse liver (*B*, ×200; *D*, ×1,000; right side of arrows marks border). (*E* and *G*) Examples of an HCC and cholangiocarcinoma, respectively, from a woodchuck (no. 4940) chronically infected with WHV. (×200.) (*F* and *H*) Presence of an HCC (*F*) and a cholangiocarcinoma (*H*) in a uPA/RAG-2 mouse after transplantation of hepatocytes from the donor woodchuck shown in *E* and *G*. (×200.)

exhibited an altered phenotype including enlarged nuclei with prominent nucleoli. This phenotype was common to woodchuck hepatocytes in the AHFs from the donor woodchuck (Fig. 5*C*, to the right of the arrows).

In another example, we detected both a primary HCC (Fig. 5*F*) and a cholangiocarcinoma (Fig. 5*H*) after transplantation of woodchuck cells from woodchuck 4940. Woodchuck 4940 was a chronic WHV carrier that had developed three HCCs and a cholangiocarcinoma (Fig. 5 *E* and *G*) in a lobe of it's liver that was removed before perfusion. The WHV DNA integration pattern in the HCC from transplanted woodchuck cells was different from the integration patterns of the three donor woodchuck HCCs (Fig. 6). Therefore, either the donor liver contained a small tumor that was not detected and was selectively amplified or an infected hepatocyte may have obtained a tumorigenic mutation during growth after transplantation leading to its malignant transformation.

DISCUSSION

We have developed a hepatitis B mouse model by transplanting xenogenic woodchuck hepatocytes into tolerant uPA/RAG-2 mice. Transplanted woodchuck hepatocytes responded to the mouse liver environment with significant proliferation and replaced more than 90% of the diseased transgenic mouse liver. Transplanted cells grew as microclones in several recipients from common donor sources of cells and their growth pattern generally restored a normal cord structure of the liver.

The experimental system reported herein combined several desirable characteristics of previous animal models for studying hepadnavirus infection and pathogenesis. The woodchuck animal model allows the study of WHV infection in a natural host setting in which complete viral clearance occurs in relatively inaccessible genetically heterogeneous animals (26–28). Although transgenic HBV mice have provided important new information regarding viral pathobiology (6–9), they are tolerant to HBV-encoded antigens and do not entirely reproduce the viral life cycle because CCC DNA cannot be detected in the nuclei of their hepatocytes. The chimeric uPA/RAG-2 mouse model offers a unique chance to study mechanisms of viral persistence in natural host hepatocytes in the absence of B and T cell-mediated immune responses. The absence of B and T cells provide potential opportunities for their replacement with either woodchuck or mouse immune system cells selected for specific B or T cell functions. Furthermore, this model provides the chance to study viral replication in rapidly proliferating hepatocytes during liver repopulation and in quiescent hepatocytes after completion of liver regeneration.

Our first antiviral study used interferon α, because this is the only currently approved treatment for persistent HBV infection (5, 29, 30). Besides exhibiting various immunomodulatory effects (31), interferon α induces the release of intracellular

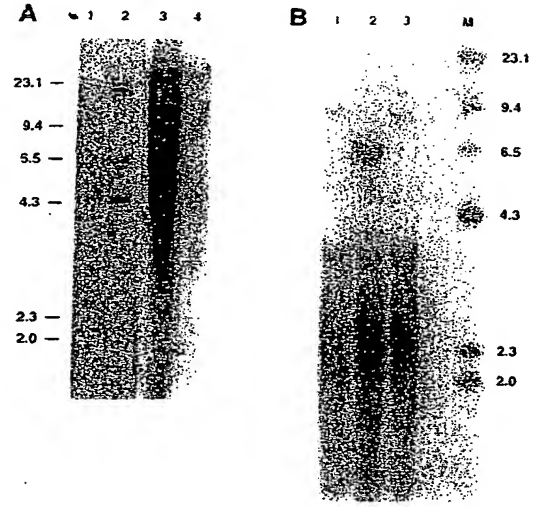

FIG. 6. (*A*) Southern blot analysis of uPA/RAG-2 mouse liver genomic DNA with a woodchuck genomic DNA probe (lanes 3 and 4). Woodchuck DNA is detectable in tumors arising in uPA/RAG-2 mice (lane 3). Lane 4 is a negative control. Unique WHV DNA integrations in DNA from the tumor of lane 3 are detected with a WHV DNA probe (lane 2, with lane 1 as negative control) that are different from WHV DNA integrations in donor woodchuck tumor DNA samples (*B*, lanes 1–3).

nzymes such as 2′,5′-oligoadenylate synthetase and double-tranded RNA-dependent protein kinase, which degrade viral nessenger RNAs and inhibit viral protein synthesis (31) *in vitro* 32) and *in vivo* (29, 33).

Patients who respond to interferon α therapy show a decrease n circulating HBV DNA levels within the first week (31). In PA/RAG-2 mice, we observed a transient reduction in WHV)NA in serum after 15 days of interferon α treatment and nhanced WHV replication by stimulation of the glucocorticoid esponsive element with dexamethasone. The immediate re-ound of viral replication after withdrawal of interferon α trongly suggests that WHV DNA was not cleared from wood-huck hepatocytes and that woodchuck hepatocytes were not liminated as a result of interferon α treatment. Further studies ould allow us to determine whether the sole remaining WHV)NA during interferon α treatment is nuclear CCC DNA. The ffectiveness of human interferon α against WHV suggests that ther human and murine reagents may cross react with their oodchuck homologues and will allow us to test a wide variety of ntiviral agents, including cytokines, for their effectiveness in earing all molecular species of WHV DNA.

A major objective for hepatocarcinogenesis studies is to define ie cellular and molecular phenotype of precancerous hepato-ytes to design early diagnostic and intervention protocols. Phe-otypic comparison of nodular woodchuck hepatocytes in uPA/ AG-2 mice with hepatocytes present in precancerous lesions in ie donor woodchuck revealed an enrichment of AHF pheno-pes in transplanted uPA/RAG-2 mice. These data suggest that ansplantation led either to a selection for altered hepatocytes iat preexisted in the woodchuck liver or progression of initiated epatocytes from the original woodchuck liver. In either case, the sy identification of amplified precancerous lesions provides a ol for studying genetic changes in those cells.

The presence of unique WHV DNA integrations in an HCC om a uPA/RAG-2 mouse liver demonstrated *in vivo* selec-on and clonal expansion of woodchuck hepatocytes, suggest-ig that tumor progression may have occurred after cell ansplantation. Such clonal expansion of hepatocytes should rovide sufficient quantities of transformed cells to investigate id better understand the roles of viral genes and WHV DNA itegrations in hepadnavirus-associated hepatocarcinogenesis.

We thank Leslie E. Rogler for helpful advice during this project and L. Johnson and B. Tennant for providing woodchucks from the experimental woodchuck colony at Cornell University, Ithaca, NY. We also thank J. Gerin, B. Korba, and P. Cote for providing WHs antiserum; W. Mason for providing WHx and WHc antisera; S. Gagandeep and R. Sokhi for technical assistance; and T. Harris for help with computer work. This work was supported by U.S. Public Health Service Grants CA 37232 and DK 46952, Center Grants P30CA13330 and P30DK41296, the Irma T. Hirschl Trust, and the Council for Tob. Res. USA Inc. C.E.R and S.G. are recipients of Irma T. Hirschl-Weiler career scientist awards. J.P. was on leave from the Department of Medicine, University Hospital Eppendorf, University of Hamburg, Germany, and was supported by the Deutsche Forschungsgemeinschaft (Pe/608 1–1), Bonn, Germany.

1. Ganem, D. & Varmus, H. E. (1987) *Annu. Rev. Biochem.* **56**, 651–693.
2. Buendia, M. A. (1992) *Adv. Cancer Res.* **59**, 167–226.
3. B. S. Blumberg, (1997) *Proc. Natl. Acad. Sci. USA* **94**, 7121–7125.
4. Rogler, C. E. (1991) *Curr. Top. Microbiol. Immunol.* **168**, 103–141.
5. Fried, M. W. (1996) *Med. Clin. N. Am.* **80**, 957–971.
6. Chisari, F. V. & Ferrari, C. (1995) *Annu. Rev. Immunol.* **13**, 29–60.
7. Chisari, F. V. (1996) *Curr. Top. Microbiol. Immunol.* **206**, 150–173.
8. Guidotti, L. G., Ando, K., Hobbs, M. V., Ishikawa, T., Runkel, L., Schreiber, R. D. & Chisari, F. V. (1994) *Proc. Natl. Acad. Sci. USA* **91**, 3764–3768.
9. Guidotti, L. G., Ishikawa, T., Hobbs, M. V., Matzke, B., Schreiber, R. & Chisari, F. V. (1996) *Immunity* **4**, 25–36.
10. Gupta, S., Rajvanshi, P., Bhargava, K. K. & Kerr, A. (1996) *Prog. Liver Dis.* **14**, 199–222.
11. Sandgren, E. P., Palmiter, R. D., Heckel, J. L., Daugherty, C. C., Brinster, R. L. & Degen, J. L. (1991) *Cell* **66**, 245–256.
12. Rhim, J. A., Sandgren, E. P., Degen, J. L., Palmiter, R. D. & Brinster, R. L. (1994) *Science* **263**, 1149–1152.
13. Rhim, J. A., Sandgren, E. P., Palmiter, R. D. & Brinster, R. L. (1995) *Proc. Natl. Acad. Sci. USA* **92**, 4942–4946.
14. Shinkai, Y., Rathbun, G., Lam, K. P., Oltz, E. M., Stewart, V., Mendelsohn, M., Charron, J., Datta, M., Young, F., Stall, A. M. & Alt, F. W. (1992) *Cell* **68**, 855–867.
15. Vemuru, R. P., Aragona, E. & Gupta, S. (1992) *Hepatology* **16**, 968–973.
16. Horton, R. M., Karachunski, P. I. & Conti-Fine, B. M. (1995) *BioTechniques* **19**, 690–691.
17. Gupta, S., Vemuru, R. P., Lee, C. D., Yerneni, P., Aragona, E. & Burk, R. D. (1994) *Hum. Gene Ther.* **4**, 249–257.
18. Rajvanshi, P., Kerr, A., Bhargava, K. K., Burk, R. D. & Gupta, S. (1996) *Hepatology* **23**, 482–496.
19. Dandri, M., Schirmacher, P. & Rogler, C. E. (1996) *J. Virol.* **70**, 5246–5254.
20. Laemmli, U. K. (1970) *Nature (London)* **227**, 680–685.
21. Gong, S. S., Jensen, A. D. & Rogler, C. E. (1996) *J. Virol.* **70**, 2000–2007.
22. Petersen, J., Buerkle, A., Zhang, L. & Rogler, C. E. (1997) *J. Virol.* **71**, 5455–5463.
23. Ogston, C. W., Jonak, G. J., Rogler, C. E., Astrin, S. M. & Summers, J. (1982) *Cell* **29**, 385–394.
24. Scotto, J., Hadchouel, M., Hery, C., Yvart, Y., Tiollais, P. & Brechot, C. (1983) *Hepatology* **3**, 279–284.
25. Gupta, S., Lee, C. D., Vemuru, R. P. & Bhargava, K. K. (1994) *Hepatology* **19**, 750–757.
26. Roggendorf, M. & Tolle, T. K. (1995) *Intervirology* **38**, 100–112.
27. Korba, B. E., Cote, P. J., Wells, F. N., Baldwin, B., Popper, H., Purcell, R. H., Tennant, B. C. & Gerin, J. L. (1989) *J. Virol.* **63**, 1360–1370.
28. Tennant, B. C. & Gerin, J. L. (1994) in *The Liver. Biology and Pathobiology*, eds. Arias, I. M., Boyer, J. L., Fausto, N., Jakoby, W. B., Schachter, D. & Shafritz, D. A. (Raven, New York), pp. 1455–1469.
29. Perillo, R. P. & Mason, A. L. (1994) *Gastroenterol. Clin. N. Am.* **23**, 581–601.
30. Perillo, R. P., Schiff, E. R., Davis, G. L., Bodenheimer, H. C., Lindsay, K., *et al.* (1990) *N. Engl. J. Med.* **323**, 295–301.
31. Haria, M. & Benfield, P. (1995) *Drugs* **50**, 873–896.
32. Yamashita, Y., Koike, K., Takashi, M. & Matsuda, S. (1988) *Microbiol. Immunol.* **32**, 1119–1126.
33. Nagahata, T., Araki, K., Yamamura, K. I. & Matsubara, K. (1992) *Antimicrob. Agents Chemother.* **36**, 2042–2045.

Hepatitis C virus replication in mice with chimeric human livers

DAVID F. MERCER[1], DANIEL E. SCHILLER[1], JOHN F. ELLIOTT[2], DONNA N. DOUGLAS[1], CHUNHAI HAO[3], ALINE RINFRET[4], WILLIAM R. ADDISON[2], KARL P. FISCHER[2], THOMAS A. CHURCHILL[1], JONATHAN R.T. LAKEY[1], DAVID L.J. TYRRELL[2] & NORMAN M. KNETEMAN[1]

[1]*Surgical-Medical Research Institute, Department of Surgery,* [2]*Department of Medical Microbiology and Immunology and* [3]*Department of Pathology, University of Alberta, Edmonton, Alberta, Canada*
[4]*Centre de Recherche du CHUM, Hôpital Saint-Luc, Montréal, Québec, Canada*
Correspondence should be addressed to N.M.K.; email: nkneteman@cha.ab.ca

Lack of a small animal model of the human hepatitis C virus (HCV) has impeded development of antiviral therapies against this epidemic infection. By transplanting normal human hepatocytes into SCID mice carrying a plasminogen activator transgene (*Alb-uPA*), we generated mice with chimeric human livers. Homozygosity of *Alb-uPA* was associated with significantly higher levels of human hepatocyte engraftment, and these mice developed prolonged HCV infections with high viral titers after inoculation with infected human serum. Initial increases in total viral load were up to 1950-fold, with replication confirmed by detection of negative-strand viral RNA in transplanted livers. HCV viral proteins were localized to human hepatocyte nodules, and infection was serially passaged through three generations of mice confirming both synthesis and release of infectious viral particles. These chimeric mice represent the first murine model suitable for studying the human hepatitis C virus *in vivo*.

Human liver disease caused by the hepatitis C virus has emerged as a major challenge to the medical community, affecting an estimated 175 million people worldwide[1]. Elucidation of the viral sequence in 1989 (ref. 2) initiated concerted study of HCV. Antiviral therapy with combination interferon and ribavirin is effective in selected patients, but many do not respond or tolerate therapy poorly, underscoring a need for improvement. Development of effective therapeutic strategies has been significantly hampered by difficulties in establishing *in vitro* and *in vivo* models of viral replication.

The *Alb-uPA* transgenic mouse, developed in 1990 to study neonatal bleeding disorders[3], carries a tandem array of four murine urokinase genes controlled by an albumin promoter. This transgene targets urokinase over-production to the liver resulting in a profoundly hypofibrinogenemic state and accelerated hepatocyte death. Through random somatic mutations, individual hepatocytes spontaneously delete portions of the transgene array, providing a significant replicative advantage over surrounding cells, and resulting in repopulation of the liver with largely nontransgenic cells[4]. This survival advantage is extended to hepatocytes transplanted from mouse, rat[5] and woodchuck donors[6], and recently in hepadnavirus systems using immortalized[7] and nonimmortalized[8] human hepatocytes.

Human graft survival correlates with *Alb-uPA* zygosity

We crossed *Alb-uPA* and C.b-17/SCID*/bg* mouse lines, and through selective backcrosses bred the SCID trait to homozygosity. In initial experiments, homozygous SCID animals carrying the *Alb-uPA* transgene in hemizygous fashion were crossed, and litters were transplanted with freshly isolated human hepatocytes. Human albumin, produced exclusively by human hepatocytes, was used as an indicator of graft function[9].

In a pilot study of 36 transplants, strong human-albumin signals at 4–5 weeks post-transplant were demonstrated in the serum of 19 recipients. We detected human-albumin bands at 2 weeks post-transplant which increased in intensity over 4–6-week time points, indicating graft expansion (Fig. 1*a*). Blinded genotype analysis revealed that all strongly human-albumin–positive animals carried *Alb-uPA*, whereas the remainder did not.

Despite initially strong human-albumin signals, some recipients showed extinction of signal around 14 weeks, whereas a second subset maintained strong signals beyond 30 weeks (Fig. 1*b*). As these graft recipients were progeny of heterozygous crosses, we hypothesized this divergence was the result of zygosity of *Alb-uPA*. Transgenic and endogenous *uPA* were distinguishable by Southern-blot analysis, with the signal ratio then used to determine the zygosity of the transgene array (Fig. 1*c*). Genomic DNA analysis confirmed that animals demonstrating sustained human engraftment were homozygous for *Alb-uPA*, whereas the subset with failing graft function was hemizygous.

Murine livers are repopulated with human hepatocytes

Sections from transplanted homozygote livers showed large nodules of hepatocytes arranged in typical cord-like structures (Fig. 2*a*). Within nodules, hepatocyte cytoplasm and nuclei appeared histologically normal compared with surrounding tissues where cells were obviously smaller, with vacuolated cytoplasm and pyknotic nuclei (Fig. 2*b*). We immunostained sections with a monoclonal antibody that intensely stained control human liver but did not cross-react with non-transplanted homozygous mouse liver, either within or outside of endogenously produced regen-

Table 1 Infection of homozygous mice with human HCV

Alb-uPA genotype	*n*	Initial human-albumin signal	Median graft duration (wk)	HCV RNA (RT-PCR)
–/–	8	none[a]	0	0/8
+/–	15	strong	15.5	0/15
+/+	4	strong	30.5[b]	4/4[c]

Association between homozygosity of the *Alb-uPA* transgene and development of both sustained human chimerism and infection with human HCV. Graft duration defined as the period of human-albumin detectability by immunoprecipitation/western-blot procedure. [a], 3/8 animals had a single weak human-albumin signal at 5-wk timepoint only. [b], $P < 0.001$ versus hemizygotes and wild type by Kruskal–Wallis test. [c], $P < 0.001$ versus hemizygotes and wild type by Pearson χ^2 test.

erative nodules (Fig. 2*c*, *d* and *e*). This showed that the nodules were clearly of human origin, expanding outward into and compressing surrounding murine-derived tissues (Fig. 2*f* and *g*). Biliary tract and portal structures appeared to be mainly host-derived, as observed by Rhim *et al.*[10]

For additional confirmation of human chimerism, we isolated genomic DNA from livers of transplanted and nontransplanted mice, and we distinguished murine and human DNAs using a PCR-based strategy to detect *Alu* elements, which are short interspersed sequence elements found only in primate genomes[11] (Fig. 2*h*). *AluSx* is the most abundant subfamily and is thought to represent the general human *Alu* consensus. We confirmed the presence of murine genomic DNA by PCR amplification of a sequence mapping to the murine *c-mos* proto-oncogene[12]. As expected, nontransplanted mouse liver DNA and mouse-tail biopsy DNA contained the proto-oncogene but no *Alu*-repeats, whereas human peripheral blood contained *Alu*-repeats but not the proto-oncogene. Analysis of DNA extracted from a transplanted mouse liver clearly showed both bands, establishing the presence of human genomic DNA within the liver.

Establishment of HCV infection in transplanted mice

With evidence of prolonged human engraftment, we next infected mice with serum from HCV-infected human donors. We transplanted non-infected human hepatocytes into 27 offspring from heterozygous crosses, and at 6 weeks after transplantation all mice were inoculated intravenously and/or intraperitoneally with 0.25 ml human serum obtained from 1 of 2 unrelated HCV-positive donors (viral genotypes 1a and 6a). We analyzed selected serum samples between 3 and 40 weeks after inoculation for the presence of positive-strand HCV RNA by reverse transcriptase (RT)-PCR (Table 1).

All eight wild-type controls showed no initial graft function and were persistently negative for HCV RNA. Hemizygous animals had initially strong human-albumin signals, but gradually showed diminishing signal intensity to a median graft duration of 15.5 weeks; we could not detect positive-strand HCV RNA in any of these animals over multiple time points. In sharp contrast, all four animals homozygous for the *Alb-uPA* transgene demonstrated sustained human chimerism (median, 30.5 wk) and were positive for HCV RNA as shown by RT-PCR analysis of serum. Quantitative HCV RNA analysis revealed that viral levels, ranging from 1.4×10^3 to 1.4×10^6 RNA copies/ml, were well within the range of infected humans. Successful infections were established with both genotypes of viral inoculum, and duration of infection ranged from 10 to 21 weeks in this initial cohort.

HCV infection is dependent on *Alb-uPA* homozygosity

Whereas positive-strand HCV RNA was persistently demonstrable in homozygous mice, we were unable to detect it in hemizygotes. We hypothesized that hemizygotes fail to support HCV replication at detectable levels after diminished initial engraftment and earlier graft loss. We developed a protein dot-blot assay using chemiluminescence and phosphoimaging to more accurately quantify human albumin production. After transplanting 1×10^6 cryopreserved human hepatocytes from a single human donor into 21 recipients (15 homozygotes and 6 hemizygotes), we sampled randomly selected animals for quantitative human-albumin analysis and/or immunohistochemical analysis.

Whereas hemizygous and homozygous animals initially showed similar human-albumin signal intensities, by 5–6 weeks a clear divergence was apparent and by 10–12 weeks human-albumin signals in homozygous mice were more than an order of magnitude higher than hemizygotes (Fig. 3*a*). To estimate the percent replacement of murine liver with human tissue, random liver sections from recipients killed at selected time points after transplantation were immunostained with a monoclonal antibody specific for hepatocytes. These immunohistochemical data confirmed the protein dot-blot findings, with human cells occupying substantial portions (> 50%) of cross-sectional liver area in homozygous mice (Fig. 3*b*). In distinct contrast, we examined multiple sections of tissue from heterozygous recipients, and found only minimal evidence of human engraftment (Fig. 3*c*).

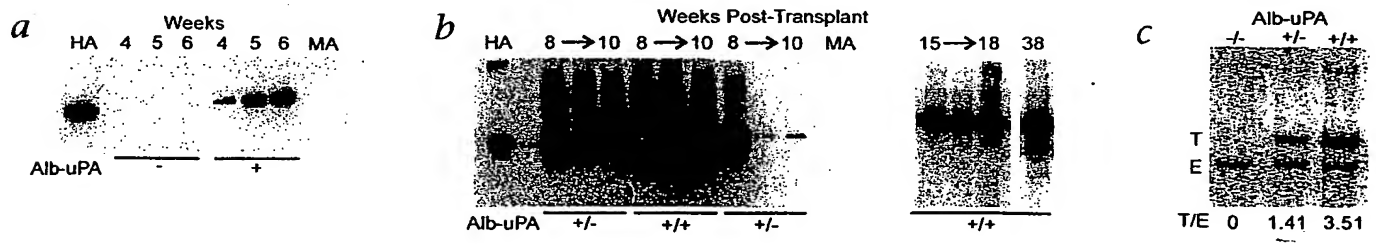

Fig. 1 Detection of human albumin (HA) produced from human hepatocytes in chimeric livers (samples represent individual mice). ***a***, Western-blot analysis showing early HA production in wild-type (–) or transgenic (+) recipients; incremental rise in HA signal indicates graft expansion. ***b***, Western-blot analysis showing long-term HA production in transplant recipients hemizygous (+/–) or homozygous (+/+) for the *Alb-uPA* transgene. Blot demonstrates diminishing signal in hemizygotes, contrasted with persisting signal in homozygotes. HA in leftmost lane, HA standard; MA in rightmost, nontransplanted mouse serum (negative control). ***c***, Southern-blot analysis for determination of *Alb-uPA* zygosity from genomic DNA. A transgenic uPA:endogenous nuPA (T/E) ratio of –2 is characteristic of hemizygous mice, whereas homozygotes have a ratio of –4.

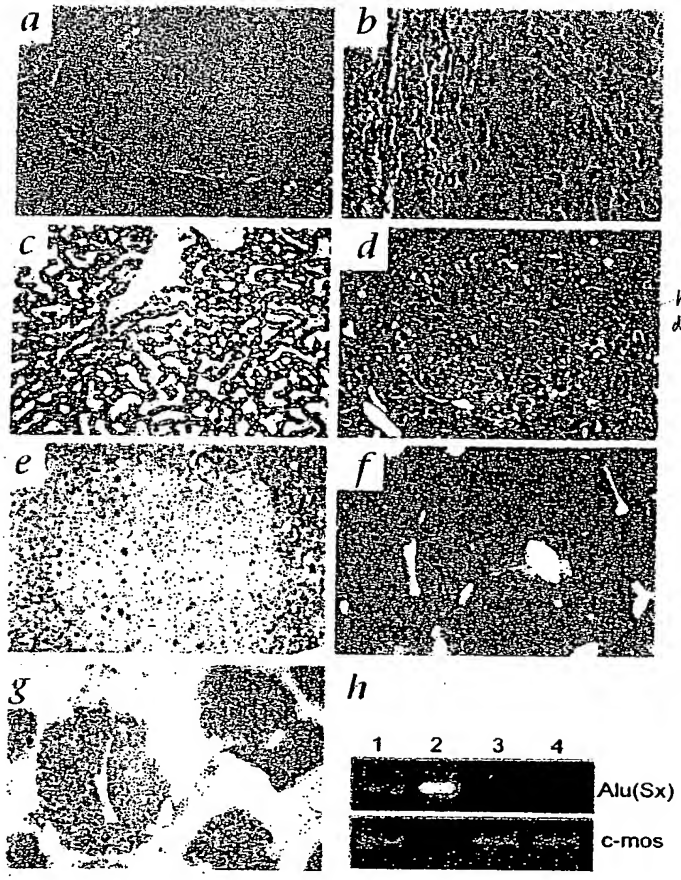

Fig. 2 Histochemical analysis of human chimerism in mouse livers. ***a*** and ***b***, Transplanted homozygote stained with H&E. ***c***, Human liver immunostained with monoclonal antibody against human hepatocytes. ***d***, Nontransplanted homozygote with mouse-derived regenerative nodule; H&E stained. ***e***, Serial section from *d* immunostained as in *c*. ***f***, Transplanted homozygote stained with H&E. ***g***, Serial section from *f* immunostained with monoclonal antibody against human hepatocytes. Magnifications, ×40 (*a*, *f*, and *g*) and ×200 (*b*, *c*, *d* and *e*). ***h***, Genomic DNA extracted from liver of a transplanted homozygous *Alb/uPA* mouse and analyzed for human-specific *AluSx* consensus sequence or murine-specific *c-mos* proto-oncogene. *AluSx* consensus was detected in genomic DNA from transplanted *Alb/uPA* murine liver (lane 1) and human peripheral blood (lane 2) but not from non-transplanted control *Alb/uPA* murine liver (lane 3) or murine control tails (lane 4).

Together, these studies indicate a substantial advantage in both the magnitude and duration of human hepatocyte engraftment for homozygous *Alb-uPA* recipients compared with their heterozygous counterparts.

By transplanting into the progeny of heterozygous crosses, we established successful infections in 4/27 mice, all homozygotes. This success rate would make the model too cumbersome for routine use. As a result of the quantitative advantage in graft size ascribed to homozygous mice, we shifted our breeding colony towards exclusive production of homozygous *Alb-uPA* mice. Using our dot-blot assay to screen early for high-level hepatocyte engraftment (human-albumin levels > 250μg/ml), approximately 75% of HCV-inoculated animals developed persistent viral titers of more than 3×10^4 copies/ml, with as many as 1×10^6 copies/ml. The rest of our viral studies were therefore performed in homozygous recipients.

Long-term persistence of HCV infection

Persistence of viral titers in humans is the result of ongoing active proliferation. However, in immunocompromised chimeric animals, it is possible that HCV persistence is due to slower viral elimination rather than true infection and replication. Five homozygous graft recipients were inoculated with 250 μl infected human serum (genotype 3a; 2.95×10^6 viral RNA copies/ml); each animal therefore received an inoculum of 7.38×10^5 RNA copies. In 3/5 recipients, viral titers increased by 16-, 27- and 36-fold, respectively, over the initial inoculum by 5 weeks after inoculation (Fig. 3*d*). In the remaining 2 recipients, titers increased modestly over 5 weeks (1.6- and 4.3-fold, respectively). In this cohort of mice, detection of positive-strand HCV RNA was confirmed at 15 weeks after inoculation in 1 animal and at 17 weeks in 2 others (one early death after blood sampling). In the fifth mouse, productive infection with HCV was ongoing at 35 weeks after inoculation with viral titers of 1.67×10^5 copies/ml. The initial rise in titers coupled with persistently high viral levels at 35 weeks is consistent with viral replication, and cannot be ascribed to carryover artifact.

A 3-log rise in viral titers after inoculation with HCV

To detect an initial rise in viral titers that might be masked by a

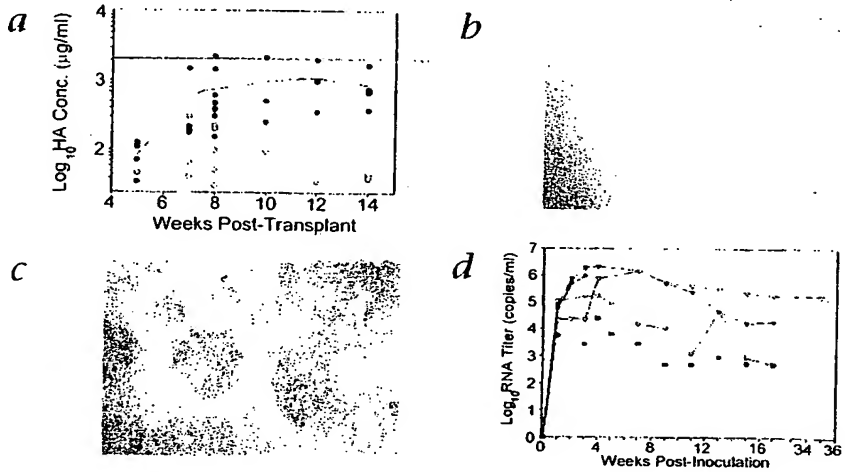

Fig. 3 Mice homozygous for the *Alb-uPA* transgene support quantitatively higher levels of human hepatocyte engraftment than hemizygotes. ***a***, Vertica-scatter plot of quantified HA production from individual homozygous (●) or hemizygous (○) recipient mouse serum samples. Median trend lines are shown for both groups. ***b*** and ***c***, Photos show representative sections taken from heterozygous (*b*) and homozygous (*c*) *Alb-uPA* graft recipients at 12 wk after transplantation immunostained with anti-human hepatocyte antibodies. ***d***, Rising serum HCV RNA titers over time in homozygous transgenic graft recipients after inoculation with HCV-infected human serum. Each different line and symbol represents serial titers from an individual graft recipient.

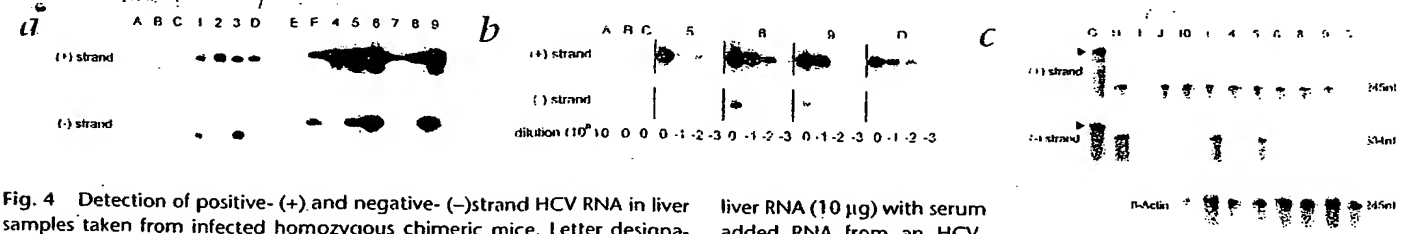

Fig. 4 Detection of positive- (+) and negative- (–)strand HCV RNA in liver samples taken from infected homozygous chimeric mice. Letter designations ('A' through 'J', specified below and consistent through the figure) represent different RNA control samples, and number designations (1 through 10, specified below and consistent through the figure) represent individual RNA samples isolated from the livers of 10 homozygous mice that were transplanted and then inoculated with HCV-infected human serum. ***a***, Detection of (+)strand RNA (upper) or (–)strand RNA (lower) by thermostable rTth reverse transcriptase RNA PCR protocol with strand-specific primers. Lanes: A, wild-type control mouse, nontransplanted, noninfected; B, heterozygous transplanted mouse inoculated with HCV; C, homozygous transplanted mouse not inoculated with HCV; D, infected human serum; E, standard DNA ladder; F, binding of labeled probe to target DNA sequences generated from (+)strand (upper) or (–)strand (lower) viral RNA; G, mouse liver RNA (10 μg) with serum added RNA from an HCV-positive human; H, mouse liver RNA (10 μg) added with 1×10^6 copies radioinert antisense (upper) or sense (lower) riboprobe; I, mouse liver RNA (10 μg) added with 1×10^6 copies radio-inert sense (upper) or antisense (lower) riboprobe; J, riboprobes hybridized with 10 μg mouse liver RNA, all subsequent steps identical except addition of RNase. ***b***, Dilution-series analysis of selected animals using thermostable rTth reverse transcriptase RNA PCR protocol. ***c***, Detection of (+)strand HCV RNA (upper), (–)strand HCV RNA (middle) or β-actin RNA (lower) by RNase protection assay. Fragments in lane G represent undigested riboprobe (arrowhead), with expected lengths greater than those of corresponding fragments protected by hybridization to their targets. Control lanes are as designated above; mouse 10 was analyzed only by the RPA method.

higher viral inoculum, we infected a sixth chimeric mouse with a much smaller viral inoculum (1.35×10^1 RNA copies), and then followed at weekly intervals. This mouse rapidly developed HCV infection, and the total serum viral load at 10 weeks after infection was measured at 1.33×10^6 copies, a 1000-fold increase. In 2 subsequent animals inoculated with 1.05×10^3 copies and 1.75×10^3 copies, titers rose to 9.5×10^5 copies/mL at 10 weeks and 3.42×10^6 copies/mL, respectively, at 5 weeks post-inoculation; rises of 905-fold and 1954-fold, which confirm the initial 10-week result. A nonproductive interaction could not reasonably sustain a 3-log increase in viral load, strongly supporting the occurrence of viral replication.

Negative-strand viral RNA in recipient livers

HCV is a positive-strand RNA virus replicating through a negative-strand intermediate; detection of negative-strand HCV RNA within the liver constitutes proof of replication. This replicative intermediate is believed to exist at levels 10–100 times lower than its positive-strand template[14,15], and hence its detection can be more difficult.

Nine homozygous graft recipients inoculated with 5×10^5 copies of viral RNA from freshly obtained human serum showed positive-strand HCV RNA at 3–4 weeks post-inoculation (Fig. 4*a*, upper). Samples of liver tissue were obtained by 50% partial hepatectomy at 2–5 weeks post-inoculation in 7 mice and 12–13 weeks in the remaining 2 mice. Analysis for negative-strand HCV RNA was performed in blinded fashion by an independent laboratory (A.R.) using a thermostable rTth RT-RNA PCR (rTth PCR) protocol and strand-specific primers (Fig. 4*a*, lower panel). In 5/9 samples analyzed, negative-strand RNA was detected; the 2 samples taken at 12–13 weeks post-inoculation did not show negative-strand RNA. To reduce the risk of false-positive results[15], we performed two additional sets of confirmatory experiments.

Using rTth PCR, we performed a dilution series on three animals to confirm dilutability of the negative-strand signal (Fig. 4*b*). Positive-strand signal was detectable over 3-log dilutions in 2/3 animals as well as control human serum. As expected, no negative-strand signal was detected in human serum. In 2/3 mice, the negative-strand signal was clearly detectable after 10-fold dilution. In the third mouse, we did not detect the negative-strand; the diminished positive-strand signal for this animal

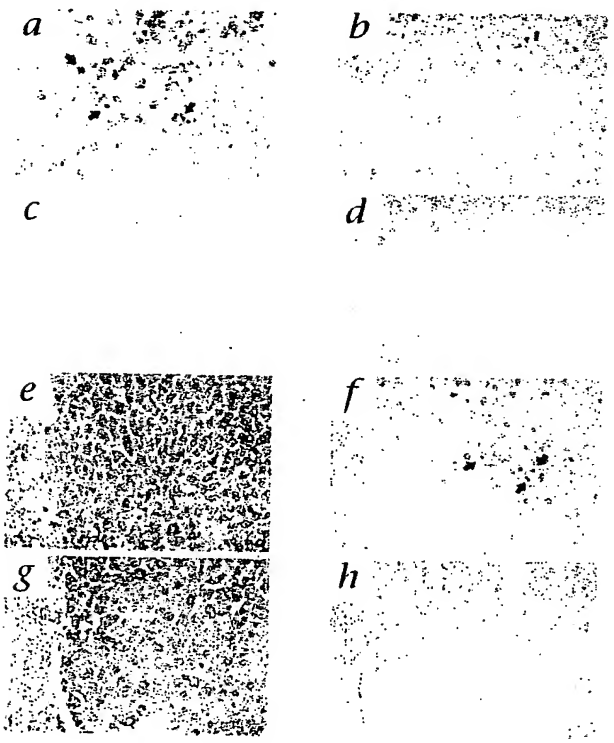

Fig. 5 Immunohistochemical detection of HCV proteins within human hepatocytes in transplanted homozygous *Alb-uPA* mice. ***a*** and ***b***, Serial sections of HCV-infected human liver stained for HCV with monoclonal antibody against NS3/NS4 (TORDJI-21) (*a*) or by an unrelated isotype-specific monoclonal antibody against melanoma (HMB-45) (*b*). ***c*** and ***d***, Serial sections from non-infected human liver stained with TORDJI-21 (*c*) or HMB-45 (*d*). ***e*** and ***f***, Serial sections from a transplanted homozygous mouse infected with HCV, stained with antibody against human hepatocytes (*e*) and HCV-specific antibody (TORDJI-21) (*f*). Arrows indicate coarse granules specific for HCV infection. ***g*** and ***h***, Serial sections from a control noninfected homozygous mouse transplanted with human hepatocytes and stained with anti-human hepatocyte antibody (*g*) or TORDJI 21 (*h*).

indicates comparatively less RNA was loaded onto these lanes of the gel. Lack of additional sample material prevented repeat analysis by this method; however, we subsequently confirmed the presence of the negative-strand using the RNase protection method.

In a further confirmatory experiment, we assayed six animals previously tested by the above PCR method (plus one additional animal) for negative-strand RNA using an RNase protection assay developed in our laboratory (Fig. 4*c*). Results from this system were concordant with the previous PCR findings in 5/6 mice, confirming presence of negative-strand RNA in 3/4 mice and absence in the remaining 2 mice, which initially tested negative by rTth PCR. We were unable to confirm presence of the negative-strand in one mouse; this variance might be attributable to the less sensitive nature of the RNase-protection assay.

These separate and independently performed assays clearly demonstrate presence of negative-strand HCV RNA within chimeric livers sampled at 2–5 weeks post-inoculation. Our previous experiments with sequential weekly analysis by quantitative RT-PCR demonstrated a rapid rise in HCV serum titer at weeks 2–4 after inoculation, corresponding to maximal rates of viral replication within the liver. We would expect this to be paralleled by maximal amounts of negative-strand viral RNA. After this period of rapid replication, viral levels stabilize, indicating that although ongoing replication clearly occurs, the rate diminishes to equal that of viral loss. This might explain why negative-strand RNA is detectable earlier in infections (5/6 animals sampled at 2–5 wk) rather than later (0/2 sampled at 12–13 wk). Together, these data conclusively support active viral replication in this mouse model.

HCV infection can be serially passaged

We intraperitoneally injected fresh serum from a human donor (250 µl; 4.75×10^5 viral RNA copies) into a naive chimeric mouse; at four weeks after inoculation, viral titers were 1.76×10^6 copies/ml. Serum taken from this mouse (125 µl; ~2.19×10^5 RNA copies) was injected intraperitoneally into a second naive chimeric mouse, which developed titers of 1.75×10^4 copies/ml at four weeks after inoculation. Serum from this first-passage recipient was then injected (100 µl; ~1.75×10^3 RNA copies) into a third naive chimeric mouse. At five weeks after inoculation, this second-passage recipient had viral titers of 3.42×10^6 copies/ml. Serum from this second-passage recipient (20 µl) was injected into two additional naive mice (third-passage recipients), both of whom subsequently developed HCV infections with viral titers of 1.6×10^5 and 4.5×10^6 at 9 and 11 weeks post-inoculation, respectively. If one assumes the null hypothesis that replication does not occur but rather the initial human inoculum persists, these third-passage recipients would have received approximately 120 copies of virus from the initial inoculum (4.75×10^5 viral copies × 1:8 dilution × 1:10 dilution × 1:50 dilution, assuming mouse serum volume ~1000 µl). At 27 weeks after the initial inoculation from human to mouse, these third-passage recipients had up to 37,500-fold more measured viral RNA than would have been received from the original human inoculum. We have replicated this experiment through two passages in two other series of mice, and through a single passage in a third leading to amplification of viral RNA from 90- to 1057-fold over the initial human inoculum. This transmission from human → mouse → mouse → mouse → mouse represents both replication of the HCV genome and production of fully infectious particles.

HCV infects human hepatocytes in transplant recipients

To colocalize HCV infection in human hepatocytes within the livers of chimeric mice, we immunostained sections of liver taken from homozygous transplanted mice with productive HCV infections with a monoclonal antibody against the NS3/NS4 portion of the viral polyprotein. Control sections of infected human liver showed staining localized to hepatocytes, with sparing of both portal triad structures and areas of bridging fibrosis (Fig. 5*a*). Using the rigorous immunohistochemical criteria defined by Brody *et al.*[16], infected cells are characterized by coarse intracytoplasmic granules (Fig. 5*a*, arrows); the diffuse fine granular cytoplasmic staining seen in sections is considered nonspecific. An unrelated isotype-specific control antibody produced no staining within hepatocytes, and sections taken from a noninfected human liver showed no staining with either antibody (Fig. 5*b–d*). Serial sections taken from the liver of a transplanted mouse with a productive HCV infection clearly show characteristic coarse cytoplasmic granules localized within nodules of human hepatocytes, with slightly diminished intensity compared with human controls (Fig. 5*e* and *f*). We detected HCV antigens only in human hepatocytes, with no staining in the surrounding hepatocytes of murine origin. Although human cells are clearly present in transplanted homozygous mice not infected with HCV, HCV antigens are not present (Fig. 5*g* and *h*). This immunohistochemical data provides convincing evidence that HCV infects human hepatocyte nodules within chimeric livers of transplanted *Alb-uPA* mice.

Discussion

These experiments establish that homozygous SCID/*Alb-uPA* mice with chimeric human livers can be infected *de novo* with HCV-positive human serum; they support HCV replication within the human portion of their livers at clinically relevant titers; and they show the capacity to transmit this infection to other chimeric mice. Successful infections were established with viral genotypes 1a, 1b, 3a and 6a, with rapid increases in viral RNA titers to levels easily detected by standard commercial assays. We successfully established infections in chimeric mice 3–8 weeks after transplantation, and did most of our inoculations between 4–6 weeks post-transplant, subject to the availability of infected human serum.

Homozygosity of *Alb-uPA* is critical to successful establishment of viral infection, and by using homozygotes as recipients, coupled with early screening of graft function by dot-blot analysis, HCV infections are routinely established in approximately 75% of all inoculated mice. Earlier reports suggested prohibitively high perinatal mortality rates associated with homozygosity of the *Alb-uPA* transgene. Since inception of our homozygous Alb-uPA colony, we have experienced a perinatal mortality rate of 32.6%, which is slowly decreasing with improvements in breeding stock. Using 8 breeding females and 4 breeding males provides ample potential recipient mice available at the ideal recipient age of 5–14 days at any one time.

The transplantation procedure requires basic microsurgical equipment and technical skills and takes 5–6 minutes per animal. While access to human hepatocytes might be limiting for some investigators, the yields from hepatocyte isolations in our laboratory average $2–3 \times 10^8$ viable human cells, similar to that of others[17,18]. Given the 9–10 day window optimal for transplantation and modest collaboration between investigators and hepatobiliary surgeons to use surplus tissue, fresh hepatocytes can almost always be available for transplantation—we have almost

no unused mice in our colony. The ability to cryopreserve surplus cells might allow for transportation to centers without human tissue access, although our experience with cryopreserved cells is considerably more limited; we have had success in both establishing long-term grafts (albeit at a lower overall success rate) and producing HCV infections within these animals.

This model should allow investigators to begin directly exploring *in vivo* strategies for inhibiting viral replication or preventing infection by passive immunity, and it should significantly advance the search for new antiviral therapies and vaccine development for hepatitis C.

Methods

Development of SCID/*Alb-uPA* strain. Animals were housed VAF, following Canadian Council on Animal Care (1993) guidelines. Experimental approval came from the University of Alberta Animal Welfare Committee. Hemizygous *Alb-uPA* mice (strain TgN(*Alb1Plau*)144Bri, Jackson, Bar Harbor, Maine) were crossed with homozygous SCID/*bg* mice (strain C.b-17/GbmsTac-SCID/*bg*N7, Taconic Farms, Germantown, New York). *Alb-uPA* was amplified from genomic DNA by PCR (Jackson). Homozygosity of the SCID trait was confirmed by quantification of total serum IgG using a sandwich ELISA.

Isolation of human hepatocytes. Ethical approval was obtained from the University of Alberta Faculty of Medicine Research Ethics Board and informed consent from all hepatocyte donors. Segments of human liver tissue (15–20 cm^3) were obtained from resection specimens normally discarded; most operations were performed for intrahepatic malignancies. After rapid cooling, hepatocytes were isolated and purified by collagenase-based perfusion[19,20], using 0.38 mg/ml Liberase CI (Boeringer) in perfusate, and stored short-term in 0°C Belzer-UW solution (DuPont, Wilmington, Delaware). Cell counts (hemocytometer) and viability (Trypan blue) were confirmed before use; viability was routinely > 80%.

Cryopreservation and thawing of human hepatocytes. Isolated hepatocytes were suspended (1×10^7 hepatocytes/ml) in cryopreservation tubes in 4 °C freeze/thaw media (50 ml FCS, 2.5 ml Pen/Strep, 447.5 ml M199 media). On ice, 2M DMSO was added in aliquots of 0.5 ml, 2 ml and 4 ml at 0, 5 and 30 min, respectively. At 45 min, tubes were transferred to a programmable ethanol freezing bath pre-set at –7.4 °C, 'nucleated' with a liquid-N_2–cooled semiconducting rod, cooled at 1 °C/min to –40 °C, and stored indefinitely in liquid N_2. Cells were rapidly reheated to 0 °C in a 37 °C water bath and spun, and supernatant was discarded. On ice, 1 ml of 0.75M sucrose was added at 0 min. Freeze/thaw media was serially added (1, 1, 2 and 4 ml at 30, 35, 40 and 45 min). At 50 min, the supernatant was separated, and cells were resuspended in Belzer-UW solution (Dupont) at 0 °C.

Transplantation of human hepatocytes. Recipients (5–14-day-old) were anesthetized with halothane/O_2, and through a small left-flank incision, 1×10^6 viable hepatocytes were injected into the inferior splenic pole; a single titanium clip was placed across the injection site for hemostasis, and the incision was closed.

Detection of human albumin in mouse serum by immunoprecipitation and western-blot analysis. Mouse serum (20 µl) was incubated with monoclonal antibody against human albumin (Clone HSA-9; Sigma) and complexes collected with protein G-agarose beads (Boehringer). Under reducing conditions, immunoprecipitates were separated by SDS–PAGE and transferred to nitrocellulose. Western blots were prepared using a biotinylated monoclonal antibody against human albumin (Clone HSA-11, Sigma), with a streptavidin-HRP conjugate and chemiluminescent substrate (Pierce, Rockford, Illinois) for detection.

Determination of zygosity of the *Alb-uPA* transgene. Mouse DNA (3 µg) was digested with PvuII, size fractionated on 0.7% agarose gel, transferred to Hybond-N+ membrane (Amersham), and hybridized to a ^{32}P-labeled probe from the final intron of the *uPA* gene (positions 7312–7920, GenBank accession #M17922). A 2.88-kb band was derived from *uPA* transgenes (T) and a 2.53-kb band from endogenous *uPA* genes (E); hybridization was quantified with a Fuji phosphoimager and Image Gauge Software (Fujifilm, Stamford, Connecticuit).

Immunohistochemistry. Mouse liver biopsies fixed in 10% formalin were paraffin embedded. Sections (5 µm) were H&E stained in standard fashion. To detect human hepatocytes, sections pre-treated with an avidin/biotin blocking kit (Zymed Laboratories, San Francisco, California) were immunostained with a monoclonal antibody against human hepatocyte (Clone OCH1E5, 1:20 dilution; DAKO, Carpinteria, California), with bound antibody detected by Super Sensitive Immunodetection System (BioGenex, San Francisco, California). For HCV proteins, sections were immunostained with monoclonal antibody against NS3/NS4 (TORDJI-22; Biogenex)[16]; isotype-specific unrelated monoclonal antibody against human melanoma (Clone HMB 45; Enzo Diagnostics, Farmingdale, New York) was used as a control.

Protein dot-blot assay for quantification of human-albumin production. Samples of mouse serum (2 µl) incubated for 5 min at 100 °C in 40 µl reducing buffer were triplicate blotted onto nitrocellulose. Dried membranes were soaked in transfer buffer, blocked with 3% PBS-Tween, and prepared as western blots. Chemiluminescence was quantified (STORM phosphoimager) from standard curves on each blot.

Detection of human DNA within transplanted mouse liver. Genomic DNA was isolated by phenol-chloroform, and *Alu* repeats amplified by PCR using *Alu Sx*-specific primers R16A/6 (5'-GGCGCGGTGGCTCACG-3') and L23A/266 (5'-TTTTTTGAGACGGAGTCTCGCTC-3')[21]. Human peripheral blood served as a positive control and *Alb/uPA* tails and non-transplanted *Alb/uPA* liver as negative controls. Murine genomic DNA was detected by amplifying a sequence from the murine *c-mos* proto-oncogene, using MUSMOS A (5'-GAATTCAGATTTGTGCATACACAGTGACT-3') and MUSMOS B (5'-AACATTTTTCGGGAATAAAAGTTGAGT-3').

Quantitative analysis of positive-strand HCV RNA in mouse serum. Blinded analysis was performed by the Alberta Provincial Laboratory of Public Health (Edmonton, Canada), or the Canadian Center for Disease Control (Winnipeg, Canada), using the Cobas Amplicor HCV Monitor system (Roche Diagnostics, Laval, Canada).

Detection of negative-strand HCV RNA by rTth PCR. Total RNA was isolated from mouse liver biopsies or infected human serum using TRIZOL (GIBCO/BRL, Burlington, Canada). RT-PCR was performed using a thermostable rTth reverse transcriptase RNA PCR kit (Perkin-Elmer, Norwalk, Connecticut). Positive-strand RNA was detected with an antisense (5'-CTCGCAAGCCCCTATCAGG-3') primer and negative-strand with a sense (5'-GAAAGCGTCTAGCCATGGCGT-3') primer for reverse transcription[22]. Strand-specific cDNA was amplified by adding the other primer to target a 240-bp region of the 5' non-coding region, using 35 cycles at 95 °C for 30 s, 66 °C for 45 s and 70 °C for 90 s, followed by 70 °C for 5 min. Reaction products were loaded onto a 2% agarose gel, transferred to Hybond-N+ nylon membrane (Amersham) and hybridized with an α-^{32}P-labeled DNA probe for HCV 5' non-coding region at 42 °C overnight.

Detection of negative-strand HCV RNA by RNase protection assay. Total RNA was isolated from mouse liver using Trizol Reagent (GIBCO/BRL) and from HCV-infected human serum using QIAamp Viral RNA Mini Kit (Qiagen, Valencia, California). Extracted RNA was probed with ^{32}P-labeled, gel-purified antisense riboprobe (detection of positive strand), sense riboprobe (detection of negative strand) and/or β-actin antisense riboprobe. Details of plasmid synthesis and riboprobe construction are available (Methods, Web Supplement). Denatured RNA samples were hybridized overnight at 42 °C, and RNase digestion was performed using an RNase protection assay kit (Ambion RPA III Kit, Austin, Texas). Products were resolved on a 5% PAGE containing 8 M urea and exposed to Kodak X-Omat AR film (Kodak, Vancouver, Canada).

Note: Supplementary information is available on the Nature Medicine website (http://medicine.nature.com/supplementary_info/).